IL
NUOVO CIMENTO
ORGANO DELLA SOCIETÀ ITALIANA DI FISICA
SOTTO GLI AUSPICI DEL CONSIGLIO NAZIONALE DELLE RICERCHE

VOL. XII, N. 6 — Serie decima — 16 Giugno 1959

Deposizione elettrolitica del rame su catodo rotante in presenza di ultrasuoni.

F. A. LEVI
Istituto di Fisica dell'Università - Perugia

(ricevuto il 10 Novembre 1958)

Riassunto. — Sono stati ottenuti depositi di rame su di un catodo rotante, un settore del quale era attraversato da ultrasuoni. Nel materiale prodotto sono state osservate modificazioni nell'abito cristallino tra le quali: una diminuzione di probabilità di formazione di centri di strutture raggiate, depositi più compatti e poveri di inclusioni gassose e formazione di geminati. Non sono state osservate modificazioni sistematiche delle dimensioni dei grani nè della microdurezza. Gli attacchi da cavitazione, che producono cavità nel metallo, dimostrano la presenza di azioni localizzate e prolungate nel tempo.

1. – Introduzione.

La presenza di ultrasuoni nel bagno elettrolitico, ed in particolare alla superficie del catodo, durante la deposizione dei metalli, può modificare le caratteristiche dei depositi ottenuti; sono noti in questo campo alcuni risul-

tati sperimentali (1-13) e qualche lavoro di carattere generale e riassuntivo (14-16).

Nelle nostre esperienze abbiamo prodotto depositi di rame di forte spessore, su di un catodo rotante attraversato da ultrasuoni di intensità generalmente superiore alla soglia di cavitazione. I depositi così ottenuti sono stati poi studiati con vari metodi, ponendo a confronto il materiale ottenuto in presenza di ultrasuoni con quello depositato contemporaneamente, in identiche condizioni, su di un settore del catodo opportunamente schermato. I primi risultati di questa ricerca sono stati riferiti altrove (17,18).

2. – Apparecchiatura e condizioni di esperienza.

Nella Fig. 1 è riprodotto il rotore (R) che porta il catodo (C) costituito da una sottile lamina di argento in forma di corona circolare. Gli ultrasuoni vengono generati entro il rotore da un trasduttore di ceramica al titanato di bario (T), che non partecipa alla rotazione; trasmessi da olio di ricino degassato, essi attraversano un settore del catodo e penetrano nel bagno elettrolitico, dove sono assorbiti da uno strato di gomma sintetica. Un altro settore del catodo, protetto da assorbitore (A) e camera d'aria, è praticamente libero da ultrasuoni, in quanto riceve solo una piccolissima frazione di energia riflessa.

La distribuzione della energia sonora nel bagno elettrolitico si controlla a mezzo di un minuscolo trasduttore di titanato di bario, montato all'estremità di un sottile supporto, che ne consente l'impiego in ogni punto del campo.

---

(1) B. Claus: *Zeits. Techn. Phys.*, **16**, 80 (1935).
(2) B. Claus e E. Schmidt: *Kolloid Beihefte*, **45**, 41 (1936).
(3) W. T. Young e H. Kersten: *Journ. Chem. Phys.*, **4**, 426 (1936).
(4) T. Rummel e K. Schmitt: *Korr. u. Metallschutz*, **19**, 101 (1943).
(5) M. Ishiguro e Y. Haramai: *Journ. Centr. Aeronaut. Res. Inst.*, **3**, 201 (1944).
(6) F. A. Levi: *Ric. Scient.*, **19**, 887 (1949).
(7) F. Müller e H. Kuss: *Helv. Chim. Acta*, **33**, 217 (1950).
(8) A. Roll: *Zeits. Metallkunde*, **42**, 238 (1951).
(9) A. Roll: *Zeits. Metallkunde*, **42**, 271 (1951).
(10) A. Roll: *Metalloberfläche*, **4**, B 49, 65, 81 (1952).
(11) O. Lindstrom: *Acta Chem. Scandin.*, **6**, 1313 (1952).
(12) W. Wolfe, H. Chessin, E. Yeager e F. Hovorka: Technical Report no. 10, Office Naval Research.
(13) W. Wolfe, H. Chessin, E. Yeager e F. Hovorka: *Journ. Electrochem. Soc.*, **101**, 590 (1954).
(14) S. Barnartt: *Quart. Rev.*, **1**, VII, 84 (1953).
(15) E. Yeager e F. Hovorka: *Journ. Acoust. Soc. Amer.*, **25**, 443 (1953).
(16) L. Bergmann: *Der Ultraschall* (Zürich, 1954).
(17) F. A. Levi: Report Nat. Phys. Lab. (Teddington, 1952).
(18) F. A. Levi: *Suppl. Nuovo Cimento*, **12**, 147 (1954).

Per far sì che l'intensità del fascio che attraversa il catodo possa raggiungere valori abbastanza alti, anche verso la fine della deposizione elettrolitica, è prevista una regolazione micrometrica della distanza dal trasduttore alla lamina di argento; si può così ottenere un intenso campo di onde stazionarie entro il rotore.

Il controllo e la regolazione della temperatura sono ottenuti mediante termometri e scambiatori di calore situati sia nell'elettrolito che nell'olio. Uno di questi scambiatori (S) è visibile nella Fig. 1.

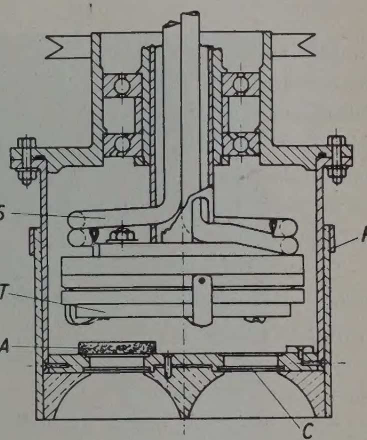

Fig. 1. – Sezione del rotore che mette in evidenza il trasduttore fisso all'interno. R, rotore; C, catodo; A, assorbitore; T, trasduttore; S, scambiatore di calore.

Nelle nostre esperienze l'intensità alla superficie del catodo non risultava perfettamente uniforme nonostante che il trasduttore fosse montato con lieve eccentricità rispetto all'asse di rotazione; erano presenti sulla superficie di deposizione figure di interferenza fisse rispetto al catodo durante la rotazione, dovute a riflessioni entro il rotore.

La maggior parte delle prove vennero condotte utilizzando come elettrolito una soluzione di solfato di rame acidificata, la cui composizione era la seguente: $CuSO_4$ 210 g/litro; H_2SO_4 75 g/litro, in acqua distillata. In tutte queste prove la temperatura della soluzione venne stabilizzata intorno ai 25 °C (*). La densità di corrente e l'intensità degli ultrasuoni variavano da prova a prova, onde sperimentare in diverse condizioni: la prima da un minimo di 109 A/m² ad un massimo di 3 260 A/m², la seconda da 1 W/cm² a 4 W/cm². La frequenza degli ultrasuoni era di 368.8 kHz. Ci si trovava dunque sempre in condizioni tali da rendere possibile la cavitazione a gas, indubbiamente favorita dal rapido ricambio e dalla continua aerazione del liquido.

La durata delle prove era quasi sempre di parecchie ore, sino a undici, dando così luogo a depositi di alcuni decimi di millimetro di spessore.

Per due prove, eccezionalmente, venne usato un elettrolita commerciale a base di fluoborato di rame, acido fluoborico e acido borico. In questi casi la temperatura nel bagno era mantenuta a circa 50 °C.

(*) La velocità di rotazione del tamburo portante il catodo era di 400 giri/m.

3. – Risultati.

Alla superficie del rame deposto elettroliticamente compaiono spesso delle escrescenze emisferiche a cui corrisponde una struttura raggiata originata da eterogeneità localizzate alla superficie di deposizione. In presenza di ultrasuoni tali strutture sono meno frequenti e tendono a formarsi con ritardo, come risulta sia dall'esame superficiale (Fig. 2), che dalla micrografia delle sezioni dei depositi da noi ottenuti; questa osservazione trova del resto conferma anche nella letteratura (7).

In uno dei nostri campioni vennero prodotte, a mezzo di periodiche interruzioni di corrente, delle superfici marcatempo, distanziate di trenta minuti: i primi strati appaiono quasi perfettamente lisci dal lato con ultrasuoni, mentre le strutture raggiate erano già evidenti nel controllo. Se ne conclude che gli ultrasuoni diminuiscono la probabilità di formazione dei centri delle strutture raggiate, cioè tendono ad impedire la localizzazione di impurità o altre cause di inomogeneità alla superficie del catodo; la diminuzione della tendenza alla crescita nei punti più sporgenti, che può aver origine dalla distruzione dei gradienti di concentrazione in prossimità del catodo, non sembra avere parte importante nella determinazione del fenomeno, forse perchè la forte agitazione del liquido agisce già in tal senso su entrambi i settori del catodo.

Nel rame prodotto con ultrasuoni si osservano con grande frequenza delle cavità rotondeggianti (del diametro di 1 o 2 decimi di millimetro), dovute, con ogni probabilità, all'attacco della cavitazione (9,10,13). L'esame microscopico di tali cavità, che interrompono nettamente le strutture cristalline che le circondano, metteva in evidenza il fatto che l'azione inibitrice o di corrosione, che le aveva originate, si era protratta per buona parte della durata della deposizione (cioè anche per diverse ore), localizzandosi non solo presso il fondo, ma anche lungo le pareti interne del foro. In una seconda fase poi la crescita dei cristalli prevaleva, il bordo della apertura, dapprima assai netto, si arrotondava e la cavità tendeva a chiudersi. Tali cavità si formavano preferenzialmente nelle zone di massima intensità e nei punti in cui, per ragioni idrodinamiche si formava una depressione (immediatamente a valle di escrescenze), il che conferma l'ipotesi che si tratti di effetti localizzati della cavitazione. In alcuni casi le cavità si disponevano con grande regolarità secondo l'andamento delle figure di interferenza (cerchi concentrici), presenti alla superficie catodica.

La presenza di tali lacune nel materiale trattato con ultrasuoni rese scarsamente significativo il confronto con i campioni di controllo nelle misure delle proprietà meccaniche, eseguite, per quanto riguarda il modulo elastico e la

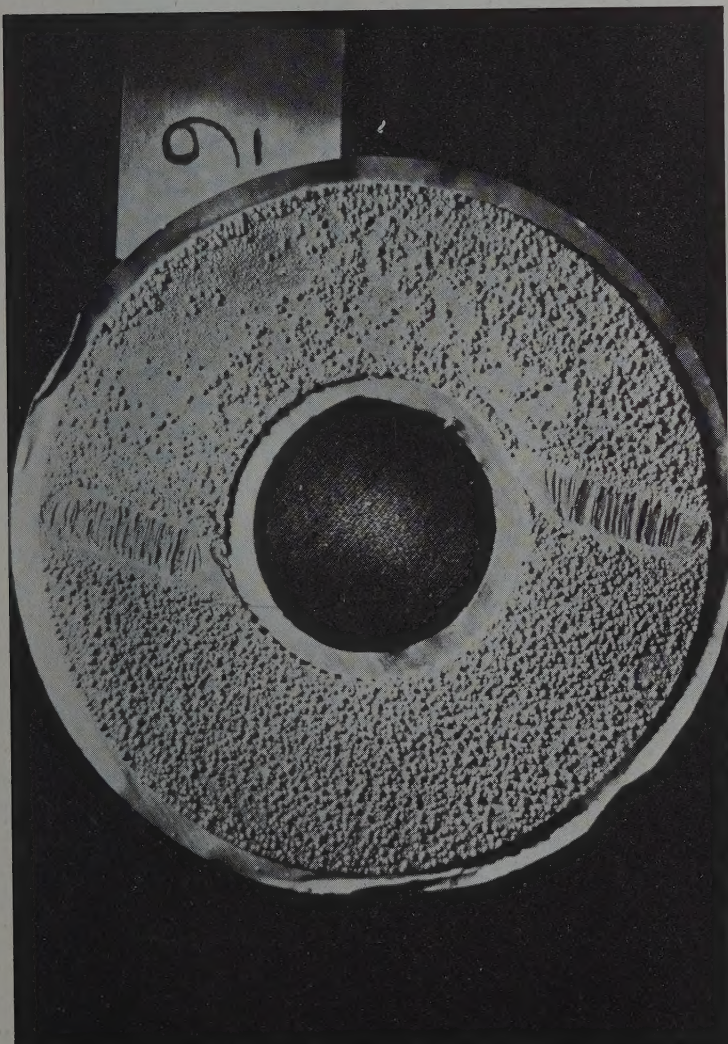

Fig. 2. – Aspetto della superficie catodica dopo una delle deposizioni, il settore attraversato dagli ultra-suoni si trova a destra.

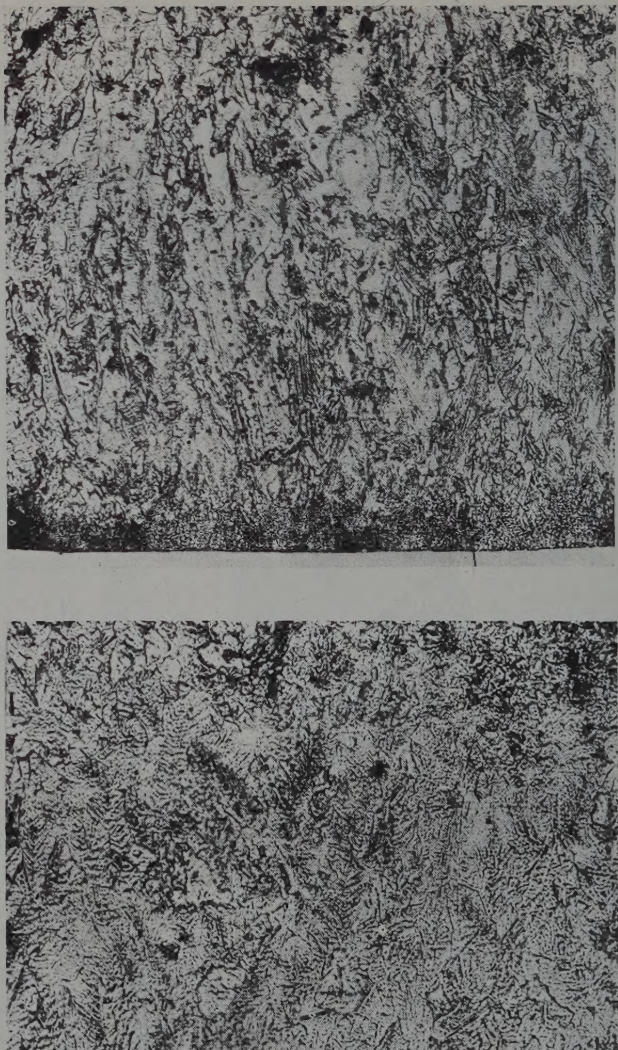

a)

b)

Fig. 3. – Sezioni trasversali (200×) dei depositi ottenuti senza ultrasuoni (*a*) e con ultrasuoni (*b*). (Densità di corrente 435 A/m²; intensità degli ultrasuoni 1 W/cm²). Campioni ricavati dalla lastra di Fig. 2.

dissipazione, con una apparecchiatura altrove descritta ([19]), e per le prove di trazione con macchine convenzionali adatte per piccoli carichi.

Dalle osservazioni microscopiche risulta poi che in generale gli ultrasuoni favoriscono la crescita regolare e uniforme dei cristalli, e diminuiscono notevolmente le inclusioni gassose, dando luogo a depositi più compatti. Quest'ultima osservazione è confermata dall'esame di campioni sottoposti a ricottura nei quali la liberazione di gas appare più scarsa quando siano stati ottenuti sulla porzione vibrante del catodo.

In certe condizioni poi la presenza di ultrasuoni altera profondamente l'aspetto micrografico delle sezioni, facendo scomparire la tendenza all'accrescimento colonnare e dando origine ad una struttura più tormentata (e più compatta) in cui si nota la presenza di numerosi geminati.

Ciò è evidente dalla Fig. 3, *a* e *b*, che mostra le sezioni di un deposito prodotto con densità di corrente non molto alta (435 A/m^2) e con la più bassa intensità degli ultrasuoni da noi impiegata (circa 1 W/cm^2); è interessante il confronto di questi risultati con quelli ottenuti da ROLL ([9,10,16]) per l'argento. Si osservi tuttavia come in altri casi la presenza di ultrasuoni sembri favorire la cristallizzazione colonnare, sempre però con depositi più compatti di quelli ottenuti senza ultrasuoni, ciò è stato osservato, ad esempio, in una delle deposizioni ottenute dal fluoborato di rame (con 651 A/m^2, intensità degli ultrasuoni 1 W/cm^2, temperatura 45 °C).

Per quanto riguarda la grossezza dei grani, che, come è noto manifesta in presenza di onde ultrasonore due opposte tendenze ([14]), non si osservavano in media nei nostri campioni differenze degne di nota tra il settore esposto agli ultrasuoni e quello schermato; ciò è risultato da numerosissimi esami micrografici, su campioni prelevati da dodici deposizioni, in punti corrispondenti dei due settori, e dalla indagine mediante diffrazione di raggi X eseguita su quattro coppie di campioni (provino assottigliato, fascio perpendicolare, camera Philips di precisione da 360 mm di circonferenza). Le stesse osservazioni ai raggi X non hanno messo in evidenza orientazioni preferenziali.

La microdurezza, misurata mediante apparecchio Tukon, non sembra subire in generale modificazioni importanti, di carattere sistematico, per effetto degli ultrasuoni.

4. – Conclusioni.

Nelle nostre esperienze la forte agitazione del liquido tendeva ad eliminare gli strati impoveriti di ioni metallici in prossimità del catodo, e riduceva quindi la probabilità di osservare quegli effetti degli ultrasuoni, che possono essere

---

([19]) G. BRADFIELD e F. A. LEVI: *Brit. Journ. Appl. Phys.*, **9**, 13 (1958).

attribuiti appunto alla distruzione di tali strati, che sono assai simili a quelli di una forte agitazione meccanica.

Non sono state osservate infatti, modificazioni sistematiche nelle dimensioni medie dei grani, nella microdurezza e nell'orientamento preferenziale. Alcuni effetti del genere erano tuttavia presenti, in qualche caso, dimostrando così che la rotazione del catodo non eliminava completamente i gradienti di concentrazione.

Altri fenomeni osservati sembrano però tipici dell'azione ultrasonora, tra questi ricordiamo la ridotta probabilità di formazione di centri di strutture raggiate; ciò è dovuto probabilmente alla microagitazione prodotta dagli ultrasuoni per effetto delle vibrazioni e della pressione di radiazione, che agisce molto attivamente proprio alla superficie del catodo, a causa della discontinuità dei mezzi di propagazione.

I depositi ottenuti con ultrasuoni risultavano più compatti e meno ricchi di inclusioni gassose; la cavitazione tende infatti ad impoverire il liquido dei gas disciolti, che si concentrano nelle bolle in formazione, mentre la agitazione ultrasonora tende ad allontanare le impurità.

Gli effetti erosivi della cavitazione si concentrano in alcuni punti dando luogo alla formazione di cavità che mostrano evidenti i segni di un'azione prolungata nel tempo. Tale azione è dovuta probabilmente a due diversi fattori: da una parte l'azione inibitrice delle bolle gassose che si formano di preferenza in quei punti, dall'altra la corrosione meccanica tipica della cavitazione accompagnata probabilmente da concomitanti azioni chimiche, non improbabili, data la potente azione ossidante degli ultrasuoni.

* * *

La prima fase di queste ricerche è stata resa possibile da una borsa di studio del British Council, ed è stata svolta presso il National Physical Laboratory in Teddington (Inghilterra); ad entrambe queste istituzioni va perciò il nostro ringraziamento.

Per avere collaborato alle osservazioni micrografiche, ringraziamo l'Istituto di Mineralogia della Università di Modena, l'Istituto Sperimentale dei Metalli Leggeri di Novara, ed il Laboratorio Metallografico delle Acciaierie di Terni. Ringraziamo pure il « Centre de Recherches Scientifiques Industrielles et Maritimes » di Marsiglia, che ha cortesemente provveduto alla esecuzione delle osservazioni coi raggi X.

Al prof. Amedeo Giacomini, Direttore dell'Istituto di Fisica della Università di Perugia, è dovuta la nostra viva gratitudine per utili discussioni e cordiale incoraggiamento.

SUMMARY

Electrodeposition of copper, as a sheet a few tenth of a millimeter thick, was obtained on a rotating cathode in the presence of ultrasonics, above cavitation level. Ultrasonic waves were transmitted through the cathode, a section of which was shielded to get a control sample. Modifications of crystalline texture, due to ultrasonic irradiation were observed, among which a reduced probability of formation of bumps (radial structures), more compact deposits with a low gas content and the presence of twins. Cavitation attacks were localised and gave evidence of an action prolonged in time. Micrographic and X-ray examination gave no evidence of grain size change or preferred orientation. Microhardness (Tukon) was not changed in the average.

1413

On the Scattering of K-Mesons by Nucleons (*).

C. Ceolin, V. De Santis and L. Taffara

Istituto di Fisica dell'Università - Padova
Istituto Nazionale di Fisica Nucleare - Sezione di Padova

(ricevuto il 1° Dicembre 1958)

Summary. — The present work deals with the problem of the scattering of K-mesons by nucleons in terms of direct pseudoscalar coupling K-Y-N. The purpose is to determine values of the pseudoscalar coupling constants g_Λ^2 and g_Σ^2 capable of fitting the experimental behaviour of K-proton elastic and K-neutron elastic and charge exchange cross-section. It has been found that, in the limits of the approximation used, no value can be determined for the ratio $Q = g_\Lambda^2/g_\Sigma^2$ which fits the experimental cross-section for all the energies investigated. Therefore it may be deduced that, assuming the quantum numbers attributed by the Gell-Mann-Nishijima scheme as correct and the theoretical procedure used as sufficiently reliable, the K-nucleon scattering phenomena cannot be interpreted in terms of K-Y-N direct coupling only.

1. – Introduction.

The problem of the interaction of heavy K-mesons by nucleons was examined by several authors during the last few years (1-5). The main purpose of

(*) Presented at the Palermo Conference (November 1958).

(1) C. Ceolin and L. Taffara: *Nuovo Cimento*, **5**, 435 (1957).

(2) D. Amati and B. Vitale: *Nuovo Cimento*, **5**, 1533 (1957); H. P. Stapp: *Phys. Rev.*, **106**, 134 (1957); C. Ceolin and L. Taffara: *Nuovo Cimento*, **6**, 425 (1957).

(3) C. Ceolin and L. Taffara: *Report of the Padua-Venice Conference* (September 1957), p. v-44.

(4) D. Amati and B. Vitale: *Nuovo Cimento*, **6**, 1013 (1957); D. Amati and B. Vitale: *Nuovo Cimento*, **9**, 190 (1958); K. Igi: *Progr. Theor. Phys.*, **19**, 238 (1958); C. Goebel: *Phys. Rev.*, **110**, 572 (1958); P. T. Matthews and A. Salam: *Phys. Rev.*, **110**, 569 (1958); S. Barshay: *Phys. Rev. Lett.*, **1**, 177 (1958).

(5) Y. Yamaguchi: *Report of Padua-Venice Conference* (September 1957), p. v-42; S. Barshay: *Phys. Rev.*, **110**, 743 (1958); *Phys. Rev. Lett.*, **1**, 97 (1958); C. Ceolin, N. Dallaporta and L. Taffara: *Nuovo Cimento*, **9**, 569 (1958).

this research was to construct a scheme capable of explaining with sufficient approximation the experimental data gradually recorded.

We already tried to explain in some previous papers [1-3] the few experimental data, which were available at that time, by means of the simplest scheme of K-Y-N interaction and always assuming the validity of the Gell-Mann-Nishijima scheme for the new particles.

The experimental evidence which we could undoubtedly rely upon was the following [6]:

a) The K-nucleon potential is repulsive;

b) The S-wave is predominant at low energies;

c) The K-proton cross-section at the energy of 100 MeV is $(10 \div 15)$ mb;

d) The R = (charge exchange/no charge exchange) ratio is 0,2 at low energies.

All these phenomena could then be explained by a simple direct pseudoscalar coupling (both for Λ and Σ-particles) with a ratio $Q = g_\Lambda^2/g_\Sigma^2 = 3$ [3]. In fact, while the nucleon-antihyperon pair term provides a sufficently large repulsive S-wave (as indicated from the experimental results *a*) and *b*)), with the value $Q = 3$ the $T = 0$ state vanishes and therefore the R-ratio takes a 0,2 value independently from the energy [1] of the incident particles: owing to its simplycity this scheme seemed to be rather coherent.

However the increase in the experimental data and particularly in the high energy data, has shown that [7], while the elastic K-neutron cross section increases up to 100 MeV and then decreases, the charge-exchange scattering cross-section (and therefore the R ratio) rapidly increases. Owing to the fact that such a rapid increase has not been found in the K-proton cross-section, one should conclude that this must be due to a not vanishing $T = 0$ phase-shift only, which is in disagreement with our assumption $Q = 3$.

With the present work we will try to see whether it is possible to explain the new experimental results by choosing new values of direct K-Y-N pseudoscalar coupling constant g_Λ^2 and g_Σ^2.

The next paragraph summarily describes the method used for the calculation of the phases. In Sect. **3** we try to determine from the experimental data on the scattering by proton the constant value $\lambda_1 = g_\Lambda^2 + g_\Sigma^2$.

Finally in Sect. **4** we try to determine a value for the ratio Q which can fit the experimental data concerning the behaviour of the total cross-section

---

(6) See ref. (1) of work (3).

(7) M. Grilli, L. Guerriero, M. Merlin, Z. O'Friel and G. A. Salandin: *Nuovo Cimento*, **10**, 163 (1958); M. Grilli, L. Guerriero, D. Keefe, A. Kernan, A. Motwill and G. A. Salandin: to be published in *Nuovo Cimento*.

for elastic and charge exange K-neutron scattering, both for high and l
energies. At the end the obtained results are discussed.

2. – Solution of integral equation.

The calculation of the phase-shift has been performed by solving
equation:

$$(E - H_0)|NK\rangle = H_{\text{int.}}|NK\rangle\,, \tag{1}$$

through the following development of $|NK\rangle$ in series of eigenstates of

$$|NK\rangle = \sum c_\alpha |l; m; n; p; q; r\rangle\,, \tag{2}$$

where:

l = nucleon number,

m = Σ-number,

n = Λ-number,

p = K-number,

q = N-$\bar{\Sigma}$ pair number,

r = N-$\bar{\Lambda}$ pair number,

and where the index α is for the quantities characteristic of a given st
The summation (2) is to be limited only to the states with strangeness 1
the following maxima numbers: $l=1$; $m=1$; $n=1$; $p=2$; $q=1$ and $r=$

By using for H_{int} the expression proposed by d'ESPAGNAT and PRENTKY
for the pseudoscalar coupling, i.e.:

$$H_{\text{int}} = \sum_{pq} \frac{1}{\sqrt{2\omega(k)\Omega}} \{ G_\Sigma \sum_{i=1}^{3} [\psi_\Sigma^{*i} \gamma_5 a^*(k) \tau_i \psi_N + \psi_N^* \tau_i \gamma_5 a(k) \psi_\Sigma^i] + \\ + G_\Lambda [\psi_\Lambda^* \gamma_5 a^*(k) \psi_N + \psi_N^* \gamma_5 a(k) \psi_\Lambda \tag{3}$$

and then by separating in the usual way the total isotopic spin and the t
angular momentum states, the following set of integral equations is obtain

$$(\omega_0 - \omega_p) c_N^{T,\mu}(p) = \lambda_T \int \omega_q \, \mathrm{d}\omega_q K_\mu(p, q) c_N^{T,\mu}(q)\,, \tag{4}$$

([8]) B. D'ESPAGNAT and J. PRENTKY: *Nucl. Phys.*, **1**, 33 (1956).

where:

$$\lambda_T = \begin{cases} \lambda_0 = 3\cdot g_\Sigma^2 - g_\Lambda^2\,, & \text{for } T=0 \\ \lambda_1 = g_\Sigma^2 + g_\Lambda^2\,, & \text{for } T=1 \end{cases} \tag{5}$$

and where the μ-index can take the three values 0,1 and 2 for the three $(l=0,\ J=\frac{1}{2})$, $(l=1,\ J=\frac{1}{2})$ and $(l=1,\ J=\frac{3}{2})$ angular momentum states.

The espression for the kernels K_μ in the approximation in which the nucleon recoil is neglected are:

$$\begin{cases} K_0(p,\,q) = \dfrac{q}{\pi(\omega_p\cdot\omega_q)^{\frac{1}{2}}(M_\mathrm{N}+M_\mathrm{Y}-\omega_0)}\,, \\ K_1(p,\,q) = \dfrac{p\cdot q^2}{6\pi M_\mathrm{Y}^2(\omega_p\cdot\omega_q)^{\frac{1}{2}}}\left[\dfrac{1}{\omega_0+M_\mathrm{N}-M_\mathrm{Y}-\omega_p-\omega_q}+\right. \\ \qquad\qquad\left.+\dfrac{1}{\omega_0-M_\mathrm{N}-M_\mathrm{Y}}-\dfrac{2M_\mathrm{Y}}{(\omega_0-M_\mathrm{N}-M_\mathrm{Y})^2}\right], \\ K_2(p,\,q) = \dfrac{pq^2}{3\pi M_\mathrm{Y}^2(\omega_p\cdot\omega_q)^{\frac{1}{2}}}\left[\dfrac{2M_\mathrm{N}^2+3M_\mathrm{Y}(M_\mathrm{Y}-2M_\mathrm{N})}{4\,M_\mathrm{N}\cdot(\omega_0+M_\mathrm{N}-M_\mathrm{Y}-\omega_p-\omega_q)}+\right. \\ \qquad\qquad\left.+\dfrac{M_\mathrm{N}-3M_\mathrm{Y}}{2M_\mathrm{N}(\omega_0-M_\mathrm{N}-M_\mathrm{Y})}-\dfrac{M_\mathrm{Y}}{(\omega_0-M_\mathrm{N}-M_\mathrm{Y})^2}\right]. \end{cases} \tag{6}$$

By the following trasformation:

$$c_\mathrm{N}^{T,\mu}(p) = \delta(\omega_p-\omega_0)+\frac{f^{T,\mu}(p)}{\omega_p-\omega_0}\,, \tag{7}$$

equation (4) becomes:

$$f^{T,\mu}(p) = \lambda_T\omega_0 K_\mu(p\,;\,k_0)+\lambda_T\int\omega_q\,\mathrm{d}\omega_q\,\frac{K_\mu(p,\,q)}{\omega_q-\omega_0}\,f^{T,\mu}(q)\,. \tag{8}$$

Solving it with Fredholm's method one obtains:

$$\operatorname{tg}\delta_{T,\mu} = \pi\cdot f^{T,\mu}(k_0) = -\,\pi\,\frac{\lambda_T\omega_0 K_\mu(k_0\,;\,k_0)}{1+\Delta_{T,\mu}}\,, \tag{9}$$

where:

$$\Delta_{T,\mu} = \lambda_T\int\omega_q\,\mathrm{d}\omega_q\,\frac{K_\mu(q\,;\,q)}{\omega_q-\omega_0}\,. \tag{10}$$

3. – K-proton scattering.

Substituting to:

$$\sigma(K^+p - K^+p) = \frac{4\pi}{k^2}\cdot(\sin^2\delta_{10} + \sin^2\delta_{11} + 2\sin^2\delta_{13})\,, \tag{11}$$

the phase-shift of $T = 1$ given by (9), the K-proton total cross-section ma
be calculated and, by comparison with the experimental data concerning th
process, the best value of λ_1 can be obtained.

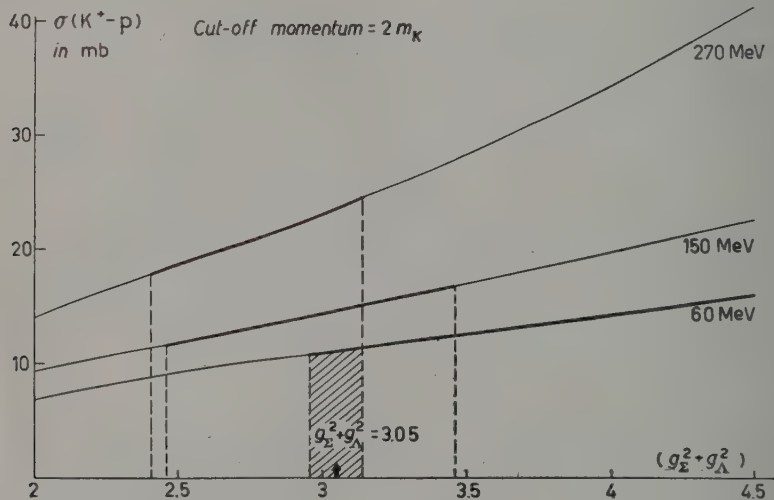

Fig. 1.

Fig. 1 shows the behaviour of $\sigma(K^+p - K^+p)$ as a function of λ_1 for thr
values of the energy. In each curve the experimental data together with the
errors are reported. It can then be seen that the best fit is obtained with th
value $\lambda_1 = 3.05$. Fig. 2 shows the theoretical cross-section calculated f
$\lambda_1 = 3.05$ and the experimental cross-section as reported in a recent work
the Padua-group [7].

Fig. 3 shows the behaviour of the three phases $T = 1$.

From the analysis of the three figures it is possible to state that, althoug
the increase of $\sigma(K^+p - K^+p)$ with the energy is slightly steeper than th
experimental one, the direct K-Y-N interaction theory with pseudoscal
coupling (both for Λ and Σ-particles) well explains the K-proton scatterin

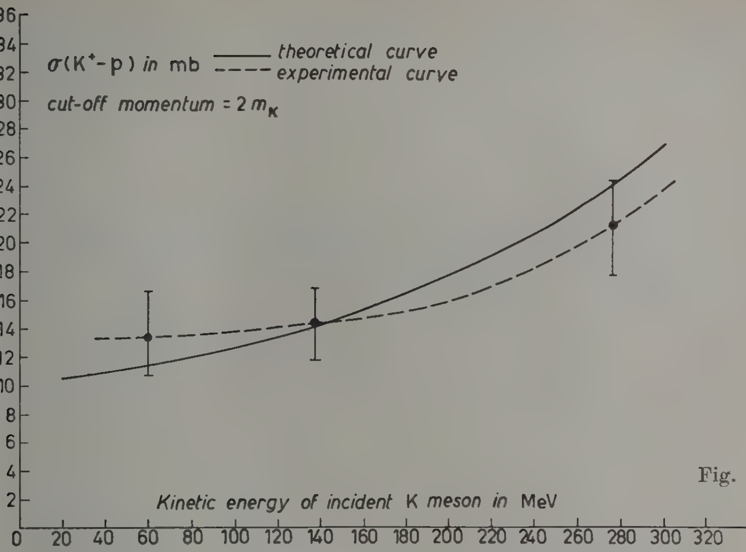

Fig. 2.

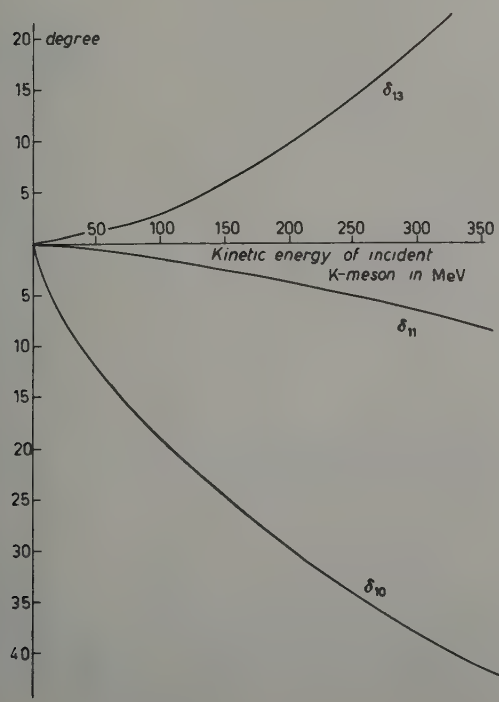

Fig. 3.

1410

in fact, with a λ_1-constant of the order of 3 it is possible to explain the repulsive S-wave at low energies and the slow increase of the total cross-section with the energy.

4. – K-neutron scattering.

The apparent agreement between the present theory and K-proton scattering experiments disappears when K-neutron scattering (both elastic and charge exchange) is analysed.

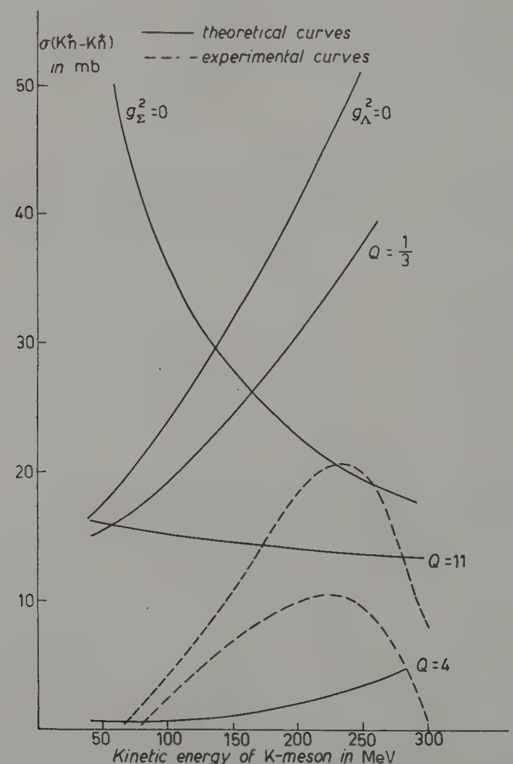

Fig. 4.

Once the constant value λ_1, and therefore the behaviour of all the phases $T=1$ is determined (see preceding paragraph), it will be necessary to know also the $T=0$ phases depending on the unknown λ_0-constant, for the calculation of $\sigma(K^+n-K^+n)$ and $\sigma(K^+n-K^0p)$ cross-sections.

In Figs. 4 and 5 we have plotted the theoretical total cross-sections $\sigma(K^-n - K^+n)$ and $\sigma(K^+n - K^0p)$ for various values of the parameter:

$$Q = \left(\frac{g_\Lambda}{g_\Sigma}\right)^2 = \frac{3\lambda_1 - \lambda_0}{\lambda_1 + \lambda_0}\,. \tag{12}$$

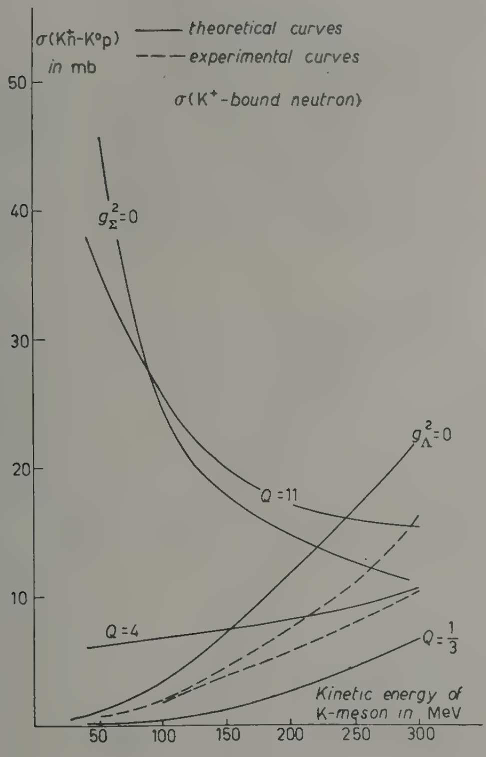

Fig. 5.

These curves were calculated from (9) by the relations:

$$\left\{\begin{aligned} \sigma(K^+n - K^0p) &= \frac{\pi}{k^2}\left[2\cdot\sin^2(\delta_{10}-\delta_{00}) + 2\sin^2(\delta_{11}-\delta_{01}) + \sin^2(\delta_{13}-\delta_{03})\right], \\ \sigma(K^+n - K^+n) &= \frac{2\pi}{k^2}\left[\sin^2\delta_{00} + \sin^2\delta_{01} + 2\sin^2\delta_{03}\right] + \\ &\qquad + \frac{1}{2}\,\sigma(K^+p - K^+p) - \sigma(K^+n - K^0p)\,, \end{aligned}\right. \tag{13}$$

and are then compared to the experimental ones reported in the quoted paper of the Padua-group (7).

The disagreement between the two curves is, in this case, evident. In fact, while from Fig. 4 the agreement may be obtained, in the limit of the errors,

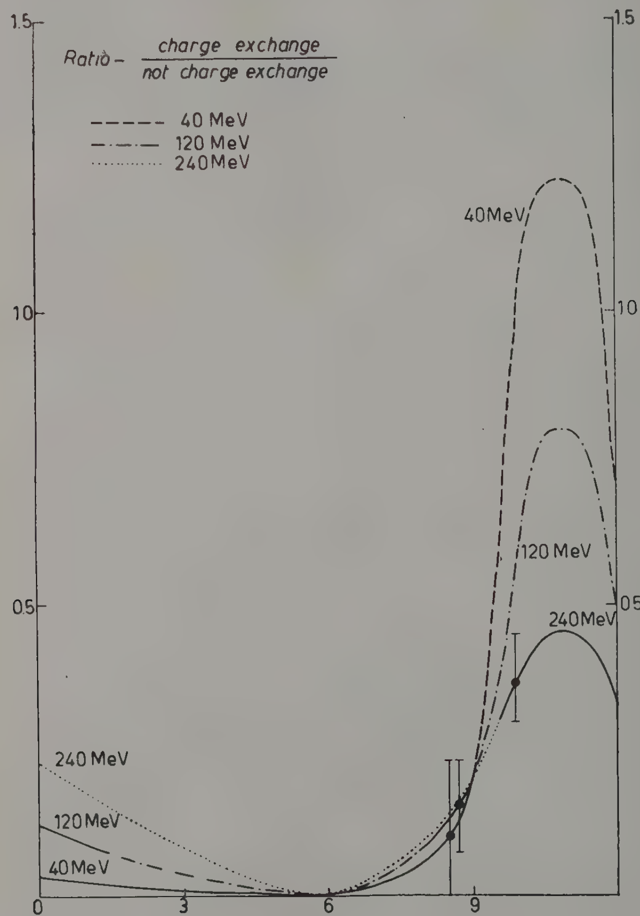

Fig. 6.

for a certain Q value between 4 and $\frac{1}{3}$ (without taking into account the strange decrease of $\sigma(K^+n - K^+n)$ over 200 MeV), with $\sigma(K^+n - K^0p)$ the agreement is possible for a Q-value in the range $0 \div \frac{1}{3}$.

The disagreement is also evident in Fig. 6 where the behaviour of the ratio R as a function of Q and the corresponding three experimental points have been

reported. The diagram 6 is such that the distance of a point on the axis of the abscissae from A is proportional to g_{Λ}^2, while the distance from B is proportional to g_{Σ}^2. One can now see that, while the fit with the experimental data at low energies is obtained with values of Q included between 6 and 9, for the agreement at high energies one should choose a value of Q greater than 9: it does not exist, therefore, a value of Q which can fit the experimental data for all energies.

5. – Concluding remarks.

The disagreement between theory and experience mentioned in the preceding Section let us think that either the method of calculation is too rough to give even qualitative results, or one of the hypotheses on which our scheme is based is uncorrect.

With respect to the method of calculation, the theoretical difficulties which arise from the calculation of strong interaction processes are well known; on the other hand, accepting for a moment that the Tamm-Dankoff method can give qualitative results only, it is necessary to point out that the approximation which consists in neglecting nucleon recoil effects is too rough and, in the case of K-nucleon scattering, could affect the results. In fact in a preceding paper (3) we have pointed out that the S-wave for $T=1$ goes down to one half at higher energies if one takes into account nucleon recoil.

With respect of the scheme of interaction adopted here, we think that, assuming for a moment that the used approximation is sufficient to give correct qualitative results, it is unlikely that better results can be obtained by other attempts to explain the K-nucleon scattering phenomena in terms of direct K-Y-N coupling in the framework of the Gell-Mann Nishijima theory.

It is known in fact, and reported in other works (2), that a scalar coupling is in disagreement from the beginning with the experiments because of the sign of the potential. On the other hand one can say, from a qualitative point of view, that it is unlikely that the possibility of opposite parities for Λ and Σ-particles may alone be sufficient, without any further assumption, to explain the experimental facts.

Therefore we are rather inclined to conclude that, either the K-Y-N interaction alone is not sufficient to explain the phenomena (and then it is necessary to consider also another type of interaction between K-meson and nucleon (5)), or that some physical assumptions as charge independence or other conservation theorems depending on the postulated simmetry properties of the new particles are uncorrect.

For example, a new possibility for escaping these contradictions could be

found in the assumption by PAIS (9), that the parity of charged K's is opposite to the parity of neutral K's. This of course should cause that, while K-proton and K-neutron elastic scattering occur essentially in S-wave, the K^0 coming out from the charge exchange reaction could be in a P-wave; and this could explain why, while the scattering cross-sections do not sensibly increase with energy, we observe on the contrary a steep increase with energy for the charge exchange.

However, it would be difficult to interpret this behaviour according to the direct K-Y-N interaction, as the assumption of different parities of K^+ and K^0 makes it necessary to treat the K-Y-N interaction according to the Gell-Mann scheme (10) in which all the hyperons are isospin doublets, and in this case the chargeexchange cross-section turns out to be zero. This can be overcome if we assumethat, for different parities for charged and neutral K's, a K-K-π interaction of the type:

$$H_{\text{int}} = k(\overline{K}^0 \cdot K^+ \pi^+ + \overline{K}^+ K^0 \pi^-) ,$$

becomes possible; then charge exchange could occur according to a graph in which the NNπ-vertex contains a $\boldsymbol{\sigma}\cdot\boldsymbol{k}$. coupling and gives a P-wave while this interaction cannot occur for a pure K-proton and K-neutron elastic scattering.

* * *

We are grateful to Prof. N. DALLAPORTA for interesting discussions during our work. We wish to thank Prof. M. GRILLI, dott. L. GUERRIERO and dott. G. A. SALANDIN for many helpful discussions on the present experimental situation relative to K-nucleon scattering.

(9) Communication privately circulated by prof. BLOCH.
(10) M. GELL-MANN: *Phys. Rev.*, **106**, 1296 (1957).

RIASSUNTO

Scopo di questo lavoro è di studiare lo scattering dei mesoni K da parte dei nucleoni, in termini di accoppiamento pseudo scalare diretto K-Y-N. Il proposito è di determinare i valori delle costanti di accoppiamento pseudo scalari g_Λ^2 e g_Σ^2 in rapporto con il comportamento sperimentale delle sezioni d'urto K-protone elastica K-neutrone elastica e cambio carica. Si è trovato che nei limiti delle approssimazioni usate, non può essere determinato nessun valore per il rapporto $Q=g_\Lambda^2/g_\Sigma^2$ che sia d'accordo con le sezioni d'urto sperimentali per tutte le energie in esame. Quindi si può dedurre che, assumendo come corretti, i numeri quantici dello schema di Gell-Mann-Nishijima e come sufficientemente valida la procedura teorica, lo scattering K-nucleone non può essere interpretato in termini solamente di accoppiamento diretto K-Y-N.

IL NUOVO CIMENTO Vol. XII, N. 6 16 Giugno 1959

Note on the Electric Quadrupole Absorption in the Nuclear Photo-Reaction.

S. Fujii

Department of Physics, College of Science and Engineering, Nihon University - Tokyo

O. Sugimoto

Department of Physics, Hiroshima University - Hiroshima

(ricevuto il 20 Dicembre 1958)

Summary — The behavior of the EQ absorption cross section in the « Giant resonance » region is discussed through the analysis of the angular distributions of emitted particles by using the direct interaction model. The difference between proton's and neutron's angular distributions is attributed to the difference between the effective charges of the proton and the neutron for EQ radiation. The excitation functions for the EQ absorption are computed for $^{40}A(\gamma\, p)^{39}Cl$ and $^{59}Co(\gamma\, p)^{58}Fe$. It is pointed out that the integrated cross sections for the EQ absorption are favorable to explain the feature of the angular distributions and the excitation curves have a peak near the maximum energy of the « Giant resonance ». The agreement between our results and the experiments for the angular distributions of the above reactions is good in part. On the whole, however, the ratio of the ED to the EQ absorption cross section is too small in comparison to that required from the experiments. The results of this model are closely discussed and the direction of the modification is also indicated.

1. – Introduction.

As is well known, the « Giant resonance » is one of the characteristic phenomena of the nuclear photo-reaction. The integrated cross-section of the « Giant resonance » is comparable with the sum-rule limit for electric dipole radiation [1].

[1] J. S. Levinger and H. A. Bethe: *Phys. Rev.*, **78**, 115 (1950); J. S. Levinger and D. C. Kent: *Phys. Rev.*, **95**, 418 (1954).

In the theories till now proposed it has been assumed that the reaction takes place mostly through ED absorption in the giant resonance region.

The validity of this treatment will be made clear from the study of the angular distribution of the emitted particles. A summary of the experimental results is as follows:

a) For neutrons; at the low energy part of the energy spectrum the angular distribution is isotropic and the high energy part is expressed as $A+B\sin^2\theta$.

b) For protons; although the angular distributions vary from nucleus to nucleus, the distribution curves show asymmetry with respect to 90° and the maxima of them generally shift to smaller angles $(60\div 70)°$.

From this summary it is clear that the multipole absorptions but the ED absorption also contribute to the giant resonance. Because the experimental results suggest that there are some interferences between nuclear excitations by ED radiation (*) and other radiations different from ED radiation in parity.

Also the fact that there exist the above interferences in the (γ, p), but not in the (γ, n) is to be noted. From this we can know that the disintegration mode of the nucleus depends to some degree on the specific way in which it absorbed the γ-ray. So it is significant that we discuss the predictions by the direct interaction model [2] for the EQ absorption. This is chiefly the aim of this note.

The angular distribution predicted by the direct interaction model depends essentially on the mechanism of the γ-ray absorption. The interactions of the neutron and the proton with electric multipole radiations are different from each other in the effective charge which will be defined in Section **2** on the basis of the translation invariance of the nucleus. For the electric multipole radiations except ED the effective charge of the neutron is nearly equal to zero, while that of the proton is approximately e. So in this model the neutron can scarcely go out of the nucleus through absorption of the electric multipole radiations except ED. Against it we shall show in Section **2** that the EQ absorption cross-section for the proton is quite large in the giant resonance region. The MD absorptions by the neutron might be so large as to be comparable with those by the proton. They, however, should be small at $\hbar\omega\sim 20$ MeV and especially in the model shown in Section **2** the MD matrix elements vanish.

(*) We shall use the abbreviations ED, EQ and MD for electric dipole, electric quadrupole and magnetic dipole respectively.

(2) E. D. Courant: *Phys. Rev.*, **82**, 703 (1951).

The important role of the EQ absorption in the (γ, p) reactions is made clearer by computing the angular distributions (*). The (γ, p) reactions chosen here are $^{40}A(\gamma, p)^{39}Cl$ and $^{59}Co(\gamma, p)^{58}Fe$. The agreement between our results and the experiments for them is good in part. It will be shown in Section **3**. On the whole, however, the ratio of the ED to the EQ absorption cross-section is too small in comparison with what is required from the experiment. Basing on the above discrepancy, we shall discuss in what direction the model should be modified. The process of direct interaction with photons was recently formulated in nuclear dispersion theory by BROWN and LEVINGER [15]. Their theory may modify somewhat our result, but the features of the result should be preserved invariably. Actually our result is consistent with their estimation that the ratio of the EQ absorption cross-section to the ED is appreciably large.

2. – The effect of electric quadrupole radiation.

At first, we discuss the feature of the angular distributions predicted by the direct interaction model in (γ, p) and (γ, n).

The interaction Hamiltonian of a nucleus with γ-ray is,

$$H' = -\sum_i \left\{\frac{e}{2Mc}\boldsymbol{p}_i\boldsymbol{A}_i + \frac{e}{2Mc}\boldsymbol{A}_i\boldsymbol{p}_i + \mu_p\frac{e\hbar}{2Mc}(\boldsymbol{\sigma}_i\cdot\boldsymbol{H}_i)\right\} - \sum_j \mu_n\frac{e\hbar}{2Mc}(\boldsymbol{\sigma}_j\cdot\boldsymbol{H}_j)$$

if there is only ordinary force in the interaction between nucleons in the nucleus. $\boldsymbol{A}_i$ is the vector potential and $\boldsymbol{H}_i$ the magnetic field. The subscript i $(1 \ldots Z)$ stands for proton and j $((Z+1), \ldots, A)$ for neutron. Let a photon of energy $\hbar\omega$ be incident in direction $\boldsymbol{n}$,

$$\boldsymbol{A}_i = \boldsymbol{\epsilon}(2\pi\hbar c^2/\omega)^{\frac{1}{2}} \exp[i\boldsymbol{k}\boldsymbol{r}_i]\,,$$

where $\boldsymbol{\epsilon}$ is the polarization vector of the photon, $\boldsymbol{k}$ its wave number vector and $\boldsymbol{k} = (\omega/c)\boldsymbol{n}$. Now we separate the co-ordinate of the nucleon into the internal co-ordinate and the co-ordinate of the center of gravity, and corresponding to this we separate the momentum of the nucleon, because the absorption of the photon is caused by the relative motion of nucleons.

(*) EICHLER and WEIDENMÜLLER [16] also referred, not in detail, on this point, basing for their estimation in the Born approximation on $A = 32$.

1427

Transforming H' parallel with the method used by AUSTERN and SACHS or MOSZKOWSKY [3],

$$(1) \qquad H' \cong -(2\pi\hbar c^2/\omega)^{\frac{1}{2}} \exp[i\boldsymbol{k}\boldsymbol{R}]I$$

and

$$(2) \quad I \doteq e\sum_{L=1}^{\infty}\sum_{i}^{Z}\left(\frac{1}{L!}\right)\left(\frac{i\omega}{c}\right)^{L}(\boldsymbol{\epsilon}\cdot\boldsymbol{r}_i-\boldsymbol{R})(\boldsymbol{n}\cdot\boldsymbol{r}_i-\boldsymbol{R})^{L-1}+$$
$$+\frac{e\hbar}{Mc}\sum_{L=1}^{\infty}\frac{1}{(L-1)!}\cdot\left(\frac{i\omega}{c}\right)^{L}\left[\sum_{i=1}^{Z}\left\{\frac{(\boldsymbol{\epsilon}'\cdot\boldsymbol{L}_i)}{L+1}+\frac{\mu_p}{2}\cdot(\boldsymbol{\sigma}_i\cdot\boldsymbol{\epsilon}')\right\}\frac{(\boldsymbol{n}\cdot\boldsymbol{r}_i-\boldsymbol{R})^{L-1}}{2}+\right.$$
$$\left.+\sum_{i=1}^{Z}\frac{(\boldsymbol{n}\cdot\boldsymbol{r}_i-\boldsymbol{R})^{L-1}}{2}\left\{\frac{(\boldsymbol{L}_i\cdot\boldsymbol{\epsilon}')}{L+1}+\frac{\mu_p}{2}(\boldsymbol{\sigma}_i\cdot\boldsymbol{\epsilon}')\right\}+\sum_{j=Z+1}^{A}\frac{\mu_n}{2}\cdot(\boldsymbol{\sigma}_j\cdot\boldsymbol{\epsilon}')(\boldsymbol{n}\cdot\boldsymbol{r}_j-\boldsymbol{R})^{L-1}\right],$$

where

$$(3) \qquad \boldsymbol{R}=\frac{1}{A}\sum_{k=1}^{A}\boldsymbol{r}_k\,,$$

$$(4) \qquad \boldsymbol{P}=\sum_{k=1}^{A}\boldsymbol{p}_k\,,$$

$$(5) \qquad \boldsymbol{L}_i=\frac{1}{\hbar}(\boldsymbol{r}_i-\boldsymbol{R})\times\left(\boldsymbol{p}_i-\frac{1}{A}\boldsymbol{P}\right),$$

and

$$(6) \qquad \boldsymbol{\epsilon}'=\boldsymbol{n}\times\boldsymbol{\epsilon}\,.$$

In deriving the eq. (2) a term, $-(e/2AMc)\sum_i\{\boldsymbol{P}\cdot\boldsymbol{A}_i+\boldsymbol{A}_i\cdot\boldsymbol{P}\}$, was neglected on account of its smallness in comparison with the other terms [3].

From the eq. (2), the effective charges of the proton and the neutron for ED-radiation are defined to be $(1-(Z/A))e$ and $(-(Z/A))e$ respectively. On the other hand, the EQ- and MD-term contain the terms which cause simultaneous excitations of two nucleons. However, the simultaneous excitations can be put out of question, because now we confine ourselves to the interference between nuclear excitations by ED- and EQ-(MD-) radiation. We can define the effective charges for EQ-radiation.

$$(7) \qquad \begin{cases} e_{\mathrm{eff}}=\left(1-\dfrac{2}{A}+\dfrac{Z}{A^2}\right)e, & \text{for protons,}\\[2ex] \quad\;\; =\dfrac{Z}{A^2}\,e\,, & \text{for neutrons.}\end{cases}$$

---

[3] R. G. SACHS and N. AUSTERN: *Phys. Rev.*, **81**, 705 (1951); S. A. MOSZKOWSKI: *Phys. Rev.*, **89**, 474 (1953).

It is clear that the excitations of the single neutron by EQ-radiation are greatly suppressed by the effective charge.

The cross-section for the MD absorption by the neutron might be so large as to be comparable with those by the proton, because the MD-term contains the spin-dependent term. It, however, should be small at $\hbar\omega \sim 20$ MeV, because around the energy there does not exist the state in which the radial wave function is similar, in form, to that in the ground state. Especially in the model, of which we mention in the following, the matrix elements for the MD absorption vanish. We may also expect that the other magnetic multipole absorption is small. Therefore the angular distributions of the neutron should be nearly symmetric with respect to 90°. This result is no longer right for the proton. The feature had already been indicated also by S. A. E. JOHANSON ([14]). And we have another result—because the signs of the effective charge for ED and EQ are same for the proton, but not for the neutron, the maximum of the proton's and of the neutron's angular distribution should tend to shift to opposite direction to each other with respect to 90° in a mirror nucleus, if we can neglect Coulomb force. For example, if the former is observed at $(60 \sim 70)°$, the latter should shift to an angle slightly larger than 90°.

Let us describe the nucleus as some kind of potential with Z protons filling the Z lowest states and suppose that the proton after absorbing a monochromatic γ-ray jumps up on the continuum level and then goes out from the nucleus suffering distortion from the potential while the other nucleons remain undisturbed. Then it is assumed that the proton in the final state is affected from the square well potential equal to that in the initial state. For the high energy proton emitted from the nucleus it is reasonable to neglect the effect of Coulomb force.

Now let a photon energy $\hbar\omega$ be incident in the z-direction. The matrix element for the MD-absorption vanishes under the above assumption, and the high multipole radiations should hardly contribute to nuclear excitation. Thus the differential cross-section and the total cross-section are given as follows,

$$(8) \qquad \frac{d\sigma}{d\Omega} \simeq 4\pi^2 \left(\frac{c}{\omega}\right) \varrho(\varkappa) \sum_{L_1=1}^{2} \sum_{L_2=1}^{2} \sum_{l_f} \sum_{l'_f} \sum_{L} (i)^{L\ \ L_2\ \ L_1} (\ \ )^{2j_i - l_i} f_{L_1} f_{L_2} \left(\frac{\omega}{c}\right)^{L_1+L_2} \cdot$$

$$\cdot (L_2 L_1 1 - 1 | L0)(L_2 l_i 00 | l'_f 0)(L_1 l_i 00 | l_f 0)\, G_{L_2}(l'_f; l_i) \cdot G_{L_1}(l_f; l_i) \cdot$$

$$\cdot Z (l'_f L_2\, l_f L_1; l_i L)\, P_L(\cos\theta)\,,$$

and

$$(9) \qquad \sigma \simeq 16\pi^3 \left(\frac{c}{\omega}\right) \varrho(\varkappa) \sum_{L=1}^{2} \sum_{l_f} (-)^{2j_i\ \ l_i} f_L^2 \left(\frac{\omega}{c}\right)^{2L} (L\, L\, 1 - 1 | 00) \cdot$$

$$\cdot (L l_i 00 | l_f 0)\ (L l_i 00 | l_f 0) |G_L(l_f; l_i)|^2 Z(l_f L l_f L; l_i 0)\,,$$

where

$$f_1 = \sqrt{\frac{4\pi}{3}}\frac{N}{A}e, \tag{10}$$

$$f_2 = \sqrt{\frac{\pi}{15}}\left(1 - \frac{2}{A} + \frac{Z}{A^2}\right)e\,, \tag{11}$$

and

$$G_L(l_f; l_i) = \int_0^\infty \bar{R}^f_{l_f} r^L R^i_{l_i} r^2 \mathrm{d}r\,, \tag{12}$$

where $\varkappa$ is the wave number of the specific proton, l_i (j_i) its orbital (total) angular momentum in the initial state and l_f the orbital angular momentum in the final state. $R^i_{l_i}$ and $R^f_{l_f}$ are the radial wave functions of the proton in the initial state and in the final state respectively. $\varrho(\varkappa)$ is the density of the final state (*), $(abcd|ef)$ the Clebsch-Gordan coefficient and $Z(l'_f L_2 l_f L_1; l_i L)$ the Z coefficient.

From the eq. (9) we obtain the cross-sections for some special processes in $^{40}A(\gamma, p)^{39}Cl$ and $^{59}Co(\gamma, p)^{58}Fe$. Some special processes mean that in the former reaction the proton in the $d_{\frac{3}{2}}$ level absorbs EQ radiation and in the latter the proton in the $f_{\frac{7}{2}}$ level as well. On the reactions we must increase the results obtained from the eq. (9) by the number of protons existing in each level, namely twice and septuple respectively, because the eq. (9) is for one proton in the level. The calculated results are shown in Fig. 1 and Fig. 2. We take $r_0 = 1.25 \cdot 10^{-13}$ cm and the well depth of nuclear potential so as to give the binding energy for the last proton.

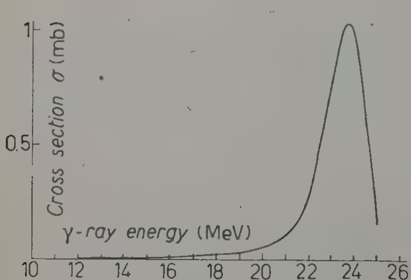

Fig. 1.

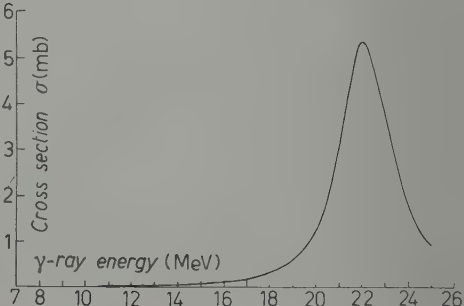

Fig. 2.

In Fig. 1 and Fig. 2 it is to be noted that there appears a large peak in each of the excitation curves for $^{40}A(\gamma, p)^{39}Cl$ and $^{59}Co(\gamma, p)^{58}Fe$. The integrated

(*) $\varrho(\varkappa) = \dfrac{M\varkappa}{8\pi^3\hbar^2}$.

1430

cross-sections of the peaks are given as follows,

$$2.3 \text{ mb-MeV} \qquad \text{for } {}^{40}\text{A}(\gamma, \text{p})^{39}\text{Cl} ,$$

and

$$17.5 \text{ mb-MeV} \qquad \text{for } {}^{59}\text{Co}(\gamma, \text{p})^{58}\text{Fe} .$$

They take a value not inconsistent with the integrated cross-section of the giant resonance. The experimental value of the latter is 540 mb-MeV for ^{40}A$(\gamma, p)^{39}$Cl (4) and 140 mb-MeV for ^{59}Co$(\gamma, p)^{58}$Fe (5). So the integrated cross-section of the above peaks are about 1/230 and 1/8 as compared with that of the giant resonance in ^{40}A$(\gamma, p)^{39}$Cl and ^{59}Co$(\gamma, p)^{58}$Fe respectively. The appearance of the peaks should be not due to the speciality of these nuclei and such results might be obtained also for the γ-reactions of the other nuclei. It will be shown by one of us in another place that a broad peak at $\hbar\omega \sim 24$ MeV appears in the excitation curve of the EQ absorption cross-section in ^{13}C$(\gamma, n)^{12}$C, too (6). In the case of ^{13}C$(\gamma, n)^{12}$C, however, the maximum value is suppressed by the effective charge of the neutron.

3. – The examination of the direct interaction model.

In the last section we indicated that the direct interaction model gives us a good description at least for the behavior of the EQ absorption.

In order to examine further the usefulness of the model we apply the eq. (8) to the angular distributions of ^{40}A$(\gamma, p)^{39}$Cl and ^{59}Co$(\gamma, p)^{58}$Fe. The results are shown in Fig. 3 and Fig. 4. Our results are obtained for the former reaction at $\hbar\omega = 18$ MeV and for the latter at $\hbar\omega = 19.5$, 21.5 MeV. The experimental data for ^{40}A$(\gamma, p)^{39}$Cl (7) and ^{59}Co$(\gamma, p)^{58}$Fe (8) are for the emitted protons with high energies in the reactions initiated by bremsstrahlung with their maximum energies 22.5 MeV and 24 MeV respectively. These protons should leave the residual nuclei on the ground state or the first

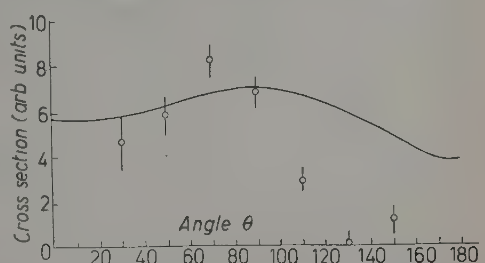

Fig. 3.

(4) D. McPherson, E. Perderson and L. Katz: *Can. Journ. Phys.*, **32**, 593 (1954).
(5) J. Halpern and A. K. Mann: *Phys. Rev.*, **83**, 370 (1951).
(6) S. Fujii: *Prog. Theor. Phys.*, **21**, 511 (1959).
(7) B. M. Spicer: *Phys. Rev.*, **100**, 791 (1956).
(8) M. E. Toms and W. E. Stephens: *Phys. Rev.*, **95**, 1209 (1954).

few excited states after absorbing some γ-ray energies near the maximum energy. So our results may be compared with these experimental results.

The qualitative agreement with the experiments is good.

From Fig. 3 and Fig. 4 it is clear that the contribution from EQ radiation is as large as that from ED radiation at $\hbar\omega \sim 20$ MeV. This is seen more clearly in Table I, where we give the ratios of the EQ- to the ED-absorption cross-section.

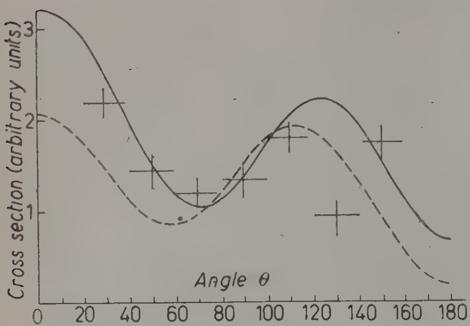

Fig. 4.

With increase of the γ-ray energy the EQ absorption plays the more important role in this model. This is due to the circumstance that the EQ absorption cross-section has a maximum at higher energy nearly equal to the giant resonance energy in each of $^{40}A(\gamma, p)^{39}Cl$ and $^{59}Co(\gamma, p)^{58}Fe$, as it was shown in Fig. 1 and Fig. 2. On the other hand the excitation functions for the ED absorption vary smoothly and do not swing upward rapidly with

TABLE I. – *Coefficient of Legendre polynomials C_L when $C_0 = 1$ and ratio of $\sigma(EQ)$ to $\sigma(ED)$.*

Nucleus	Potential depth (MeV)	γ-ray energy (MeV)	C_1	C_2	C_3	C_4	$\frac{\sigma(EQ)}{\sigma(ED)}$
$^{59}_{32}Co^{27}$	38.0	21.5	0.035	0.27	0.73	−0.11	3.21
		19.5	−0.07	−0.22	0.77	0.06	0.334
$^{40}_{22}A^{18}$	39.2	22.0	0.06	0.15	0.83	0.09	1.65
		20.0	0.09	−0.20	0.39	0.08	0.156
		18.0	0.11	−0.25	0.003	0.01	0.0116

increase of the γ-ray energy in the model. So in the higher energy region the EQ absorption cross-section accounts for a great part of the total cross-section and then the angular distribution, if we compute, bears little resemblance to the experiments. Our result for the ED absorption is not to be so amazing

but corresponding to Burkhardt's (9) obtained by using a similar model for $^{64}Cu(\gamma, n)^{63}Cu$. He computed the excitation function for the (γ, n) on the supposition that all the nucleons in ^{64}Cu move independently of each other. As result it was indicated that most of the ED absorptions take place in a considerably lower energy region than the giant resonance energy and so the ED absorption cross-section in the giant resonance region takes a small value.

We computed the cross-section for the (γ, p) on the supposition that the emitted proton couples weakly with the other nucleons not only in the final state but also in the initial state and made a qualitative comparison with the experiments. Though this supposition may extremely simplify the real nucleus, our result at least for the EQ absorption is reasonable. So in the EQ absorption the proton in a nucleus seems to be excited to a certain degree independently of the motions of the other particles at the γ-energy of 20 MeV. On the other hand, in comparison with the EQ absorption cross-section, the value for the ED absorption that is predicted by the above model is much smaller than what is required by the experiments. This may suggest the existence of a many-body effect which modifies the above results for the ED absorption more largely than for the EQ absorption.

Some many-body effects that may explain the giant resonance energy have already been indicated. They are, for instance, the nuclear dipole vibration mode by GOLDHABER and TELLER (10) or the velocity-dependence of the nuclear potential by WILKINSON (11). Above all, the model introduced by U. L. BUSINARO and S. GALLONE (12) or S. TAKAGI and one of us (13) is very interesting from the point of the above discussion. They supposed that, while the centre of mass of the protons vibrates relatively to that of the neutrons, the protons (or the neutrons) interact still between themselves only through the nuclear potential. In these models ED radiation excites the dipole vibration mode, while the EQ absorption by the individual particle should still be allowed. So we consider that these models may give reasonable results for the angular distribution of the (γ, p) and the (γ, n).

(9) J. L. BURKHARDT: *Phys. Rev.*, **91**, 420 (L) (1953).
(10) M. GOLDHABER and E. TELLER: *Phys. Rev.*, **74**, 1046 (1948).
(11) D. H. WILKINSON: *Physica*, **22**, 1039 (1956).
(12) U. L. BUSINARO and S. GALLONE: *Nuovo Cimento*, **1**, 1285 (1955).
(13) S. TAKAGI and S. FUJII: *Progr. Theor. Phys.*, **14**, 402, 405 (L) (1955).
(14) S. A. E. JOHANSON: *Phys. Rev.*, **97**, 434 (1955).
(15) G. E. BROWN and J. S. LEVINGER: *Proc. Phys. Soc.*, **71**, 733 (1958).
(16) J. EICHLER and H. A. WEIDENMÜLLER: *Zeits. f. Phys.*, **152**, 261 (1958).

* * *

The authors wish to express their sincere thanks to Prof. M. KOBAYASHI, K. SAKUMA, S. NAKAMURA and S. TAKAGI for their kind encouragement and affording facility to this joint research. They are also indebted to colleagues of their laboratories and members of the Kobayashi Laboratory for their valuable discussion.

RIASSUNTO (*)

Si discute il comportamento della sezione d'assorbimento nella regione della «Risonanza gigante» mediante l'analisi delle distribuzioni angolari delle particelle emesse usando un modello d'interazione diretta. La differenza fra le distribuzioni angolari dei protoni e dei neutroni si attribuisce alla differenza fra le cariche effettive del protone e del neutrone per la radiazione EQ. Si calcolano le funzioni d'eccitazione per l'assorbimento per $^{40}A(\gamma\ \pi)^{39}Cl$ e per $^{59}Co(\gamma\ \pi)^{58}Fe$. Si fa rilevare che le sezioni d'urto integrate per l'assorbimento EQ si prestano all'interpretazione del comportamento delle distribuzioni angolari e che le curve di eccitazione hanno un picco nelle vicinanze della massima energia della «Risonanza gigante». L'accordo tra i nostri risultati e le esperienze sulle distribuzioni angolari delle reazioni di cui sopra è relativamente buono. Nel complesso, tuttavia, il rapporto delle sezioni d'urto d'assorbimento ED ed EQ è troppo piccolo rispetto a quello richiesto dalle esperienze. Si discutono esaurientemente i risultati del presente modello e si indica in qual senso modificarlo.

(*) *Traduzione a cura della Redazione.*

IL NUOVO CIMENTO Vol. XII, N. 6 16 Giugno 1959

A Tentative Evaluation of the N Ξ Mass Difference.

N. DALLAPORTA and G. PATERGNANI

Istituto di Fisica dell'Università - Padova
Istituto Nazionale di Fisica Nucleare - Sezione di Padova

(ricevuto il 16 Febbraio 1959)

Summary. — An attempt is made to evaluate the NΞ mass difference by using a Lee model consisting in a bare baryon B with no electric charge nor hypercharge which may be clothed either with K-mesons giving thus the nucleon or with $\overline{\text{K}}$-mesons giving thus the Ξ. The mass difference between these two states is then attributed to a hypercharge dependent perturbation consisting in the simultaneous emission and absorption of two K-mesons. The order of magnitude of this perturbation is discussed in order to obtain the experimental mass difference. The values thus obtained for it are such as to make this two K-interaction of small importance in K-nucleon scattering processes.

The main tendency for the interpretation of the scheme of the elementary particle states observed up to now has principally consisted in the search of symmetries to which the regularities for the charge states, the coupling types and the values of the interaction constants could be attributed; and several models based on some highly symmetric lagrangian have been proposed (1,2). More recent works however (3) seem to indicate that these postulated symmetries are less general than was first supposed: and an explanation for this failure may be found if, apart from the initial interaction terms in the lagrangian to which the high symmetry was attributed, there are also some other terms with a less pronounced degree of symmetry which act as a perturbation

(1) B. D'ESPAGNAT and J. PRENTKI: *Nucl. Phys.*, **1**, 33 (1956); J. SCHWINGER: *Phys. Rev.*, **104**, 1164 (1956); J. TIOMNO: *Nuovo Cimento*, **6**, 69 (1957).
(2) N. DALLAPORTA: *Nuovo Cimento*, **7**, 200 (1957).
(3) A. PAIS: *Phys. Rev.*, **110**, 574 (1958); **112**, 624 (1958).

on the initial scheme and are therefore responsible for the appearance of the irregularities now observed in different interaction phenomena [3].

The occurrence of such irregularities in the interaction is however less surprising if one considers that the symmetrical schemes to which the previous lagrangians of reference [1,2] were applied, have been obtained with the assumption of neglecting the mass differences between baryons, which are by no means small (the N Ξ mass difference is about 25% of the nucleons mass). These mass differences may also be naturally attributed to some disturbing feature in the symmetry of the interactions [1,2]: so that the same fundamental disturbing cause could be responsible for both effects.

While most of the work, up to now, has been principally directed to the explanation of the irregularities of the interactions, the present paper is instead an attempt to interpret the mass splitting of the baryon levels.

Such a possibility has already been indicated in a previous paper [4] in which it was shown that symmetric lagrangians such as d'Espagnat-Prentki's one are not only invariant for ordinary charge-conjugation, but also for what was termed in this paper the boson and the spinor conjugation alone; the first of which being defined as the reversal of the sign of electric charge and hypercharge of all the component field operators of the lagrangian without changing anything to their spinor structure, and the second being on the contrary the transformation of all spinor states into their antiparticle states without changing anything to the charge and hypercharge part of the fields: the product of these operations being of course the ordinary charge conjugation. It was then remarked that if, apart from the ordinary interaction terms which are invariant for all the three kinds of conjugation, one would introduce in the lagrangian also some other term which should be invariant for charge conjugation but not for boson and spinor conjugations taken separately, this term could split the N and Ξ baryon masses and be responsible for the mixing of the two $\Sigma^+ Y$ and $Z\Sigma^-$ doublets of the Gell-Mann scheme into the Λ singlet and the Σ triplet. As a simple example for such a non-invariant term, was proposed the indirect interaction of two K-mesons with any baryon B expressed by the term (*) [4]

$$H'' = -iG_{2K}\bar{B}\gamma_\alpha B\left[\bar{K}\frac{\partial K}{\partial x_\alpha} - \frac{\partial \bar{K}}{\partial x_\alpha}K\right], \tag{1}$$

where K, defined as φ_Δ in [1], is the isospinor boson K field.

(*) A rather different attempt to explain the baryon mass differences consisting in the assumption of different coupling types in the fundamental interactions themselves has been made by KATSUMORI: *Progr. Theor. Phys.* **19**, 342 (1958).

(4) P. BUDINI, N. DALLAPORTA and L. FONDA: *Nuovo Cimento*, **2**, 316 (1958).

In the following a first approximation calculation will be made of the splitting of the nucleon and Ξ particle masses due to this interaction term. This may be obtained in a rather simple way according to a Lee model (5) already proposed in a previous paper (2,4). Let us assume as fundamental baryon a fermion B without electric charge nor hypercharge and let us clothe it with all the known meson states to obtain the real baryons. In this way the clothing of B with K's gives the two nucleon states and its clothing with $\bar{K}$'s the two Ξ states. The fundamental interaction leading from the bare baryon B to these clothed states is assumed to be of the type

$$H' = G_K[\bar{N}\Gamma BK + \bar{\Xi}\Gamma B + \text{h. c.}] + \delta m_N \bar{N}N + \delta m_\Xi \bar{\Xi}\Xi \,, \tag{2}$$

Γ is the type of coupling of the K field to baryons. As no precise indications of its type are so far available (3), it is assumed for semplicity to be a scalar.

N indicates the bare nucleon spinor field.

Ξ indicates the bare Ξ spinor field.

This interaction is responsible for the fundamental self mass contribution due to the diagrams of type a (Fig. 1) equal for nucleons and for Ξ's, as it is invariant for boson conjugation. The perturbation (1) is then supposed to act in the B state and gives the further self mass contribution (diagram b) which is not invariant for boson conjugation and gives a self mass contribution of opposite sign for nucleons and Ξ's.

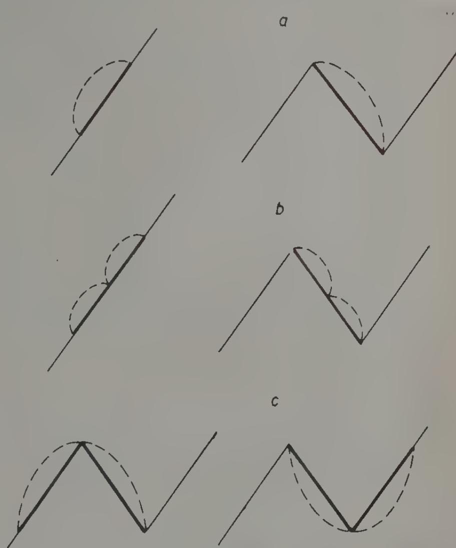

—— B —— N or Ξ K or $\bar{\text{K}}$

Fig. 1.

The following assumptions will be further made to simplify the treatment of the problem:

a) Isospin connecting the two nucleon states or the two Ξ states will be neglected: that is, our model will consider the building of either the pair neutron Ξ^0 by neutral K's, or of the pair proton Ξ^- by charged K's, without

(5) T. D. Lee: *Phys. Rev.*, **95**, 1329, (1954).

considering the transitions from the charged to neutral baryons thus formed. It is believed that, should this model be an adequate approximation to the real situation, the results would not be substantially changed by the introduction of the adequate isospin interactions.

b) Equally, self masses due to pion interactions between baryons will be disregarded, as they are assumed to give self mass contribution similar for nucleons and Ξ's.

Of course this model with such simplifications is inadequate to construct the other hyperon states, which according to the main idea of the scheme have to be considered as built either directly from B by pion additions or indirectly by a further clothing of the nucleons with K's or of the Ξ with K's, with due allowance for the combination of the two isospins of the baryon doublet and the K doublet to give the singlet Λ and the triplet Ξ. The solution of such a problem represents a more complicated step in the construction of clothed states and will not be considered in this paper.

c) Diagrams *b*) refer obviously to the case in which in the intermediate state the baryon is either in a positive or in a negative state. Of course, also the situation indicated in diagram *c*) (Fig. 1) could be considered, in which the baryon goes from a negative to a positive state or viceversa in the vertex of the interaction [1]. However, owing to the fact that the diagram is much more complicated and contains one further particle in the intermediate state, it has not been considered in the present calculation.

Of course, the proposed model is intended to be just an idealization of the much more complicated real situation and the calculation just a test if, with the very simple assumptions adopted and the first order process considered, one is led to reasonable values for the interaction constants and the cut-offs which have to be introduced in order to obtain the experimental mass difference. If this turns out to be so, there will be some hope that the model adopted may have some connection with the real physical situation and that the values obtained for these parameters to fit the NΞ mass difference could then be used to deduce some other physical quantity of the particle. According to our previous assumptions, let us take for the hamiltonian density of the system the following expression

$$H = H_0 + H' + H'' ,$$

where H' is given by (2), H'' by (1),

$$H_0 = m_N \overline{N} \cdot N + m_B \overline{B} \cdot B + \tfrac{1}{2}(\pi_K^2 + m_K K^2 + \Delta K^2) , \tag{3}$$

with $\pi_K = \dot{K}$.

We then expand the clothed baryon state $|\boldsymbol{N}\rangle$ according to the expression

$$(4)\qquad |\boldsymbol{N}\rangle = Z^{\frac{1}{2}}\Big[|N\rangle - G_K \sum_{KB} f(k_K)\,|KB\rangle - G_K \sum_{\bar{K}\bar{B}} \bar{f}(k_K)\,|K\bar{B}\rangle\Big]$$

in which $\bar{B}$ is a negative energy B particle.

The $f(k)$ refer to the positive energy states and the $\bar{f}(k)$ to the negative energy states for B.

We have then to resolve the Schrödinger equation

$$(5)\qquad H|\boldsymbol{N}\rangle = m_N|\boldsymbol{N}\rangle$$

with the condition

$$(5a)\qquad H_0|N\rangle = m_N|N\rangle\,.$$

According to the well known procedure (4), we obtain

$$(6a)\qquad \delta m_N - \sum_{KB}^{k_{K\max}} f(k_K)\langle KB|H'|N\rangle - \sum_{\bar{K}\bar{B}}^{k_{\bar{K}\max}} \bar{f}(k_{\bar{K}})\langle K\bar{B}|H'|N\rangle = 0\,,$$

$$(6b)\qquad f(k_K)\left[\omega + E_B - m_N\right] = -\frac{\langle KB|H'|N\rangle}{G_K} - \sum_{K'B'}^{k_{K\max}} f(k_K)\langle KB|H''|K'B'\rangle\,,$$

$$(6b')\qquad \bar{f}(k_K)\left[\omega - 2E_B - m_N\right] = -\frac{\langle \bar{K}\bar{B}|H'|N\rangle}{G_K} - \sum_{\bar{K}'\bar{B}'}^{k'_{\bar{K}\max}} \bar{f}(k_K)\langle \bar{K}\bar{B}|H''|\bar{K}'\bar{B}'\rangle\,.$$

From (6b) we obtain approximately

$$(7a)\qquad f(k_K) \simeq \frac{\langle KB|H'|N\rangle}{\omega + E_B - m_N}\Bigg/\left(1 + \sum_{K'B'}^{k_{K\max}} \frac{\langle KB|H''|K'B'\rangle}{\omega + E_B - m_N}\right),$$

$$(7a')\qquad \bar{f}(k_K) \simeq \frac{\langle KB|H'|N\rangle}{\omega + 2E_B - m_N}\Bigg/\left(1 + \sum_{K'B'}^{k_{K\max}} \frac{\langle \bar{K}\bar{B}|H''|\bar{K}'\bar{B}'\rangle}{\omega + 2E_B - m_N}\right),$$

and hence in (6a)

$$(8)\qquad \delta m_N \sim \sum_{KB}^{k_{K\max}} \frac{|\langle KB|H'|N\rangle|^2}{\omega + E_B - (m_N + A)} - \sum_{\bar{K}\bar{B}}^{k_{\bar{K}\max}} \frac{|\langle \bar{K}\bar{B}|H'|N\rangle|^2}{\omega + 2E_B - (m_N + A)}\,,$$

with

$$A = -\sum^{k'_{K\max}} \langle KB|H''|K'B'\rangle = -\frac{G_{2K}/4\pi}{\{1 + [p/(E_B+1)]^2\}^{\frac{1}{2}}\sqrt{\omega}}\cdot \int_0^{p'_{\max}} \frac{(\omega + \omega')(E'_B + 1) - p'^2}{[(E'_B+1)^2 + p'^2]^{\frac{1}{2}}\sqrt{\omega'}}\, p'^2 \mathrm{d}p'.$$

1433

Similar formulas are obtained for the Ξ with the systematic substitutions

$$\Xi \rightarrow \mathrm{N}$$

$$\bar{\mathrm{K}} \rightarrow \mathrm{K}$$

$$\mathrm{K} \rightarrow \mathrm{K}$$

$$\mathrm{A} \rightarrow -\mathrm{A}$$

The formula (8) depends on the following physical quantities: the bare baryon mass, the G_k interaction constant, the cut-off parameter and A. If we assume for G_k the probable values indicated by scattering experiments on K^-, we can calculate the baryon bare mass and A as a function of the cut-off parameter in order to fit the experimental $m_\Xi - m_\mathrm{N}$ values. This calculation has been done and is presented in Table I for the two values of $G_k = 1$ and $G_k = 3$.

It is seen that the bare mass is always greater for scalar coupling than the clothed mass. Moreover, for reasonable values of the cut-off parameter it is also seen that the reduction of the clothed mass is rather important and that the perturbation term A is rather conspicuous if compared to the clothed mass.

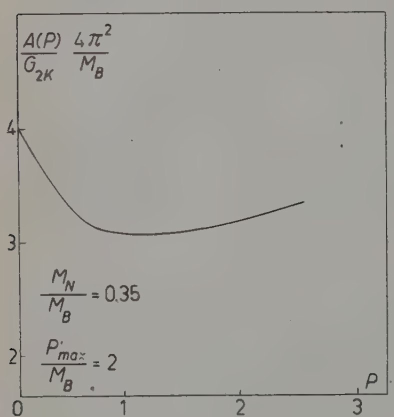

Fig. 2.

The A term consists in an integral which is also divergent and depends on the momentum p of the second meson; however, the dependence of p is rather flat and the approximation in considering A as a constant in the main calculation is justified; this dependence on p is shown for one of the cases in which it has been calculated (Fig. 2).

A has been calculated with with $p'_{\max} = k_{\max}$ and $p'_{\max} = \frac{1}{2} k'_{\max}$.

The values obtained for G_{2k} with the second cut-off are marked with a star in Table I. As was to be expected, the value of G_{2k} depends very sensibly on cut-off.

As a general remark to the values obtained in Table I, one may say that the order of magnitude of what we have called the « perturbation » whose contribution to the self mass problem is represented by the two K-meson

term A. is of the same order of magnitude as the self mass difference due to the direct K interaction given by column 3. This, of course, constitutes a limitation to the reliability of the present approach based on the consideration of the diagrams *a*) and *b*) only.

TABLE I.

cut off / bare mass	cut off / clothed mass	clothed m_N / m_{bare}	Λ / bare mass	$\dfrac{m^2_{\text{bare}}\,G_{2K}}{4\pi^2}$	$\sigma\cdot 10^{29}$ cm²	
2.2	3.66	0.6	0.72	0.166 0.473 (*)	33 268.3 (*)	$G_K = 1$
3.9	7.7	0.6	0.6	0.0344 0.115 (*)	6.55 66.81 (*)	
1.2	2.4	0.5	0.24	0.283 1.43 (*)	45.2 11.58 (*)	
1.8	4.5	0.4	0.20	0.082 0.248 (*)	1.67 15.26 (*)	$G_K = 3$
2	5.7	0.35	0.175	0.039 — 0.133 (*)	0.41 4.74 (*)	

(*) This value was obtained with a cut-off for Λ which is $\frac{1}{2}$ of the value indicated.

The assumption of a direct two K-mesons interaction with nucleons has as a direct consequence that, should this assumption be true, one should expect a contribution to the $K^{\pm}$ nucleon scattering due to this direct two K interaction. In fact, one can easily evaluate the cross-section for scattering due to such an interaction and one finds, in non-relativistic first order approximation

$$\sigma = 4\,\frac{G^2_{2K}}{4p}\left(\frac{m_N\, m_K}{m_N + m_K}\right)^2. \tag{9}$$

If we put in this formula the G_{2K} value obtained from the fitting of the NΞ mass difference, one finds for the cross-section the values given in Table I (col. 6).

The values so obtained are much too small in respect to the experimental value of about 15 mb. This is an indication that, should in fact the direct two K interaction be responsible for the NΞ mass splitting, the strength necessary for it to obtain this splitting should not be great enough to make this

process particularly important in the K nucleon scattering phenomenon. Therefore, the present assumption for explaining the NΞ mass difference is quite consistent with K^+ nucleon scattering and its ordinary tentative explanation, as in any case the direct two K interaction postulated to explain the NΞ mass difference would account for a small amount of the K nucleon scattering.

RIASSUNTO

Si fa un tentativo di calcolare la differenza di massa NΞ, usando un modello di Lee consistente in un barione nudo B privo di carica elettrica e di ipercarica che può essere rivestito con mesoni K, dando il nucleone, o con mesoni $\bar{K}$, dando la Ξ. La differenza di massa tra questi due stati è attribuita ad una perturbazione dipendente dalla stranezza consistente nell'emissione e nell'assorbimento simultaneo di due mesoni K. Si discute l'ordine di grandezza di questa perturbazione per ottenere la differenza di massa sperimentale. I valori così ottenuti sono tali da rendere questa interazione a due K di piccola importanza nei processi di scattering K nucleone.

1412

IL NUOVO CIMENTO Vol. XII, N. 6 16 Giugno 1959

Observations of Hyperfragments.

F. Breivik, O. Skjeggestad and S. O. Sörensen
Institute of Physics, University of Oslo - Blindern

A. Solheim
The Norwegian Institute of Technology - Trondheim

(ricevuto il 18 Febbraio 1959)

Summary. — The disintegration of 23 hypernuclei is described, involving 7 mesonic and 16 non mesonic decays. An event is observed which possibly represents the mesonic decay of a $^6He_\Lambda$ hypernucleus according to the scheme $^6He_\Lambda \to {}^4He + {}^2H + \pi^-$ with $B_\Lambda(^6He_\Lambda) = (3.8 \pm 0.7)$ MeV.

1. – Introduction.

A stack of stripped Ilford G-5 emulsions, each 600 μm thick, has been exposed at high altitudes by means of free balloons. An additional stack was exposed to 5.7 GeV protons from the Berkeley Bevatron. In scanning for stable heavy fragments from nuclear disintegrations, 23 events involving hypernucleus decay have been observed. Most of the scanning in the present investigation was performed under relatively low magnification ($\times 10$, $\times 25$), a method which results in a tendency to lose hypernuclei of hydrogen. Furthermore, a number of double stars have been observed with short interconnecting tracks representing either hypernuclei or ejected σ mesons. These events have been excluded from the present material.

The charges of the tracks occurring in the present investigation have been determined by combining the following methods:

1) Measurements of the total ionization of the tracks by the « planimeter method » previously described (1).

(1) O. Skjeggestad, A. Solheim and S. O. Sörensen: *Phys. Rev.*, **106**, 1280 (1957).

2) Conservation of charge in the decay.

3) An inspection of the general appearance of the tracks (scattering, grain density, δ-ray density, etc.).

We have investigated each hypernucleus disintegration in detail. In most cases, however, an unambiguous identification of the hypernucleus and determination of the binding energy of the Λ^0 particle could not be made for either one of two reasons:

a) The visible kinetic energy, plus the energy required by one neutron to give momentum balance, was not consistent with the energy release of a bound Λ^0 particle, thus indicating the emission of two or more neutrons.

b) One of the particles emitted in the disintegration left the stack of plates before being brought to rest in the emulsion, thus making an exact analysis impossible if in addition a neutron is emitted.

In all calculations we have used the range-energy relation given by BARONI *et al.* (2). In the determination of the binding energies we have used the mass values for light nuclei given by BETHE and MORRISON (3). We have used $Q_\Lambda = 37.2$ MeV for the Q value in the decay of a free Λ^0 particle (4).

2. – Event 1. Observation of a possible ${}^6\mathrm{He}_\Lambda$ hypernucleus.

From a nuclear disintegration of type 20+0 p a particle is emitted at an angle of 84°.2 with the direction of the primary. The particle comes to rest after 191 μm and gives rise to a three prong star A, B, C, Fig. 1. The prong C shows the characteristic multiple scattering and change in grain density of a π-meson. It stops after traversing 16 548 μm of emulsion, and a low energy electron track is associated with its ending, indicating that the particle was a negative π-meson. Further characteristics of the secondary star are given in Table I.

The tracks A, B and C are coplanar within the error of measurement. This strongly suggests that no neutral particle was emitted in the decay. Assuming this to be the case, and track A = ^{4}He and track B = ^{2}H, a mo-

(2) G. BARONI, C. CASTAGNOLI, G. CORTINI, C. FRANZINETTI and A. MANFREDINI: *Bureau of Standards CERN Bulletin* no. 9 (unpublished).

(3) H. BETHE and P. MORRISON: *Elementary Nuclear Theory* (London, 1956).

(4) W. E. SLATER: *Thesis* (The University of Chicago, 1958).

TABLE I. – *Relevant data for the secondary star* A, B, C.

Track	A	B	C
Range in microns	9.3	17.3	16 548
Angle with the direction of C, projected on the plane of the emulsion	$(25.0 \pm 3.0)^\circ$	$(70.8 \pm 1.0)^\circ$	0
Angle of dip with the plane of the emulsion	$(20.2 \pm 2.0)^\circ$ down	$(27.8 \pm 2.0)^\circ$ up	$(4.4 \pm 1.0)^\circ$ up

mentum-balance of (1 ± 6) MeV/c is obtained. The event is therefore interpreted as:

$$ {}^6\mathrm{He}_\Lambda \to {}^4\mathrm{He} + {}^2\mathrm{H} + \pi^- + Q \,, \tag{1}$$

where $Q = 35.6$ MeV. The binding energy B_Λ (${}^6\mathrm{He}_\Lambda$) is calculated to be: $Q_\Lambda + B$ (deuteron) $- Q = (3.8 \pm 0.7)$ MeV.

As no uniquely defined examples of ${}^6\mathrm{He}_\Lambda$ hypernuclei have been reported, the event was carefully investigated for alternative possibilities of interpretation.

Measurements of the total ionization of the track producing the star A, B, C using the method described by SKJEGGESTAD *et al.* [1] show that the particle most probably carried a charge $Z = 2$. Further, the Q value 35.6 MeV is very near to the Q value 37.2 MeV characteristic for the decay of a free Λ^0 particle. This very strongly suggests that the track was due to a hypernucleus of helium, and we regard the interpretation of the event as the nuclear capture of a negative K particle or hyperon as very remote.

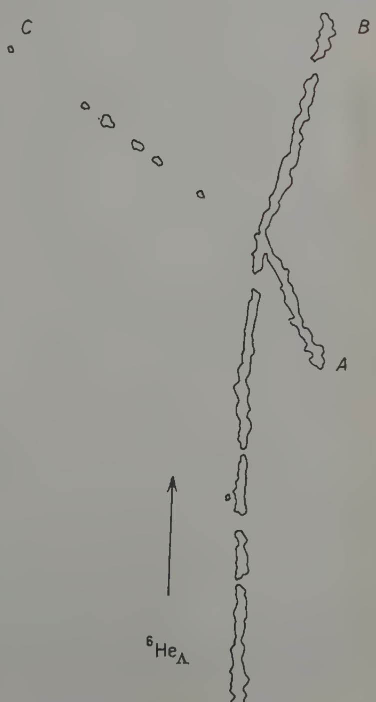

Fig. 1. – Projection drawing of a hypernucleus which decays into two heavily ionizing particles A and B and a negative π-meson C. The event possibly represents the mesonic decay of a ${}^6\mathrm{He}_\Lambda$ hypernucleus according to the scheme ${}^6\mathrm{He}_\Lambda \to {}^4\mathrm{He} + {}^2\mathrm{H} + \pi^-$ with $B_\Lambda({}^6\mathrm{He}_\Lambda) = (3.8 \pm 0.7)$ MeV.

1145

Going through all the permutations of the assignments of charge and mass numbers to the prongs A and B, no other three body hypernucleus decay could give momentum balance. The nearest possible alternative interpretation is the decay of a ${}^4\mathrm{He}_\Lambda$ hypernucleus according to:

$$(2) \qquad {}^4\mathrm{He}_\Lambda \to {}^4\mathrm{He} + {}^1\mathrm{H} + \pi^- .$$

This gives a momentum unbalance of (17 ± 6) MeV/c which makes the process (2) unprobable compared to (1). The interpretation (2) however, cannot be excluded, particularly as it leads to the correct binding energy $B_\Lambda({}^4\mathrm{He}_\Lambda) = (2.1 \pm 0.7)$ MeV.

For the event under discussion all hypernucleus disintegration schemes with the emission of one or more neutrons give negative binding energies for the Λ^0 particle and are therefore excluded.

The decay mode (1) resulting in an α-particle and a deuteron formed by the p neutron in the ${}^5\mathrm{He}$ « core » and the decay proton of the Λ^0 particle is a very probable type of decay for the hypothetical ${}^6\mathrm{He}_\Lambda$ hypernucleus. Further, the binding energy $B_\Lambda({}^6\mathrm{He}_\Lambda) = (3.8 \pm 0.7)$ MeV is reasonable when compared with the corresponding well established values for the neighbouring hypernuclei (5) $B_\Lambda({}^5\mathrm{He}_\Lambda) = (2.8 \pm 0.1)$ MeV and $B_\Lambda({}^7\mathrm{Li}_\Lambda) = (5.3 \pm 0.3)$ MeV.

If this event represents a genuine example of a ${}^6\mathrm{He}_\Lambda$ hypernucleus decay, the following conclusions can be drawn:

1) Since the « core » nucleus ${}^5\mathrm{He}$ in ${}^6\mathrm{He}_\Lambda$ is extremely unstable with a lifetime $\sim 2.4 \cdot 10^{-21}$ s, the present observation seems to indicate that the presence of a Λ^0 particle sufficiently alters the nuclear configuration to permit an additional neutron to be bound to an α-particle.

2) Owing to the additional Coulomb repulsions, the hypothetical ${}^6\mathrm{Li}$ hypernucleus should have a B_Λ value less by ~ 1 MeV (6) than that of a ${}^6\mathrm{He}_\Lambda$, *i.e.* according to the present observation $B_\Lambda({}^6\mathrm{Li}_\Lambda) \sim (2.8 \pm 0.7)$ MeV. This, however, is very near the observed value $B_\Lambda({}^5\mathrm{He}_\Lambda) = (2.8 \pm 0.1)$ MeV (5). The present observation therefore throws considerable doubt on the stability of the ${}^6\mathrm{Li}_\Lambda$ hypernucleus against the decay:

$$(3) \qquad {}^6\mathrm{Li}_\Lambda \to {}^5\mathrm{He}_\Lambda + {}^1\mathrm{H} .$$

3. – Three measurable mesonic decays.

In three events the mode of disintegration was such that an analysis of the event could be made. A detailed description of these follows.

---

(5) R. Levi-Setti, W. E. Slater and V. L. Telegdi: *Proc. 7th Annual Rochester Conf.* (April 1957), recomputation and addition of data (circulating preprint) (May 1958).

(6) R. H. Dalitz and B. W. Downs: *Phys. Rev.*, **111**, 967 (1958).

3·1. *Event* 2. – From a nuclear disintegration of type $28+0p$ a slow unstable particle F is emitted at an angle of $52^\circ.1$ relative to the direction of the primary. The particle comes to rest after 405 μm and gives rise to a star with three prongs A, B and C. The prong C shows the characteristic multiple scattering of a π-meson, and leaves the stack of emulsions after traversing 11 600 μm. Measurements of the multiple scattering of the track C gives that the π-meson was ejected with kinetic energy (29.9 ± 3.0) MeV. Further characteristics of the secondary star are given in Table II.

TABLE II. – *Relevant data for the secondary star* A, B, C.

Track	A	B	C
Range in microns	91	3.8	11 600
Angle with the direction of C, measured clockwise projected on the plane of the emulsion	$(231.6 \pm 1.0)^\circ$	$(146.0 \pm 1.0)^\circ$	0
Angle of dip with the plane of the emulsion	(56.0 ± 2.0) down	(34.5 ± 4.0) up	(13.8 ± 2.0) up

Going through all the permutations of the assignments of charge and mass numbers to the prongs A and B, no three body hypernucleus decay could give momentum balance.

Assuming the emission of a single neutron in the disintegration, the only possible hypernucleus decay scheme is:

$$ {}^{3}\mathrm{H}_{\Lambda} \to {}^{1}\mathrm{H} + {}^{1}\mathrm{H} + \mathrm{n} + \pi^{-} + Q \,, \tag{4}$$

where $Q = (35.4 \pm 3.0)$ MeV and the binding energy of the Λ^0 particle is $B_\Lambda({}^3\mathrm{H}_\Lambda) = -(0.4 \pm 3.0)$ MeV.

The particle F has an angle of dip of $(37.9 \pm 2.0)^\circ$ in the emulsion, making measurements of ionization of the track very difficult. The general appearance of the track, however, is consistent with the particle being of unit charge.

3·2. *Event* 3. – From a nuclear disintegration of type $14+1p$ a slow unstable particle F is ejected at an angle of $80^\circ.2$ relative to the direction of the primary. The particle comes to rest after 23 μm, and gives rise to a star with three prongs A, B and C. The prong C shows the characteristic multiple scattering and change in grain density of a π-meson. It ends, after traversing 8 210 μm of emulsion, in a σ star, indicating that the particle was a negative π-meson. Further characteristics of the secondary star are given in Table III.

Going through all the permutations of the assignments of charge and mass numbers to the prongs A and B, no three body hypernucleus decay could give momentum balance.

TABLE III. – *Relevant data for the secondary star* A, B, C.

Track	A	B	C
Range in microns	141	2	8210
Angle with the direction of C, measured clockwise, projected on the plane of the emulsion	$(44.6 \pm 1.0)°$	$(216.5 \pm 5.0)°$	0
Angle of dip with the plane of the emulsion	$(21.7 \pm 2.0)°$	Not measurable	$(7.9 \pm 2.0)°$

Assuming the emission of a single neutron in the disintegration, the only possible hypernucleus decay schemes are:

$$^{3}\mathrm{H}_{\Lambda} \to {}^{1}\mathrm{H} + {}^{1}\mathrm{H} + \mathrm{n} + \pi^{-} + Q_1 \,, \tag{5}$$

where $Q_1 = 35.6$ MeV and the binding energy of the Λ^0 particle is $B_{\Lambda}(^{3}\mathrm{H}_{\Lambda}) = -(0.6 \pm 0.7)$ MeV, and

$$^{9}\mathrm{Li}_{\Lambda} \to {}^{7}\mathrm{Li} + {}^{1}\mathrm{H} + \mathrm{n} + \pi^{-} + Q_2 \,, \tag{6}$$

where $Q_2 = 27.9$ MeV and $B_{\Lambda}(^{9}\mathrm{Li}_{\Lambda}) = (7.4 \pm 0.7)$ MeV.

The ionization and multiple scattering of F strongly suggest that the particle producing the track had unit charge. We therefore regard the event as representing the decay of a $^{3}\mathrm{H}_{\Lambda}$ hypernucleus, and consider the alternative interpretation (6) as very remote.

3·3. *Event* 4. – From a nuclear disintegration 7+0p a slow unstable particle F is ejected at an angle of 66°.1 relative to the direction of the primary. The particle comes to rest after 251 μm and gives rise to a star with three prongs A, B and C. The prong C shows the characteristic multiple scattering and change in grain density of a π-meson. It ends, after traversing 11243 μm of emulsion, in a σ star, indicating that the particle was a negative π-meson. Further characteristics of the secondary star are given in Table IV.

Going through all the permutations of the assignments of charge and mass numbers to the prongs A and B, the only two alternatives consistent with momentum balance and reasonable binding energies for the Λ^0 particle are $\mathrm{A} = {}^{3}\mathrm{He}$ or $^{4}\mathrm{He}$ and $\mathrm{B} = {}^{1}\mathrm{H}$, leading to the two possible decay schemes:

$$^{4}\mathrm{He}_{\Lambda} \to {}^{3}\mathrm{He} + \mathrm{H}^{1} + \pi^{-} + Q \,, \tag{7}$$

with $Q = 35.7$ MeV and $B_{\Lambda}(^{4}\mathrm{He}_{\Lambda}) = (1.5 \pm 0.7)$ MeV, and

$$^{5}\mathrm{He}_{\Lambda} \to {}^{4}\mathrm{He} + {}^{1}\mathrm{H} + \pi^{-} + Q \,, \tag{8}$$

with $Q = 35.6$ MeV and $B_{\Lambda}(^{5}\mathrm{He}_{\Lambda}) = (1.6 \pm 0.7)$ MeV.

TABLE IV. – *Relevant data for the secondary star* A, B, C.

Track	A	B	C
Range in microns	2	590	11243
Angle with the direction of C, measured clockwise, projected on the plane of the emulsion	$(0.0 \pm 5.0)^\circ$	$(3.8 \pm 1.0)^\circ$	0
Angle of dip with the plane of the emulsion	Not measurable	$(24.8 \pm 2.0)^\circ$ up	$(21.2 \pm 2.0)^\circ$ down

Both alternatives, (7), (8), are in agreement with the now well established binding energies of the Λ^0 particle in the $^4\mathrm{He}_\Lambda$ and $^5\mathrm{He}_\Lambda$ hypernuclei (5).

3·4. *Events* 5-23. – 19 cases of hypernucleus decay were observed where no reasonable values for the binding energy of the Λ^0 particle could be obtained. The relevant data for the 19 events are summarized in Table V and Table VI.

TABLE V. – *Characteristics of the hyperfragments of events* 5-23.

Event	Primary star	Range in microns	Charge	Angle with the incident direction of the star-primary
5	8+0	75	2	—
6	24+1p	46	2	34.0°
7	6+0	194	2	—
8	12+0p	66	1, 2	68.1°
9	15+0p	110	2	95.9°
10	13+0p	66	4, 5	61.5°
11	19+0p	347	4, 5	128.4°
12	16+0p	97	3	73.2°
13	17+0p	280	2	28.6°
14	14+0p	70	2	66.5°
15	21+0p	73	3	82.5°
16	23+1p	49	4, 5, 6	54.6°
17	22+0p	46	3, 4	65.0°
18	13+0p	48	4, 5	59.0°
19	20+4p	93	4	77.0°
20	21+6p	56	3	26.0°
21	26+0p	125	4, 5, 6	62.7°
22	19+2p	63	4, 5	63.5°
23	20+0p	48	3	153.8°

TABLE VI. – *Relevant data for the secondary stars in events 5-23.*

Event	Track	Range in microns	Charge	Angle with the direction of A projected on the plane of the emulsion	Angle of dip with the plane of the emulsion	Identity
5	A	14235	1	0	$(12.7\pm2.0)°$ up	p, d, t
	B	231	1	$(98.4\pm1.0)°$	$(0\ \ \pm2.0)°$	p, d, t
6	A	> 2300	1			p, d, t
	B	0.5	?			?
7	A	114	1	0	$(40.0\pm2)°$ down	p, d, t
	B	370	1	$(172.0\pm1.0)°$	$(42.3\pm2)°$ down	p, d, t
	C	87	1	$(195.6\pm1.0)°$	$(53.2\pm2)°$ up	p, d, t
	D	> 5580	1	$(348.0\pm1.0)°$	$(36.9\pm2)°$ up	π
8	A	172	1	0	$(52.0\pm2)°$ down	p, d, t
	B	2	1, 2	$(127.4\pm1.0)°$	$(0\ \ \pm5)°$	p, d, t, ^{3}He, ^{4}He
	C	> 1000	1	$(228.4\pm1.0)°$	$(53.3\pm2)°$ up	π, p, d, t
9	A	67	1	0	$(6.6\pm2)°$ down	p, d, t
	B	$4\div8$	1	$(0.0\pm1.0)°$	?	p, d, t
	C	> 2500	1	$(177.0\pm1.0)°$	$(17.4\pm2)°$ down	π
10	A	63	1, 2	0	$(39.4\pm2)°$ up	p, d, t, ^{3}He, ^{4}He
	B	2396	1	$(175.2\pm1.0)°$	$(26.5\pm2)°$ down	p, d, t
	C	23	1, 2	$(181.6\pm5.0)°$	$(84.8\pm4)°$ up	p, d, t, ^{3}He, ^{4}He
	D	1103	1	$(253.6\pm1.0)°$	$(35.6\pm2)°$ down	p, d, t
11	A	3604	1	0	$(41.6\pm2)°$ up	p, d, t
	B	1877	1	$(146.8\pm1.0)°$	$(56.0\pm2)°$ down	p, d, t
	C	2	?	$(343.5\pm3.0)°$	?	recoil
12	A	> 3751	1	0	$(24.7\pm2)°$ down	p, d, t
	B	1421	1	$(1.7\pm1.0)°$	$(33.4\pm2)°$ down	p, d, t
	C	7220	1	$(173.4\pm1.0)°$	$(25.1\pm2)°$ up	p, d, t
13	A	1034	1	0	$(0\ \ \pm2)°$	p, d, t
	B	2651	1	$(41.8\pm1.0)°$	$(72.0\pm2)°$ up	p, d, t
14	A	1845	1	0	$(21.1\pm2)°$ down	p, d, t
	B	> 2544	1	$(90.1\pm1.0)°$	$(60.0\pm2)°$ down	p, d, t
15	A	318	1	0	$(47.2\pm2)°$ up	p, d, t
	B	51	1	$(4.2\pm1.0)°$	$(42.4\pm2)°$ up	p, d, t
	C	> 2376	1	$(165.8\pm1.0)°$	$(54.1\pm2)°$ down	p, d, t

TABLE VI (*continued*).

Event	Track	Range in microns	Charge	Angle with the direction of A projected on the plane of the emulsion	Angle of dip with the plane of the emulsion	Identity
16	A	71	1, 2	0	$(31.2 \pm 2)^\circ$ down	p, d, t, ^{3}He, ^{4}He
	B	14	?	$(29.1 \pm 1.0)^\circ$	$(53.5 \pm 2)^\circ$ up	?
	C	21	?	$(52.9 \pm 1.0)^\circ$	$0 \quad \pm 2)^\circ$	?
17	A	51	1	0	$(21.4 \pm 2)^\circ$ up	p, d, t
	B	79	1	$(97.7 \pm 1.0)^\circ$	$(28.1 \pm 2)^\circ$ up	p, d, t
	C	13	?	$(153.3 \pm 1.0)^\circ$	$(82.7 \pm 4)^\circ$ up	?
18	A	60	1, 2	0	$(52.6 \pm 2)^\circ$ up	p, d, t, ^{3}He, ^{4}He
	B	16	1, 2	$(71.8 \pm 1.0)^\circ$	$(8.1 \pm 2)^\circ$ up	p, d, t, ^{3}He, ^{4}He
	C	4 860	1	$(170.2 \pm 1.0)^\circ$	$(17.6 \pm 2)^\circ$ down	p, d, t
19	A	131	2	0	$(63.2 \pm 2)^\circ$ down	^{3}He, ^{4}He
	B	1 027	1	$(83.0 \pm 1.0)^\circ$	$(32.3 \pm 2)^\circ$ down	p, d, t
	C	> 5 600	1	$(206.3 \pm 1.0)^\circ$	$(48.6 \pm 2)^\circ$ up	p, d, t
20	A	4	?	0	$(47.4 \pm 5)^\circ$ down	?
	B	11	1, 2	$(180.0 \pm 5.0)^\circ$	$(21.3 \pm 3)^\circ$ down	^{3}He, ^{4}He
	C	952	1	$(215.3 \pm 5.0)^\circ$	$(24.8 \pm 2)^\circ$ down	p, d, t
21	A	55	2, 3	0	$(32.5 \pm 2)^\circ$ down	He, Li
	B	97	1, 2	$(35.1 \pm 1.0)^\circ$	$(15.3 \pm 2)^\circ$ down	p, d, t, ^{3}He, ^{4}He
	C	4 348	1	$(45.3 \pm 1.0)^\circ$	$(14.9 \pm 2)^\circ$ up	p, d, t
22	A	6	1, 2	0	$(23.7 \pm 3)^\circ$ up	p, d, t, ^{3}He, ^{4}He
	B	335	1	$(95.0 \pm 1.0)^\circ$	$(5.4 \pm 2)^\circ$ up	p, d, t
	C	8	1, 2	$(105.1 \pm 1.0)^\circ$	$(8.6 \pm 3)^\circ$ down	p, d, t, ^{3}He, ^{4}He
	D	> 5 447	1	$(265.4 \pm 1.0)^\circ$	$(39.8 \pm 2)^\circ$ down	p, d, t
23	A	18	?	0	$(67.9 \pm 2)^\circ$ up	?
	B	74	1	$(171.5 \pm 1.0)^\circ$	$(40.4 \pm 4)^\circ$ down	p, d, t
	C	7 105	1	$(220.6 \pm 1.0)^\circ$	$(17.2 \pm 2)^\circ$ up	p, d, t

* * *

The authors are indebted to Professor J. HOLTSMARK and Professor R. TANGEN for providing laboratory facilities. Some of the plates used in the present investigation were supplied by the Institute of Theoretical Physics, Copenhagen, for which we thank Professor J. BÖGGILD. We are further in-

debted to Professor C. F. POWELL, University of Bristol, for arranging balloon exposure and to Dr. W. H. BARKAS, Radiation Laboratory of Berkeley, California, for giving us the proton exposed emulsions. We thank the Royal Norwegian Council for Scientific and Industrial Research for financial support.

RIASSUNTO (*)

Si descrive la disintegrazione di 23 ipernuclei di cui 7 sono decadimenti mesonici e 16 non mesonici. È stato osservato un evento che probabilmente corrisponde al decadimento mesonico di un ipernucleo $^6He_\Lambda$ secondo lo schema $^6H_\Lambda \to {}^4He + {}^2H + \pi^-$ con $B_\Lambda(^6He_\Lambda) = (3.8 \pm 0.7)$ MeV.

(*) *Traduzione a cura della Redazione.*

IL NUOVO CIMENTO Vol. XII, N. 6 16 Giugno 1959

On the Asymptotic and Causality Conditions in Quantum Field Theory.

F. Kaschluhn

Joint Institute for Nuclear Research, Laboratory of Theoretical Physics - Dubna

(ricevuto il 18 Febbraio 1959)

Summary. — It is shown that the mathematical proceeding of Lehmann, Symanzik and Zimmermann leads necessarily to a causal field theory in which the commutators of the field operators vanish for space-like distances. In order to study this fact from a more general point of view we use extensively variational derivatives of the S-matrix with respect to the free-field operators as proposed by Bogoljubov *at al.* The manner in which Lehmann, Symanzik and Zimmermann apply the asymptotic condition is investigated in more detail. Concluding we make some general statements about the concept of causality in quantum field theory. It is indicated that only the causality condition in the form used by Bogoljubov *et al.* (and not the commutator condition) is sufficient for a general approach to quantum field theory as needed, for instance, in the theory of dispersion relations.

1. – Introduction.

Lehmann, Symanzik and Zimmermann [1] have recently discussed the concept of a causal S-matrix using retarded multiple commutators of field operators. In their discussion they derived the following commutation relation for the field operator $\varphi(x)$ of a real scalar Bose-field with the destruction operator $a_{\text{in}}(\boldsymbol{q})$ of the corresponding incoming field [*]

$$(1)\qquad [a_{\text{in}}(\boldsymbol{q}), \varphi(x)] = \frac{1}{(2\pi)^{\frac{3}{2}}}\int \mathrm{d}y\, \frac{\exp[iqy]}{\sqrt{2q^0}}\,(\Box_y - m^2)\, \overline{R}\,(x, y)\,, \qquad q^0 = +\sqrt{m^2 + \boldsymbol{q}^2}\,,$$

[1] H. Lehmann, K. Symanzik and W. Zimmermann: *Nuovo Cimento*, 6, 319 (1957).

[*] We use a slightly different notation as in [1].

where $\overline{R}(x, y)$ is the retarded commutator

$$\overline{R}(x, y) = -i\theta(x-y)[\varphi(x), \varphi(y)] \tag{2}$$

(they indeed derived expressions for generalized R-products of n field operators, however, for our purposes (1), (2) are sufficient). In their derivation they assumed that $\varphi(x)$ may also be a non-causal field operator which does not necessarily satisfy the causality condition in the commutator form

$$[\varphi(x), \varphi(y)] = 0 \qquad \text{if } x \sim y, \tag{3}$$

where $x \sim y$ means that $(x-y)$ is space-like. However, it is easily shown that the operator $\varphi(x)$ in (1), (2) has *necessarily* to be a *causal* operator which satisfies (3). For the purposes of a more general and—as far as possible—complete discussion of this fact we derive in Section **2** some commutation relations of the S-matrix with the free-field operators in terms of variational derivatives of the S-matrix with respect to these operators as proposed by BOGOLJUBOV *et al.* [2]. However, we distinguish explicitly between incoming and outgoing fields. In Section **3** we show that the application of the asymptotic condition as performed by LEHMANN, SYMANZIK and ZIMMERMANN leads immediately to a causal field theory. This fact is investigated in more detail which leads us to the result that their application of the asymptotic condition is not sufficiently defined. The function $\theta(x-y)$ in (2), (1), for instance, is quite arbitrary: it has only to fulfil the condition $\theta(x-y) = 1$ if $y^0 = -\infty$ and $\theta(x-y) = 0$ if $y^0 = +\infty$ with vanishing derivatives at these limits. In Section **4** we make some general statements about the concept of causality in quantum field theory. The investigations indicate that only the causality condition in the form used by BOGOLJUBOV and co-workers (and not the commutator condition (3)) is sufficient for a general approach to quantum field theory as needed, for instance, in the theory of dispersion relations.

2. – S-matrix and causality condition.

We assume the following structure for the S-matrix [2] [*]

$$S = \sum_{n=0}^{\infty} \int \mathrm{d}x_1 \dots \mathrm{d}x_n \, f_n(x_1, \dots, x_n) : \varphi_{\text{in}}(x_1) \dots \varphi_{\text{in}}(x_n) : \tag{4}$$

[2] N. N. BOGOLJUBOV, B. V. MEDVEDEV and M. K. POLIVANOV: *Problems of the Theory of Dispersion Relations* (Moscow, 1958); abridged translation in German in *Fortschr. d. Phys.*, **6**, 169 (1958). N. N. BOGOLJUBOV: *Isv. Akad. Nauk SSSR, Ser. Fiz.*, **19**, 237 (1955); N. N. BOGOLJUBOV and D. V. SHIRKOV: *Usp. Fiz Nauk*, **55**, 149 (1955); German translation in *Fortschr. d. Phys.*, **3**, 439 (1955).

[*] We remark that the elements of S with respect to states with a finite number of particles are represented by finite sums, so that no problems of convergence arise.

where $\varphi_{in}(x)$ describes the incoming particles

$$(5) \qquad (\Box - m^2)\varphi_{in}(x) = 0\,, \qquad [\varphi_{in}(x), \varphi_{in}(y)] = i\Delta(x-y)\,.$$

We write

$$(6) \qquad \begin{cases} \varphi_{in}(x) = \dfrac{1}{(2\pi)^{\frac{3}{2}}}\displaystyle\int \dfrac{d\boldsymbol{q}}{\sqrt{2q^0}}\{\exp[iqx]a^*_{in}(\boldsymbol{q}) + \exp[-iqx]a_{in}(\boldsymbol{q})\}\,, \\ q^0 = +\sqrt{m^2 + \boldsymbol{q}^2}\,, \end{cases}$$

where

$$(7) \qquad [a_{in}(\boldsymbol{q}), a^*_{in}(\boldsymbol{q}')] = \delta(\boldsymbol{q} - \boldsymbol{q}')\,, \qquad [a_{in}(\boldsymbol{q}), a_{in}(\boldsymbol{q}')] = 0\,.$$

Then it follows immediately from the assumption (4) and (6) and (7)

$$(8) \qquad \begin{cases} [a_{in}(\boldsymbol{q}), S] = \dfrac{1}{(2\pi)^{\frac{3}{2}}}\displaystyle\int dx \dfrac{\exp[iqx]}{\sqrt{2q^0}} \dfrac{\delta S}{\delta\varphi_{in}(x)}\,, \\ [S, a^*_{in}(\boldsymbol{q})] = \dfrac{1}{(2\pi)^{\frac{3}{2}}}\displaystyle\int dx \dfrac{\exp[-iqx]}{\sqrt{2q^0}} \dfrac{\delta S}{\delta\varphi_{in}(x)}\,, \\ q^0 = +\sqrt{m^2 + \boldsymbol{q}^2}\,. \end{cases}$$

Of course, we assume

$$(9) \qquad SS^\dagger = S^\dagger S = 1\,.$$

Further we introduce the field operator $\varphi_{out}(x)$ which describes the outgoing particles

$$(10) \qquad \varphi_{out}(x) = S^\dagger\varphi_{in}(x)S\,.$$

Because of (9) it is possible to write (4) in the same manner for the outgoing fields

$$(11) \qquad S = \sum_{n=0}^{\infty}\int dx_1 \dots dx_n f_n(x_1, \dots, x_n) : \varphi_{out}(x_1) \dots \varphi_{out}(x_n) :\,.$$

The relations (5)–(8) are valid also for the outgoing fields without any change (replace only the index in by out).

Following Bogoljubov we define the current operator by (*) (**)

$$(12) \qquad j(x) = iS^\dagger \frac{\delta S}{\delta\varphi_{in}(x)} = i\frac{\delta S}{\delta\varphi_{out}(x)} S^\dagger\,.$$

(*) Strictly speaking Bogoljubov *et al.* use only the second expression for the outgoing field.

(**) Another definition for a current would be $j'(x) = i[\delta S/\delta\varphi_{in}(x)]S^\dagger$, however, because of $[\delta S/\delta\varphi_{in}(x)]S^\dagger = S[\delta S/\delta\varphi_{out}(x)]S^\dagger S^\dagger$ this definition seems not very useful (compare also (21), where such an expression does not appear).

1455

Because of (10) the two expressions on the right define indeed the same $j(x)$ since for the S-matrix we have (4) and (9). The last implies

$$j^\dagger(x) = -i \frac{\delta S^\dagger}{\delta\varphi_{in}(x)} S = -iS \frac{\delta S^\dagger}{\delta\varphi_{out}(x)} = j(x) . \tag{13}$$

Then we get

$$\frac{\delta j(x)}{\delta\varphi_{in}(y)} = iS^\dagger \frac{\delta^2 S}{\delta\varphi_{in}(y)\,\delta\varphi_{in}(x)} + ij(y)j(x) , \tag{14}$$

$$\frac{\delta j(x)}{\delta\varphi_{out}(y)} = i \frac{\delta^2 S}{\varphi_{out}\,\delta(y)\,\delta\varphi_{out}(x)} S^\dagger + ij(x)j(y) . \tag{14'}$$

Because of

$$\frac{\delta^2 S}{\delta\varphi_{\substack{in\\out}}(y)\,\delta\varphi_{\substack{in\\out}}(x)} = \frac{\delta^2 S}{\delta\varphi_{\substack{in\\out}}(x)\,\delta\varphi_{\substack{in\\out}}(y)} , \tag{15}$$

it follows

$$\frac{\delta j(x)}{\delta\varphi_{\substack{in\\out}}(y)} - \frac{\delta j(y)}{\delta\varphi_{\substack{in\\out}}(x)} = \mp i[j(x), j(y)] . \tag{16}$$

Following BOGOLJUBOV we define a causal S-matrix by

$$\frac{\delta j(x)}{\delta\varphi_{in}(y)} = 0 , \qquad \text{if } y \gtrsim x \tag{17}$$

$$\frac{\delta j(x)}{\delta\varphi_{out}(y)} = 0 , \qquad \text{if } y \lesssim x \tag{17'}$$

where $y \gtrsim x$ respectively $y \lesssim x$ means that y is later respectively earlier than x or $(x-y)$ is space-like. From (16) the causality condition follows then in the usual commutator form

$$[j(x), j(y)] = 0 \qquad \text{if } x \sim y \tag{18}$$

and also the representation

$$\frac{\delta j(x)}{\delta\varphi_{\substack{in\\out}}(y)} = i \begin{Bmatrix} -\theta(x-y) \\ \theta(y-x) \end{Bmatrix} [j(x), j(y)] . \tag{19}$$

We remark that it is not possible to derive from (18) the condition (17), (17') or the representation (19) (compare (14) and (16); from (16), for instance, it follows only

$$\frac{\delta j(x)}{\delta\varphi_{\substack{in\\out}}(y)} = \frac{\delta j(y)}{\delta\varphi_{\substack{in\\out}}(x)} , \qquad \text{for } x \sim y ;$$

see also the discussion in Section 4). On the other hand the representation (19) yields immediately the causality condition in the form (17), (17′) since it follows from (19)

$$\frac{\delta j(x)}{\delta\varphi_{\substack{\text{in}\\ \text{out}}}(y)} = 0\,, \qquad \text{for } y \gtrless x, \tag{20}$$

and for the reason of covariance that has to held also for $x \sim y$. The last statement yields immediately from (19) also the causality condition in the commutator form (18) (without using any further relation). Thus we arrive at the result: *the representation* (19) *defines already a causal field theory.*

Concluding this Section we derive a further relation needed for the following. From (10), (9), (6) and (8) it follows

$$\begin{aligned}\varphi_{\text{out}}(x) &= S^\dagger\varphi_{\text{in}}(x)S = \varphi_{\text{in}}(x) + S^\dagger[\varphi_{\text{in}}(x), S] = \\ &= \varphi_{\text{in}}(x) + [\varphi_{\text{out}}(x), S]S^\dagger = \varphi_{\text{in}}(x) + \int \Delta(x-y)j(y)\,\mathrm{d}y\,,\end{aligned} \tag{21}$$

where $j(x)$ is defined by (both expressions) (12) and $\Delta(x-y)$ as usually. (21) may be used for a reasoning of the definition (12) for the current operator.

3. – S-matrix and asymptotic condition.

LEHMANN, SYMANZIK and ZIMMERMANN proceed a step further and introduce a field operator $\varphi(x)$ by

$$\varphi(x) = \varphi_{\substack{\text{in}\\ \text{out}}}(x) - \int \Delta_{\substack{\text{ret}\\ \text{adv}}}(x-y)j(y)\,\mathrm{d}y\,, \tag{22}$$

$$(\Box - m^2)\varphi(x) = j(x)\,, \tag{22′}$$

which « interpolates » between past and future, *i.e.* between $\varphi_{\text{in}}(x)$ and $\varphi_{\text{out}}(x)$ for which we have the connection (10) and (21). They further assume the asymptotic condition (*)

$$\lim_{t\to\mp\infty} a(\boldsymbol{q}, t) = a_{\substack{\text{in}\\ \text{out}}}(\boldsymbol{q})\,, \tag{23}$$

(*) In their mathematically more rigorous treatment they use a discrete orthonormal system $\{f_\alpha(x)\}$ instead of $\{(1/(2\pi)^{\frac{3}{2}})(\exp[-iqx]/\sqrt{2q^0})\}$ which indeed is necessary in the last step in (27), where an integration by parts is performed. Also the relation (23) is defined in such a manner that the operators stay within a matrix element. However, for our purposes the above treatment is sufficient. We remark that there is a difference in sign in (1) between (18) and the application of the asymptotic condition on p. 328.

where

$$(24)\qquad a(\boldsymbol{q}, t) = \frac{-1}{(2\pi)^{\frac{3}{2}}}\, i\int \mathrm{d}\boldsymbol{x}\varphi(x)\, \frac{\overleftrightarrow{\partial}}{\partial x^0}\, \frac{\exp[iqx]}{\sqrt{2q^0}} = \frac{-1}{(2\pi)^{\frac{3}{2}}}\, i\int \mathrm{d}\boldsymbol{x}\left\{\varphi(x)\,\frac{\partial}{\partial x^0}\,\frac{\exp[iqx]}{\sqrt{2q^0}} - \frac{\partial}{\partial x^0}\,\varphi(x)\,\frac{\exp[iqx]}{\sqrt{2q^0}}\right\},$$

$$(25)\qquad \begin{cases} \varphi(x) = \dfrac{1}{(2\pi)^{\frac{3}{2}}}\displaystyle\int \frac{\mathrm{d}\boldsymbol{q}}{\sqrt{2q^0}}\{\exp[iqx]a^*(\boldsymbol{q}, t) + \exp[-iqx]a(\boldsymbol{q}, t)\}; \\ q^0 = +\sqrt{m^2 + \boldsymbol{q}^2}\,. \end{cases}$$

Using the condition (23) in connection with (24), (25) they calculate the commutator

$$(26)\qquad [a_{\text{in}}(\boldsymbol{q}), \varphi(x)]$$

to the form (1), (2) according to

$$(27)\qquad \begin{cases} [a_{\text{in}}(\boldsymbol{q}), \varphi(x)] = \lim\limits_{y^0\to-\infty}[a(\boldsymbol{q}, y^0), \varphi(x)] = \\ \quad = \lim\limits_{y^0\to-\infty} \dfrac{1}{(2\pi)^{\frac{3}{2}}}\, i\displaystyle\int \mathrm{d}\boldsymbol{y}[\varphi(x), \varphi(y)]\, \frac{\overleftrightarrow{\partial}}{\partial y^0}\, \frac{\exp[iqy]}{\sqrt{2q^0}} \\ \quad = \lim\limits_{y^0\to-\infty} \dfrac{1}{(2\pi)^{\frac{3}{2}}}\displaystyle\int \mathrm{d}\boldsymbol{y}\, i\theta(x-y)[\varphi(x), \varphi(y)]\, \frac{\overleftrightarrow{\partial}}{\partial y^0}\, \frac{\exp[iqy]}{\sqrt{2q^0}} \\ \quad = \dfrac{1}{(2\pi)^{\frac{3}{2}}}\displaystyle\int \mathrm{d}y\, \frac{\partial}{\partial y^0}\left\{-i\theta(x-y)[\varphi(x), \varphi(y)]\, \frac{\overleftrightarrow{\partial}}{\partial y_0}\, \frac{\exp[iqy]}{\sqrt{2q^0}}\right\} \\ \quad = \dfrac{1}{(2\pi)^{\frac{3}{2}}}\displaystyle\int \mathrm{d}y\, \frac{\exp[iqy]}{\sqrt{2q^0}}\, (\Box_y - m^2)\bar{R}(x, y)\,, \quad q^0 = +\sqrt{m^2 + \boldsymbol{q}^2}, \end{cases}$$

where $\bar{R}(x, y)$ is defined by (2).

Applying $(\Box_x - m^2)$ on (27) and using (22′) we get

$$(28)\qquad [a_{\text{in}}(\boldsymbol{q}), j(x)] = \frac{1}{(2\pi)^{\frac{3}{2}}}\int \mathrm{d}y\, \frac{\exp[iqy]}{\sqrt{2q^0}}\, (\Box_x - m^2)(\Box_y - m^2)\bar{R}(x, y)\,.$$

We remark that the commutation relation (28) is not uniquely defined: if we directly replace $\varphi(x)$ by $j(x)$ in (27) we get instead of (28)

$$(29)\qquad [a_{\text{in}}(\boldsymbol{q}), j(\boldsymbol{x})] = \frac{1}{(2\pi)^{\frac{3}{2}}}\int \mathrm{d}y\, \frac{\exp[iqy]}{\sqrt{2q^0}}\, (\Box_y - m^2)\{-i\theta(x-y)(\Box_x - m^2)[\varphi(x), \varphi(y)]\},$$

i.e. the operator $(\Box_x - m^2)$ stays now to the right of $\theta(x-y)$. However, it is

$$(30)\qquad (\Box_x - m^2)\{\theta(x-y)[\varphi(x), \varphi(y)]\} - \theta(x-y)(\Box_x - m^2)[\varphi(x), \varphi(y)] = \\ = P\left(\frac{\partial}{\partial x^0}\right)\delta(x^0 - y^0)$$

where $P(\partial/\partial x_0)$ is a polynomial (of first order) in $\partial/\partial x_0$ with coefficients which depend on $\boldsymbol{x}$, $\boldsymbol{y}$ and x^0. On the other hand $\theta(x-y)$ is only defined for $x^0 \gtrless y^0$ but not for $x^0 = y^0$ so that (30) yields no further indefinitness of the theory (*)(**). In the same manner we see that (28) of (29) is equivalent to

$$(31)\quad [a_{\text{in}}(\boldsymbol{q}), j(x)] = \frac{1}{(2\pi)^{\frac{3}{2}}}\int \mathrm{d}y\, \frac{\exp[iqy]}{\sqrt{2q^0}}\{-i\theta(x-y)[j(x), j(y)]\},\quad q^0 = +\sqrt{m^2 + \boldsymbol{q}^2}.$$

Now the next step is the following: from Section **2** we know that the commutator (31) may also be written in the form

$$(32)\qquad [a_{\text{in}}(\boldsymbol{q}), j(x)] = \frac{1}{(2\pi)^{\frac{3}{2}}}\int \mathrm{d}y\, \frac{\exp[iqy]}{\sqrt{2q^0}}\,\frac{\delta j(x)}{\delta\varphi_{\text{in}}(y)},\qquad q^0 = +\sqrt{m^2 + \boldsymbol{q}^2}.$$

Thus we arrive at the result that $-i\theta(x-y)[j(x), j(y)]$ must have the same transformation properties as $\delta^k(x)/\delta\varphi_{\text{in}}(y)$, *i.e.* has to be a scalar, and from considerations similar to those made after (20) we conclude that the application (27) of the asymptotic condition (23) leads immediately to a causal field theory, in which the commutator condition (18) has to be fulfilled.

The situation is now the following: in (22) there was constructed a field operator $\varphi(x)$ where $j(x)$ may be assumed as a causal operator or a non-causal one (in the last case we expect that $\varphi(x)$ is also a non-causal one). However, the application (27) of the asymptotic condition (23) in connection with (24), (25) yields the result that in *any* case the operator $j(x)$ has necessarily to be a causal one, which satisfies (18). Thus we have to conclude that either the definition of the asymptotic condition or its application or even both of them are not sufficiently defined.

We show that the second is indeed the case: the function $\theta(x-y)$ introduced in (27) is quite arbitrary; it has only to fulfil the condition $\theta(x-y) = 1$ if $y^0 = -\infty$ and $\theta(x-y) = 0$ if $y^0 = +\infty$ and if we assume that

(*) Compare the same situation in the definition of the T-product in (2) footnote (1) on p. 185 in the German translation.

(**) Also the derivation (27) is only defined in the same uncomplete manner since $\overleftrightarrow{\partial}/\partial y^0$ may operate on $\theta(x-y)$ or may not. We assumed the first case.

$\overleftrightarrow{\partial}/\partial y^0$ acts also on $\theta(x-y)$, then the time-derivatives of $\theta(x-y)$ have to vanish correspondingly at these limits (see also the Appendix). That expresses the fact that it is well possible to represent a function at a fixed point as an integral over a definite interval, however, the integrand is not uniquely defined.

Thus we conclude: the application of the asymptotic condition is not sufficiently defined in the approach of LEHMANN, SYMANZIK and ZIMMERMAN.

4. – The concept of causality.

We generalize our above considerations and state: a field theory into which expressions like the T-product

$$T(x, y) = T\, j(x)j(y) \tag{33}$$

or the R-product

$$R(x, y) = -i\theta(x-y)[j(x), j(y)] \tag{2'}$$

enter as scalar quantities (as it is the case in the approach of LEHMANN, SYMANZIK and ZIMMERMANN) has to be a causal field theory, in which the commutator condition (18) has to be fulfilled. The proof for this statement is quite simple (these things are by no means new in principle): the T-product of some scalar operators may be a scalar, *i.e.* an invariant expression, if and only if these operators commute in space-like regions since time-ordering has a covariant meaning only in time-like regions. The R-product (2′) may be also a scalar if and only if the operators $j(x)$, $j(y)$ commute in space-like regions since it vanishes for $x<y$ and for the reason of covariance it has to vanish also in the whole space-like region.

On the other hand if we write (compare (14) and (16))

$$S^\dagger \frac{\delta^2 S}{\delta\varphi_{\text{in}}(x)\,\delta\varphi_{\text{in}}(y)} = j(y)j(x) + i\,\frac{\delta j(x)}{\delta\varphi_{\text{in}}(y)} = \tag{34}$$

$$= Tj(x)j(y) + i\theta(x-y)\,\frac{\delta j(y)}{\delta\varphi_{\text{in}}(x)} + i\theta(y-x)\,\frac{\delta j(x)}{\delta\varphi_{\text{in}}(y)}\,,$$

we cannot conclude that $Tj(x)j(y)$ has to be a scalar (*i.e.* $j(x)$ has to be a causal operator, which satisfies (18)) since only the *whole* expression on the right of (34) has to be a scalar. In such a formalism we arrive at no contradiction. If we require causality in the form (17) the last two terms in (34) vanish and $Tj(x)j(y)$ is also a scalar. However, if we assume causality only

in the commutator form (18) we may conclude only that

$$i\theta(x-y)\,\frac{\delta j(y)}{\delta\varphi_{\text{in}}(x)}+i\theta(y-x)\,\frac{\delta j(x)}{\delta\varphi_{\text{in}}(y)}\,, \tag{35}$$

is a scalar which in addition is indeterminable. We *cannot* conclude that (35) has to vanish identically (for the rest it would follow from this the causality condition in the form (17)). Thus we arrive once more at the result: the causality condition in the commutator form (18) is not sufficient to determine (34) as the T-product (that is the same situation as for the representation (19)) which is needed, for instance, in the theory of dispersion relations.

Let us, however, proceed a step further. The essential physical difference between the causality condition (17), (17′) and (18) is that the first distinguishes *time* and also yields a causality condition for *time-like* regions. The causality condition in the commutator form (18) says nothing about causality for time-like distances and seems therefore uncomplete. Thus the question arises: how it is possible that this condition may be sufficient to define a field theory uniquely as a causal one which only uses the S-matrix and field operators but nothing more. Of course, LEHMANN, SYMANZIK and ZIMMERMANN use the wave equation (22′) but only as a definition for $\varphi(x)$ according to (22) and it seems quite impossible that the asymptotic condition could also be a substitute for a causality condition in time-like regions (which obviously is a condition for finite times). In Section **3** it was shown that their approach leads indeed to quite arbitrary and even contradictious results. On the other hand it was shown above that the causality condition (17), (17′) used by BOGOLJUBOV *et al.* is a mathematically sufficient expression for causality in the sense that such a condition leads immediately to a prescribed time-ordering in time-like regions which, of course, is irrelevant in space-like regions, where, indeed, time does *not* appear as a distinguished quantity (commutator condition (18)). If we add to a relativistic theory the condition of causality we necessarily distinguish time, however, that does not violate the requirement for covariance (that would only be the case if we required a defined time-ordering in space-like regions (*)). In a theory of dispersion relations we need indeed this form of causality.

The following statement may also be important (which was already mentioned in footnote 8 of [3]): the causality condition (17), (17′) has such a form that it also defines causality in a non-relativistic theory (where the commu-

(*) In order to be even more strict: causality does not distinguish a time-*direction* but only prescribes a defined time-*ordering*. The use of incoming or outgoing fields is completely equivalent.

[3] F. KASCHLUHN: *Zeits. f. Naturfor.*, **13a**, 183 (1958).

tator condition (18) loses its meaning). We have simply to replace $y \geqslant x$ by $y > x$ in (17) or $y \geqslant x$ by $y < x$ in (17′) respectively. Then a cut-off meson theory, for instance, which treats the nucleons non-relativistically is necessarily a *causal* theory (the Hamiltonian is time-independent). Of course, such a theory is *not* a *local* one. Further it is not necessary to make a second-quantization procedure to define a current operator in a field-theoretical way: the usual treatment with Schrödinger wave functions is sufficient ($j(x)$ is well defined by (12)). Especially this is valid for the static Chew model ([4]) which we have to define as a causal but non-local theory ([**]) (it is interesting to look at the remarks after equation (61) in ([4]) from our point of view).

* * *

I would like to thank Dr. MEDVEDEV for reading the manuscript and a valuable discussion.

APPENDIX

One can try to examine the proceeding of LEHMANN, SYMANZIK and ZIMMERMANN for the case where $a(\boldsymbol{q}, t)$ is not given by (24) but, for simplicity, by the relation

$$\text{(A.1)} \qquad a(\boldsymbol{q}, t) = \frac{1}{(2\pi)^{\frac{3}{2}}}\int \mathrm{d}\boldsymbol{x}\, \varphi(x)\sqrt{2q^0}\exp[iqx]\,,$$

and require the asymptotic condition as in (23)

$$\text{(A.2)} \qquad \lim_{t\to\mp\infty} a(\boldsymbol{q}, t) = a_{\substack{\text{in}\\ \text{out}}}(\boldsymbol{q})\,.$$

Then we write instead of (27)

$$\text{(A.3)} \quad \left\{ \begin{aligned} [a_{\text{in}}(\boldsymbol{q}), \varphi(x)] &= \lim_{y^0\to-\infty} [a(\boldsymbol{q}, y^0), \varphi(x)] \\ &= \lim_{y^0\to-\infty} \frac{1}{(2\pi)^{\frac{3}{2}}}\int \mathrm{d}\boldsymbol{y}\,[\varphi(y), \varphi(x)]\sqrt{2q^0}\exp[iqy] \\ &= \lim_{y^0\to-\infty} \frac{1}{(2\pi)^{\frac{3}{2}}}\int \mathrm{d}\boldsymbol{y}\,\theta(x-y)[\varphi(y), \varphi(x)]\sqrt{2q^0}\exp[iqy] \\ &= \frac{1}{(2\pi)^{\frac{3}{2}}}\int \mathrm{d}y\, \frac{\partial}{\partial y^0}\{\theta(x-y)[\varphi(x), \varphi(y)]\sqrt{2q^0}\exp[iqx]\}\,. \end{aligned} \right.$$

([4]) G. F. CHEW and F. E. LOW: *Phys. Rev.*, **101**, 1570 (1956).

([**]) A relativistic form factor theory is, of course, non-causal and non-local, however, for a non-relativistic theory these things need not be the same.

1462

For the reason of covariance $(\sqrt{2q^0}[a_{in}(\boldsymbol{q}), \varphi(x)]$ has to be a scalar and consequently $\theta(x-y)[\varphi(x), \varphi(y)])$ we may then conclude that $\varphi(x)$ has to be a causal operator; which satisfies (A.3). However, we have to notice that the introduction of the θ-function is not well defined: the only requirement is that the function $\theta(x-y)$ introduced in (A.3) has to satisfy

$$\lim_{y^0 \to \mp\infty} \theta(x-y) = \begin{cases}1\\0\end{cases}, \tag{A.4}$$

which yields a great lot of arbitrariness (of course, we assume that (A.4) does not influence the limiting value of its co-factor in (A.3)). Nevertheless it may be that using the appropriate modifications — the proceeding (A.3) (or (27) respectively) is useful for an approach to quantum field theory which avoids the explicit use of variational derivatives.

Note added in proof:

Recently Dr. MEDVEDEV has called my attention to the work of Y. OKABAYASHI (*Suppl. Nuovo Cimento*, **9**, 599 (1958)), where the first part of our conclusions is also reached, namely that the mathematical scheme of LEHMANN, SYMANZIK and ZIMMERMANN does not work for non-causal interactions. I would like to thank Dr. MEDVEDEV once more for useful discussions. In the meantime I had also occasion to discuss the main points of this work with Academician Bogoljubov to whom I am extremely grateful for his great interest and valuable remarks. Quite recently I received a letter from Prof. LEHMANN and Dr. ZIMMERMANN, in which the main point of this work is accepted, *i.e.* the statement that their introduction of the retarded commutators is not sufficiently defined (the same is, of course, true for the introduction of the T-products in: H. LEHMANN, K. SYMANZIK, W. ZIMMERMANN: *Nuovo Cimento*, **1**, 205 (1955)). However, then it is necessary to introduce a further condition in their scheme for the case of a casual theory (besides the usual commutator condition), which we may exspect to be equivalent to that condition which follows from Bogoljubov's causality condition for time-like distances. We emphasize once more that the introduction of the T-products or the retarded products as done by LEHMANN, SYMANZIK and ZIMMERMANN leads to wrong transformation properties in the general non-causal case (compare (34), where besides the T-product two additional terms occur which are non-zero and non-scalar quantities in the non-causal case and which are completely absent in their scheme. We notice that these terms are also important for a discussion of a possible non-causal structure of quantum field theory in the framework of the theory of dispersion relations in addition to the deviations from the commutator condition (18)). I would like to thank Prof. LEHMANN and Dr. ZIMMERMANN for their letter and for pointing out a mistake involved in the preprint of this work (which was also brought to my attention in a discussion with Dr. MEDVEDEV).

RIASSUNTO (*)

Si dimostra che il procedimento matematico di Lehmann, Symanzik e Zimmermann conduce necessariamente ad una teoria di campo causale, in cui i componenti degli operatori di campo si annullano a distanze spaziali. Per studiare questo fatto da un punto di vista più generale usiamo derivate estesamente variazionali della matrice S rispetto agli operatori del campo libero come proposto da Bogoljubov e collaboratori. Si esamina dettagliatamente il modo in cui Lehmann, Symanzik e Zimmermann definiscono e applicano la condizione asintotica. Concludendo presentiamo qualche affermazione generale sul concetto di causalità nella teoria quantistica dei campi. Si rileva che solo la condizione di causalità nella forma usata da Bogoljubov e collaboratori (e non le condizioni imposte ai commutatori) è sufficiente per un trattamento della teoria quantistica dei campi, quale è richiesto, ad esempio, nella teoria delle relazioni di dispersione.

(*) *Traduzione a cura della Redazione.*

IL NUOVO CIMENTO VOL. XII, N. 6 16 Giugno 1959

Feldgleichungen für nichtlokalisierbare Felder.

G. HEBER

Theoretisch-Physikalisches Institut der Universität - Jena

(ricevuto il 19 Febbraio 1959)

Summary. — In the special cases of a real, scalar field and of electrodynamics the conventional, differential field equations are substituted by covariant integral laws. These integral equations are then modified in such a manner, that we get accord with the possibilities of measurement. The modified integral equations are then once more changed to differential field laws. It is shown, that for the scalar field these equations are different from the conventional ones, but for electrodynamics we find identical field equations. However the meaning of the field quantities does change by our modification and as a result we get commutation relations between the new field quantities, which are no longer c-numbers; they are certain q-numbers. The meaning of this fact is still an open question. In the appendix a short discussion about critical points of the series of papers [1-3], which led us to this work, is given.

1. – Einführung.

Es handelt sich im folgenden um eine Fortführung des in früheren Veröffentlichungen [1-3] entwickelten Programmes: Ein möglichst einfaches, isoliertes Modell-Feld soll auf solche Weise quantisiert werden, daß die schließlich entstandene Theorie mit den realen Meßmöglichkeiten völlig im Einklang steht. Oder etwas anders ausgedrückt: Die bei Verwendung von in der Natur vorkommenden Probekörpern auftretenden Meßbarkeits-Beschränkungen sollen organisch in der Theorie enthalten sein.

(1) G. HEBER: *Nuovo Cimento*, **7**, 677 (1958).
(2) G. HEBER: *Nuovo Cimento*, **8**, 327 (1958).
(3) G. HEBER: *Max-Planck-Festschrift*, in *Deutscher Verlag der Wissenschaften* (Berlin, 1959).

Wir haben bisher einen wesentlichen Zug dieser neuen Theorie herausgearbeitet: Die Notwendigkeit des Auftretens von Operatoren $\xi_\mu(y)$, die sich wie Vierer-Vektoren transformieren, von den Koordinaten y_ν eines Minkowski-Kontinuums abhängen und mit den aus der konventionellen Quanten-Feldtheorie bekannten Feldoperatoren $F_\lambda(y)$ i. a. nicht kommutieren.

Die physikalische Bedeutung der Größen $\xi_\mu(y)$ für festes y läßt sich einfach erklären: Es sind die 4 Koordinaten, die den Weltpunkt der Messung der Feldgröße $F_\lambda(y)$ festlegen. Da die Messung mit Hilfe eines der Quantenmechanik zu unterwerfenden Probekörpers erfolgen soll, müssen die ξ_μ Operatoren sein. Da ferner die an den verschiedenen Weltpunkten y verwendeten Probekörper i. a. nichts miteinander zu tun haben, muß man für jeden Punkt des y-Kontinuums solche Operatoren einführen; deshalb haben wir $\xi_\mu = \xi_\mu(y)$.

Trotz dieser Abhängigkeit von y können die $\xi_\mu(y)$ natürlich nicht als Feldoperatoren aufgefaßt werden, wie in ([2]) erläutert wurde. Darin lag die eigentliche Schwierigkeit bei der sachgemäßen Aufstellung von Feldgleichungen, die ja die $\xi_\mu(y)$ irgendwie organisch enthalten sollen. Verf. glaubt jetzt, einen natürlichen Gesichtspunkt für die Aufstellung der Bewegungsgleichungen gefunden zu haben. Darüber soll hier berichtet werden.

Der Grundgedanke dieser Arbeit ist sehr einfach: Um die beschränkten Meßmöglichkeiten in die Theorie einbauen zu können, muß man die Theorie so formulieren, daß die Grundgleichungen direkt nachgemessen werden können. Das ist kaum möglich bei Differentialgesetzen, wohl aber bei Integralgesetzen. Wir schreiben also integrale Bewegungsgleichungen auf. Nehmen wir an, eine solche Gleichung habe in der konventionellen Theorie die Gestalt

$$\oint_C F_\nu(x)\,\mathrm{d}x^\nu = 0\,.$$

Dann besteht unser Einbau der Größen ξ in dieses Gesetz im Ersatz dieser Gleichung durch:

$$\oint_C F_\nu(y)\,\mathrm{d}\xi^\nu(y) = 0\,,$$

wobei der Weg C im y-Raum definiert ist. Das ist ein sachgemäßes Verfahren, denn beim Nachmessen einer solchen Integralgleichung wird man stets so vorgehen: Man setzt an die Punkte $y_k \in C$ Probekörper, mißt an jedem dieser Punkte $F_\nu(y_k)$ und mißt die Abstände der zugehörigen Probekörper: $\Delta\xi^\nu(y_k) = \xi^\nu(y_{k-1}) - \xi^\nu(y_k)$. Dann bildet man für möglichst dicht auf C gelegte Meßpunkte.

$$\sum_k F_\nu(y_k)\,\Delta\xi^\nu(y_k)\,.$$

Der Grenzübergang zu beliebig dicht liegenden y_k liefert dann genau obiges Gesetz.

Unter der Annahme $\mathrm{d}\xi^\nu(y) = \mathrm{d}y^\nu$ enthält dies auch die konventionelle Gleichung; wie in (2) ausgeführt, möchten wir jedoch diese Annahme ausschließen. Dann hat man wegen des Operator-Charakters von $\xi^\nu(y)$ und $\mathrm{d}\xi^\nu(y)$ eine gewisse « Verschmierung » des geschlossenen Integrationsweges C erreicht. Wir diskutieren nun die formalen Folgen dieses Vorgehens an zwei Spezialfällen.

2. – Skalares, reelles Feld der Ruhmasse Null.

Für dieses Feld lauten bekanntlich die konventionellen Feldgleichungen:

$$\Box U(x) = 0\,, \qquad \text{oder} \qquad \partial_\mu F_\nu(x) - \partial_\nu F_\mu(x) = 0\,, \tag{1}$$

$$\partial^\mu F_\mu(x) = 0\,. \tag{2}$$

Wir möchten (1) und (2) in kovariante Integralgleichungen überführen. Dies läßt sich besonders elegant mit Hilfe des Kalküls der Differentialformen (4) ausführen. Im vorliegenden Spezialfall benötigen wir zur Formulierung von (1) und (2) zwei Differentialformen $\mathcal{H}$ und $\mathcal{H}'$, nämlich:

$$\mathcal{H} = F_\nu(x)\,\mathrm{d}x^\nu\,, \tag{3}$$

$$\mathcal{H}' = F_\nu(x)\,\mathrm{d}x^\mu\,\mathrm{d}x^\lambda\,\mathrm{d}x^k\,, \tag{4}$$

mit $(\nu, \mu, \lambda, k) = (0, 1, 2, 3)$ + zyklisch Vertauschte (*).

Den Gleichungen (1) und (2) sind nun mit (3) und (4) genau äquivalent

(4) E. Cartan: *Leçons sur les invariants intégraux* (Paris, 1922); W. V. D. Hodge: *The theory and applications of harmonic integrals*, S. 68-79 (Cambridge, 1952); E. Kähler: *Einführung in die Theorie der Systeme von Differentialgleichungen*, S. 1-10 (Leipzig-Berlin, 1934); A. Lichnerowicz: *Lineare Algebra und lineare Analysis*, S. 137-180 (Berlin, 1956).

(*) Wenn $\mathcal{H}$ ein Skalar ist, muß $\mathcal{H}'$ ersichtlich ein Pseudoskalar sein. Alle hier und unten auftretenden Produkte zwischen den Differentialen $\mathrm{d}x^\nu$ sind « alternierende » Produkte mit der Eigenschaft: $\mathrm{d}x^\mu\,\mathrm{d}x^\nu = -\mathrm{d}x^\nu\,\mathrm{d}x^\mu$ für alle μ, ν. Also gilt stets: $(\mathrm{d}x^0)^2 = 0$, $(\mathrm{d}x^1)^2 = 0$, usw. Das alternierende Produkt entspricht also dem üblichen Vektorprodukt und ist besonders geeignet zur Formulierung von Integrationen über Flächen mit Richtungssinn. Wegen weiterer Einzelheiten des verwendeten Kalküls und besonders dessen Begründung vgl. (4).

die Gesetze

$$d\mathcal{H} = 0\,; \tag{5}$$

$$d\mathcal{H}' = 0\,. \tag{6}$$

Hier bedeutet $d\mathcal{H}$ das totale Differential von $\mathcal{H}$, welches nach den geltendend Regeln (vgl. ([4])) so zu bilden ist:

$$d\mathcal{H} = d(F_\nu)\, dx^\nu = \frac{\partial F_\nu}{\partial x^\mu}\, dx^\mu\, dx^\nu = \sum_{\nu<\mu} \frac{\partial F_\nu}{\partial x^\mu}\, dx^\mu\, dx^\nu + \sum_{\nu>\mu} \frac{\partial F_\nu}{\partial x^\mu}\, dx^\mu\, dx^\nu =$$
$$= \sum_{\nu<\mu} \left(\frac{\partial F_\nu}{\partial x^\mu} - \frac{\partial F_\mu}{\partial x^\nu}\right) dx^\mu\, dx^\nu\,.$$

$d\mathcal{H} = 0$ ist aber nach ([4]) gleichbedeutend damit, daß die Koeffizienten aller linear unabhängigen Differentiale in $d\mathcal{H}$ einzeln verschwinden. Aus der letzten Gestalt unseres angeschriebenen Ausdruckes für $d\mathcal{H}$ folgt dann sofort die Äquivalenz von (5) mit (1). Analog beweist man die Äquivalenz von (6) mit (2).

In ([4]) wird ferner gezeigt, daß dann, wenn das totale Differential $d\mathcal{H}$ der Differentialform $\mathcal{H}$ identisch verschwindet, für diese Form die Integralbeziehung

$$\oint_C \mathcal{H} = 0\,, \tag{7}$$

gilt, wo C eine beliebige geschlossene Kurve im 4-dimensionalen Weltkontinuum sein darf. Entsprechend folgt aus $d\mathcal{H}' = 0$ die Beziehung

$$\iiint_{C'} \mathcal{H}' = 0\,, \tag{8}$$

wo jetzt C' eine 3-dimensionale Mannigfaltigkeit ist, die als Rand einer beliebigen 4-dimensionalen Mannigfaltigkeit definiert ist. (7) und (8) sind die gesuchten, zu (1) und (2) äquivalenten, kovarianten Integralgleichungen.

Jetzt bauen wir in (7) und (8), wie oben erläutert, unsere $\xi^\mu(y)$ ein, indem wir statt

$$\oint_C F_\nu(x)\, dx^\nu = 0\,, \tag{7}$$

und

$$\iiint_{C'} F_\nu(x)\, dx^\mu\, dx^\lambda\, dx^k = 0\,, \tag{8}$$

schreiben

(9) $$\oint_C F_\nu(y)\,\mathrm{d}\xi^\nu(y) = 0\,,$$

und

(10) $$\iiint_{C'} F_\nu(y)\,\mathrm{d}\xi^\mu(y)\,\mathrm{d}\xi^\lambda(y)\,\mathrm{d}\xi^k(y) = 0\,.$$

(9) und (10) sehen wir jetzt als die Feldgleichungen unserer Theorie an. Wir möchten sie aber verständlicherweise auch in differentieller Form aufschreiben. Hierzu muß man die Gleichungen (9) und (10) nur in die Gestalt von (7) und (8) bringen. Das gelingt nach Beachtung von

$$\mathrm{d}\xi^\mu(y) = \frac{\partial\xi^\mu(y)}{\partial y^\lambda}\,\mathrm{d}y^\lambda\,,$$

sowie

$$\mathrm{d}\xi^\beta(y)\,\mathrm{d}\xi^\gamma(y)\,\mathrm{d}\xi^\varepsilon(y) = \sum_{\mu<\lambda<k}\frac{\partial(\xi^\beta,\,\xi^\gamma,\,\xi^\varepsilon)}{\partial(y^\mu,\,y^\lambda,\,y^k)}\,\mathrm{d}y^\mu\,\mathrm{d}y^\lambda\,\mathrm{d}y^k \quad (^*)\,,$$

und Einführung der neuen Feldgrößen

(11) $$B_\nu(y) = F_\lambda(y)\,\partial_\nu\,\xi^\lambda(y)$$

und

(12) $$H_\nu(y) = \sum_{\alpha=1}^{4} F_\alpha(y)\,\frac{\partial(\xi^\beta,\,\xi^\gamma,\,\xi^\varepsilon)}{\partial(y^\mu,\,y^\lambda,\,y^k)}\,,$$

mit $(\alpha, \beta, \gamma, \varepsilon) = (0, 1, 2, 3)$ oder zyklisch vertauschte Indexanordnung und ebenso mit $(\nu, \mu, \lambda, k) = (0, 1, 2, 3)$ oder zyklisch vertauschte Indexanordnung.

Die Gleichungen (9) und (10) erhalten dann die Gestalt:

$$\oint_C B_\nu(y)\,\mathrm{d}y^\nu = 0\,;$$

$$\iiint_{C'} H_\nu(y)\,\mathrm{d}y^\mu\,\mathrm{d}y^\lambda\,\mathrm{d}y^k = 0\,.$$

Diese Gleichungen sind identisch mit (7) bzw. (8), also sind sie äquivalent zu:

(13) $$\partial_\nu B_\mu - \partial_\mu B_\nu = 0\,,$$

(*) Das hier erstmalig auftretende Differentialsymbol $\frac{\partial(\dots)}{\partial(\dots)}$ ist die bekannte Funktional-Determinante.

bzw.

$$\partial_\nu H^\nu = 0 \,. \tag{14}$$

Die Gleichungen (13), (14) sind natürlich nicht ausreichend zur Bestimmung der Feldgrößen; man muß noch den Zusammenhang zwischen B_ν und H_ν kennen. Dieser folgt aus (11) und (12), die wir symbolisch als

$$B = F\cdot\theta \qquad \text{und} \qquad H = F\cdot\vartheta$$

schreiben wollen, in der Form

$$H = B\cdot\theta^{-1}\cdot\vartheta \,. \tag{15}$$

Da $\theta^{-1}\cdot\vartheta$ i.a keineswegs gleich 1 sein wird, sind die Gleichungen (13), (14), (15) komplizierter als (1), (2). Wir möchten eine Diskussion des Inhalts dieser Gleichungen zurückstellen. Vielmehr möchten wir jetzt zeigen, daß bei entsprechender Anwendung der eben vorgeführten Prozedur auf die isolierte Elektrodynamik die Grundgleichungen im Gegensatz zu dem eben diskutierten Fall überhaupt nicht verändert werden. Vielleicht ist dieser keineswegs triviale Unterschied u.a. wichtig für die Erklärung des geringen Erfolges der konventionellen Feldtheorien in der Mesonenphysik verglichen mit der Elektrodynamik.

3. – Isolierte Elektrodynamik.

Die Maxwellschen Gleichungen im Vakuum lauten bekanntlich:

$$\partial_\lambda F_{\mu\nu} + \partial_\mu F_{\nu\lambda} + \partial_\nu F_{\lambda\mu} = 0 \,, \tag{16}$$

$$\partial^\mu F_{\nu\mu} = 0 \,. \tag{17}$$

Hier hat der Feldstärken-Tensor $F_{\mu\nu} = -F_{\nu\mu}$ die übliche Bedeutung:

$$F_{\mu\nu} = \begin{pmatrix} 0 & -\mathfrak{E} \\ \mathfrak{E} & \mathfrak{B} \end{pmatrix}.$$

(16) kann man nach Einführung der Differentialform $\mathcal{H} = \frac{1}{2} F_{\mu\nu}\, \mathrm{d}x^\mu\, \mathrm{d}x^\nu$ in der Gestalt

$$\mathrm{d}\mathcal{H} = 0 \quad (^*) \tag{18}$$

(*) Zur Untersuchung der Maxwellschen Gleichungen mit Hilfe des äußeren Differentialkalküls siehe E. KÄHLER: *Bemerkungen über die Maxwellschen Gleichungen*, in *Abh. Math. Sem. Hamburg*, **12**, 1 (1938).

schreiben. Wenn man die andere Form

$$\mathcal{H}' = \tfrac{1}{2}\,\hat{F}_{\mu\nu}\,\mathrm{d}x^\mu\,\mathrm{d}x^\nu\,,$$

mit

$$\hat{F}_{\mu\nu} = \left(\begin{array}{c:c} 0 & \mathfrak{B} \\ \hdashline -\mathfrak{B} & \mathfrak{E} \end{array}\right)(^*)\,,$$

einführt, ist (17) mit

$$\mathrm{d}\mathcal{H}' = 0 \tag{19}$$

äquivalent. Die Gleichungen (18), (19) sind wiederum in kovariante Integralgleichungen überführbar, nämlich in (vgl. ([4])):

$$\oint\!\!\oint_C \mathcal{H} = 0\,, \tag{20}$$

$$\oint\!\!\oint_{C'} \mathcal{H}' = 0\,. \tag{21}$$

In diesen beiden Gleichungen sind C und C' zwei 2-dimensionale Mannigfaltigkeiten, die zwei beliebige 3-dimensionale Teilräume des Minkowski-Raumes begrenzen (**).

Entsprechend unserem obigen Vorgehen werden jetzt (20) und (21) ersetzt durch:

$$\oint\!\!\oint_C F_{\mu\nu}(y)\,\mathrm{d}\xi^\mu(y)\,\mathrm{d}\xi^\nu(y) = 0\,,$$

und

$$\oint\!\!\oint_{C'} \hat{F}_{\mu\nu}(y)\,\mathrm{d}\xi^\mu(y)\,\mathrm{d}\xi^\nu(y) = 0\,;$$

dafür aber kann man auch schreiben:

$$\oint\!\!\oint_C B_{\lambda k}(y)\,\mathrm{d}y^\lambda\,\mathrm{d}y^k = 0\,, \tag{22}$$

(*) $\hat{F}$ wird oft zu F «dual» genannt. Es besteht offensichtlich eine Relation der Form

$$\hat{F}_{\mu\nu} = \varepsilon_{\mu\nu}{}^{rs}\,F_{rs} \qquad \text{mit} \qquad \varepsilon_{\mu\nu}{}^{rs} = 0,\ \pm 1\,.$$

(**) Schreibt man sich die Gleichungen (20), (21) explizit auf, so sieht man, wie es natürlich sein muß, daß sie mit den über die Zeit integrierten, kovariant geschriebenen, bekannten Integralgesetzen der Maxwellschen Theorie identisch sind.

mit

$$B_{\lambda k}(y) = \sum_{\mu<\nu} F_{\mu\nu}(y) \frac{\partial(\xi^\mu, \xi^\nu)}{\partial(y^\lambda, y^k)}, \tag{23}$$

und

$$\oiint_{C'} \hat{H}_{\lambda k}(y)\, \mathrm{d}y^\lambda\, \mathrm{d}y^k = 0, \tag{24}$$

mit

$$\hat{H}_{\lambda k}(y) = \sum_{\mu<\nu} \hat{F}_{\mu\nu} \frac{\partial(\xi^\mu, \xi^\nu)}{\partial(y^\lambda, y^k)}. \tag{25}$$

Die Gleichungen (22) und (24) wiederum sind äquivalent mit

$$\partial_\lambda B_{\mu\nu} + \partial_\mu B_{\nu\lambda} + \partial_\nu B_{\lambda\mu} = 0, \tag{26}$$

und

$$\partial^\mu H_{\nu\mu} = 0,$$

mit

$$\hat{H}_{\mu\nu} = \varepsilon_{\mu\nu}{}^{rs} H_{rs} \qquad (\varepsilon \text{ wie oben}).$$

Formal haben wir also die Grundgleichungen der Maxwellschen Theorie ohne Ladungen, aber in irgendeinem Medium erhalten. Entscheidend für den Inhalt der Gleichungen (26), (27) ist natürlich der Zusammenhang zwischen B und H. Um ihn abzuleiten, schreiben wir (23) und (25) symbolisch:

$$B = F \cdot T \ (^*); \qquad \hat{H} = \hat{F} \cdot T;$$

ferner beachten wir:

$$\hat{F} = \varepsilon \cdot F; \qquad \hat{H} = \varepsilon \cdot H.$$

Dann folgt:

$$H = \varepsilon^{-1} \cdot \hat{H} = \varepsilon^{-1} \cdot \hat{F} \cdot T = F \cdot T = B.$$

Wegen

$$H = B \tag{28}$$

erhalten wir also genau die Grundgleichungen der Elektrodynamik im Vakuum wieder. Dieses durchaus nichttriviale Resultat hängt ersichtlich eng einerseits mit der Tatsache, daß die elektrodynamischen Feldgrößen einen schiefsymmetrischen Tensor zweiter Stufe bilden und andererseits mit der 4-Dimensionalität unserer Welt zusammen.

(*) T ist der Tensor $\dfrac{\partial(\xi^\mu, \xi^\nu)}{\partial(y^\lambda, y^k)}$.

4. – Vertauschungsregeln zwischen den Feldgrößen der Elektrodynamik.

Die Übereinstimmung der Feldgleichungen für F und B bedeutet jedoch keineswegs, daß sich unsere Theorie von der konventionellen Quantenelektrodynamik nicht unterscheidet. Vielmehr lauten die Vertauschungsregeln wesentlich anders. Geht man nämlich von den in (³) angeschriebenen Vertauschungsregeln aus

$$(29)\ (^*)\qquad \begin{cases} [F(y), F(y')] = D(y-y')\,; & [\xi, \xi] = 0\,; \\ [F(y), \xi(y')] = G(y-y')\,, \end{cases}$$

so erhält man sofort für $B = F \cdot T$ die Regeln:

$$(30)\qquad [B(y), B(y')] = D(y-y')\cdot T(y')\cdot T(y) - \\ - A(y', y)\cdot F(y)\cdot T(y') + A(y, y')\cdot F(y')T(y)\,,$$

mit

$$A(y, y') = [F(y), T(y')]\,.$$

Unter der Voraussetzung, daß D und G in (29) c-Zahl-Charakter haben, wird also $[B, B]$ nach (30) ganz sicher q-Zahl-Charakter erhalten. Vielleicht könnte man in (29) die Größen D und G als solche q-Zahlen anzetsen, daß (30) eine c-Zahl-Funktion wird. Aber das erscheint, wenn überhaupt möglich, außerordentlich gekünstelt und soll hier nicht diskutiert werden.

q-Zahl-Vertauschungsregeln für die Feldgrößen sind bisher meines Wissens nicht in Betracht gezogen worden. Im Rahmen unserer Überlegungen stoßen wir jedoch zwangsläufig auf sie. Es ist zu vermuten, daß sie den Inhalt einer Feldtheorie wesentlich verändern. In welcher Weise und in welcher Richtung dies geschieht, hofft der Autor später darlegen zu können.

Verf. ist übrigens keineswegs überzeugt davon, daß nach ihrer Fertigstellung die hier begründete Theorie eine brauchbare Theorie der Elementarteilchen sein wird. Verf. hofft lediglich, daß die hier untersuchte Theorie allgemeiner sein wird als die konventionelle Feldtheorie. Die lokalen, konventionellen Feldtheorien sind ja offensichtlich zu eng, um zu einer Theorie der Elementarteilchen ausgebaut werden zu können. Vielleicht wird die hier angestrebte Feldtheorie sich bei weiterer Entwicklung zur Formulierung einer Theorie der Elementarteilchen verwenden lassen.

(*) Tensorindizes seien der Übersichtlichkeit wegen fortgelassen. D und G sollen c-Zahl-Charakter besitzen.

1473

* * *

Herrn Dr. A. Uhlmann, Jena, ist Verf. für den Hinweis auf den Kalkül der Differentialformen und hilfreiche Erläuterungen zu demselben zu Dank verpflichtet.

Anhang

Zur Diskussion über den vorgliegenden Ansatz zu einer modifizierten Feldtheorie.

In verschiedenen Diskussionen mit einigen Fachkollegen, für die Verf. diesen Herren sehr dankbar ist, wurden einige Bedenken gegen die hier und in (1) bis (3) verfolgte Absicht vorgebracht. Verf. möchte sich an dieser Stelle zusammenfassend dazu äußern, weil diese Auseinandersetzungen zur Erläuterung des vorliegenden Ansatzes recht nützlich sein dürften.

Kritik. – Zwecks Messung wird das untersuchte Feld vom Verf. an Probekörper gekoppelt, die der gewöhnlichen Quantenmechanik gehorchen. Wäre es nicht richtiger, stattdessen die zur Messung dienende Kopplung an ein anderes (quantisiertes) Feld vorzunehmen? Dann wären die Unschärferelationen für die Probekörper automatisch erfüllt und brauchten nicht mehr zusätzlich eingebaut zu werden!

Antwort des Verf. – Will man zwei Felder aneinanderkoppeln, muß man vorher wissen, was die isolierten Felder bedeuten. Kopplung zweier Felder hat nur dann einen Sinn, wenn man die beiden Felder vorher unabhängig voneinander definiert hat. Dazu gehört auch eine Meßvorschrift. Eben damit befaßt sich der Autor. Übrigens haben schon Bohr und Rosenfeld gezeigt, daß makroskopische Objekte wesentlich besser zur Feldmessung geeignet sind als z. B. Elektronen (Landau und Peierls).

Aber die Meßvorschriften von Bohr und Rosenfeld sind sehr unreal; mit realen Meßmitteln kann man Felder nicht beliebig genau ausmessen; das ist der Ausgangspunkt unserer Überlegungen.

Kritik. – Sollte man nicht damit zufrieden sein, die Feldtheorie axiomatisch aufzubauen? Die möglichen Meßwerte sind dann bekanntlich die Eigenwerte der betreffenden Operatoren. Der konventionelle Apparat der quantisierten Feldtheorien enthält dann schon alle Aussagen über den Meßprozeß.

Antwort des Verf. – Der vom Kritiker skizzierte Standpunkt mag den Mathematiker befriedigen. Der Physiker hingegen muß die mathematisch formulierte Meßvorschrift auch physikalisch verifizieren. Gelingt dies nicht, so besteht eine Diskrepanz zwischen mathematischer Theorie und physikalischer Wirklichkeit. Die Beseitigung dieser in der konventionellen Feldtheorie

vorhandenen Diskrepanz ist gerade das Anliegen des Verf. Vgl. hierzu auch S. 81 des Buches von JAUCH und ROHRLICH (5) und S. 206 des Artikels von KÄLLÉN im *Handb. d. Phys.* (6).

(5) J. M. JAUCH and F. ROHRLICH: *The Theory of Photons and Electrons* (Cambridge, 1955).
(6) G. KÄLLÉN: *Quantenelektrodynamik*, in *Handb. d. Phys.*, 5, Teil I (Berlin, 1958).

RIASSUNTO (*)

Nei casi speciali di campo scalare reale e dell'elettrodinamica si sostituiscono le convenzionali equazioni differenziali del campo con leggi integrali covarianti. Si modificano poi queste equazioni integrali in modo che ci sia accordo con le possibilità di misurazione. Si trasformano poi ancora le equazioni integrali ad esprimere le leggi del campo in forma differenziale. Si dimostra che per campo scalare queste equazioni sono differenti da quelle convenzionali, ma per l'elettrodinamica si trovano equazioni di campo identiche. Tuttavia, il significato delle grandezze di campo non cambia con le nostre modificazioni e come risultato otteniamo relazioni di commutazione tra le nuove grandezze di campo che non sono più numeri c; sono numeri q. Il significato di ciò è ancora in discussione. Nell'appendice diamo una breve discussione sui punti critici della serie di lavori (1-3) che ci hanno condotto al presente lavoro.

(*) *Traduzione a cura della Redazione.*

IL NUOVO CIMENTO Vol. XII, N. 6 16 Giugno 1959

Results on Antiproton-Proton Elastic Scattering.

G. Baroni, G. Bellettini, C. Castagnoli, M. Ferro-Luzzi
and A. Manfredini

Istituto di Fisica dell'Università - Roma
Istituto Nazionale di Fisica Nucleare - Sezione di Roma

(ricevuto il 23 Febbraio 1959)

Summary. — Fifteen antiproton-proton elastic scatterings are described: the angular distribution and the cross-section $\sigma_{el} = (65.7 \pm 17)$ mb are obtained. By averageing our results with those obtained by other laboratories under similar conditions, it is found $\sigma_{el} = (70.9 \pm 12.7)$ mb. Both angular distribution and cross-section are in agreement with the predictions of Ball-Chew's theory. Four events were used for an accurate determination of the antiproton mass: $m_{\bar{p}} = (0.998 \pm 0.015)$ proton masses.

1. – Introduction.

Until now 16 events interpreted as $\bar{p}$-H elastic scatterings have been observed in nuclear emulsions [1,2] and 33 in propane bubble chambers [3]. Here 15 more $\bar{p}$-H elastic scatterings are reported which have been observed in this laboratory during the scanning of an emulsion stack exposed to the enriched antiproton beam at Berkeley. The results are compared with the theoretical predictions of Fulco [4], based on Ball and Chew's theory [5].

Four events have been used for an accurate determination of the antiproton mass.

(1) G. Goldhaber, T. Kalogergroulos and R. Silberger: *Phys. Rev.*, **110**, 1474 (1958).

(2) A. G. Ekspong and B. E. Ronne: private communication.

(3) L. Agnew, T. Elioff, W. B. Fowler, L. Gilly, R. Lander, L. Oswald, W. Powell, E. Segrè, H. Steiner, H. White, C. Wiegand and T. Ypsilantis: *Phys. Rev.*, **110**, 994 (1958).

(4) J. Fulco: *Phys. Rev.*, **110**, 784 (1958).

(5) J. S. Ball and G. F. Chew: *Phys. Rev.*, **109**, 1385 (1958).

2. – Experimental method.

The energy of the incident antiprotons was 250 MeV and their tracks were followed up to the antiproton annihilation. For the study of elastic scatterings, the fulfilment of the following conditions was required:

a) Within experimental errors the track of the scattered antiproton should be coplanar with the tracks of the incident antiproton and of the recoiling proton.

b) The angle between the proton and antiproton tracks should be $90° - \eta$, where η is the relativistic correction

$$\operatorname{tg} \eta = \frac{\operatorname{tg} \theta \, (\gamma - 1)}{(\gamma + 1) \operatorname{tg}^2 \theta - 2}$$

In this relationship θ is either the antiproton or the proton scattering angle and $\gamma = E/m$ refers to the incident antiproton.

c) The residual range of the incident antiproton at the scattering point, the angle of emission and range of the recoiling proton, the scattering angle and—when possible—the range of the antiproton after the collision, should be consistent with a two body collision between particles of protonic mass. Since the identification of a $\bar{p}$-H collision in emulsion requires the visibility of the recoiling proton, we have set a lower limit of 2 μm for the range of this particle. This implies a cut-off of the scattering angle of the antiproton of 1°30′ at 260 MeV, 2°10′ at 140 MeV and 4°40′ at 30 MeV. The corresponding centre of mass cut-off angles are 3°11′, 4°19′, 9°20′ respectively. Thus the loss of solid angle is small enough to be neglected in the calculation of the cross-section for elastic scattering.

A second remark concerns the determination of the coplanarity. So far, the majority of the authors who have studied this type of event in emulsion, bubble chambers or cloud chambers have tested the coplanarity of the tracks by means of the angle δ between the incident track and the plane determined by the tracks of the two outgoing particles [2,6]. Such a test however, is very insensitive since in the case of $\bar{p}$-H scattering, the angle of deflection of the antiproton is always very small and the angle between the two outgoing tracks,

(6) P. J. Duke, W. O. Lock, P. W. March, W. M. Gibson, J. G. McEven, I. S. Hughes and H. Muirhead: *Phil. Mag.*, **2**, 204 (1957).

is very close to 90°. Therefore we decided to test the coplanarity by means of the spherical excess ε of each event. Fig. 1 shows the ratio ε/δ computed for $\delta \leqslant 4°$ as a function of the antiproton scattering angle. The solid part of the curve corresponds to the range of values covered by our antiprotons. We see that ε is always larger than δ and that the ratio increases rapidly with increasing antiproton scattering angle.

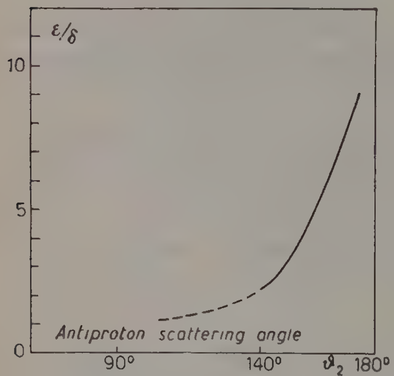

Fig. 1.

The error on the spherical excess ε, — for $\theta_1 \sim \pi/2$ — is given by

$$(\Delta\varepsilon)^2 = \\ = (\sin^2\theta_3 - \cos^2\theta_2)^{-1} \sum_{K=1}^{3} (H_{ij} \sin\theta_K)^2 (\Delta\theta)^2,$$

where

$$H_{ij} = \{(\cos\theta_i + \cos\theta_j)/(1 + \cos\theta_K)\} - 1 .$$

By θ_K we indicate the angle in space between tracks i and j. For the error on the angle measurements we adopt the mean value of the deviations of our measurements $\Delta\theta = 0.01$ rad.

Events with ε larger than $\Delta\varepsilon$ were not considered as due to elastic scattering. Thus, the stipulation of the requirements *a*), *b*) and *c*) brought us to exclude 4 events which will be analyzed later as due to inelastic scattering.

Angular measurements have been corrected for distortion effects, which were always rather small.

3. – Results and discussion.

3·1. *Cross-section for* $\bar{\text{p}}$-H *elastic scattering.* – The 15 elastic collisions considered above have been found on a total length of antiproton track $l = 72.17$ m; thus the mean free path turns out to be $\lambda = 4.81$ m. Table I shows the details of the events. Since our emulsions had a density of (3.847 ± 0.019) g/cm³, corresponding to a hydrogen concentration $c = (3.16 \pm 0.04) \cdot 10^{22}$ H-atoms/cm³, one obtains for the $\bar{\text{p}}$-H elastic scattering cross-section in the energy interval $(250 \div 30)$ MeV corresponding to a mean energy of 150 MeV

$$\sigma_{el} = \frac{1}{\lambda c} = (65 \pm 17) \text{ mb} .$$

1478

The mean value obtained from emulsions by other laboratories [1,2,8] is (77 ± 19) mb.

TABLE I.

Event	T (MeV)	$\Delta T/T$ (%)	$c = \varepsilon/2\pi$	$\cos\theta^*$
46	112.8	10	1.00 ± 0.12	0.79
48	200	6	0.90 ± 0.15	0.86
53	179.2	11	0.98 ± 0.17	0.65
91	159.0	4	1.00 ± 0.11	0.88
105	170	7	1.00 ± 0.11	0.77
211	81.0	39.5	0.96 ± 0.17	-0.07
214	240	29	0.95 ± 0.11	0.26
320	238.0	3	0.91 ± 0.14	0.87
321	232.1	4	0.96 ± 0.26	0.92
434	128.3	34	0.94 ± 0.09	0.28
436	180	17	0.99 ± 0.24	0.71
488	194.2	9	0.98 ± 0.21	0.79
494	98.2	23	1.00 ± 0.26	0.57
498	164.0	65	1.00 ± 0.14	-0.39
513	209	11	1.00 ± 0.08	0.83

T = antiproton energy at interaction.
ΔT = energy loss in collision.
θ^* = antiproton scattering angle in the C. M. S.

Since the two groups of measurements are homogeneous we can put together all present emulsion data with the result:

$$\sigma_{el} = (70.9 \pm 12.7) \text{ mb}$$

for $T_{\bar{p}}$ between 30 and 250 MeV (average kinetic energy 140 MeV). This value agrees, remarkably well, with the theoretical results of BALL and CHEW who give, at 140 MeV, $\sigma_{el} = 73$ mb.

We recall that as pointed out by BALL and CHEW σ_{el} is the cross-section which is the most sensitive to the details of the adopted nucleon-antinucleon interaction: thus for example, if the central well should deviate from complete absorption even only by a small amount the cross-section for elastic scattering would strongly decrease.

The value of σ_{el} obtained from 33 events observed in a propane bubble chamber amounts to $\sigma_{el} = (41 \pm 10)$ mb and refers to antiprotons scattered between 17° and 165° in the c.m.s. If one takes into account the solid angle

(7) A. C. E.: *Phys. Rev.*, **105**, 1037 (1957).
(8) A. G. EKSPONG, S. JOHNSON and B. E. RONNE: *Nuovo Cimento*, **8**, 84 (1958).

loss according to the angular distribution given by FULCO (1), one obtains $\sigma_{el} = (45.2 \pm 11)$ mb at 120 MeV. This value is significantly smaller than that found from emulsion work as well as from scintillation counter experiments: $\sigma_{el} = (72 \pm 10)$ mb at 133 MeV. The result of the latter authors are corrected geometrically according to Fulco's theory, taking a minimum cut-off angle of 14° and a maximum cut-off angle $\sim 90°$ in the centre of mass system.

3·2. *Angular distribution.* – The angular distribution of all events found so far in emulsions is shown in Fig. 2*a*, where θ^* is the antiproton scattering angle in the centre of mass system. The curve is that given by FULCO at 140 MeV. A comparison of the theory with the experimental results can be made because the shape of the angular distribution is rather insensitive to energy changes.

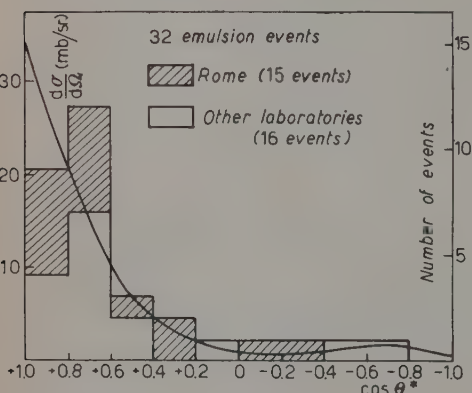

Fig. 2*a*.

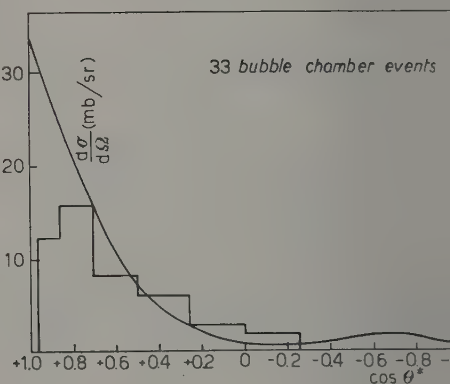

Fig. 2*b*.

The agreement is as satisfactory as we can expect because of the poor statistics. The theoretical minimum occurs at $\theta^* \sim 90°$, and the backwards cross-section comes out very small: the theoretical value, integrated over the forward and backward hemispheres is 68 and 5 mb against 28 and 4 events actually observed.

Fig. 2*b* shows a similar hystogram for the bubble chamber data. Some discrepancy between emulsion and bubble chamber data appears to arise from the region between 20° and 60°.

4. – Antiproton mass.

Previous determinations of the antiproton mass are accurate only within 3% (7,8).

Therefore we thought worth-while to use four of our elastic scatterings for

a determination of the mass of the antiproton, by a method different from those used by previous workers and which allows a more accurate result (9).

Only those events have been used in which after collision the antiproton annihilates at rest; and furthermore, the plane of three particles makes a small angle with the plane of the emulsion. With the latter requirement the correction for distortion was always smaller than 30′. In these events, both the proton and antiproton ranges after collision as well as the angles formed by these tracks with the incident antiproton track, are very accurately measured.

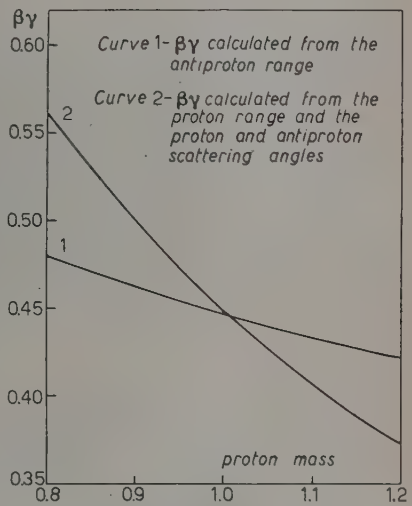

Fig. 3.

From these measurements one can obtain the value of the $\beta\gamma$ of the antiproton after collision, in two different ways, as a function of the antiproton mass.

For example, curve 1 in Fig. 3 has been obtained from the measurement of the antiproton range of the event $\bar{p}$ 434. Curve 2 has been obtained from the measurement of the proton range and of the angles, by means of transverse momentum balance. The point of intersection of the two curves provides the value of the antiproton mass.

Table II lists the mass-values. The errors quoted arise mainly from range measurements: the errors on the angles do not contribute appreciably. Due account was taken for the 1% uncertainty in the range energy relation (10).

TABLE II.

Event	Mass
46	0.985 ± 0.031
434	1.005 ± 0.030
494	1.035 ± 0.027
498	0.962 ± 0.029

(9) W. W. CHUPP, G. GOLDHABER, S. GOLDHABER, W. R. JOHNSON and J. E. LANNUTTI: *Phys. Rev.*, **99**, 1042 (1955).

(10) UCRL-2426 (rev.), vol. **2**.

As final result we obtained

$$m_{\bar{p}} = (0.998 \pm 0.015) \text{ proton masses },$$

where the error has been computed from the errors of the single determinations and agrees very well with the external error of the distribution: 0.014.

* * *

We express our deep gratitude to Dr. E. J. LOFGREN, head of the Bevatron and to Prof. E. SEGRÈ, Prof. O. CHAMBERLAIN and Prof. G. GOLDHABER for preparing the beam and carrying out the exposure. We thank Professor AMALDI for his continuous interest and help throughout this work.

RIASSUNTO

Vengono riportati i dati relativi a 15 scattering elastici antiprotone-protone. Si ricava la distribuzione angolare e la sezione d'urto $\sigma_{el} = (65.7 \pm 17)$ mb. Mediando con i valori ottenuti in emulsione presso altri laboratori si ricava: $\sigma_{el} = (70.9 \pm 12.7)$ mb. Distribuzione angolare e sezione d'urto sono in buon accordo con le previsioni teoriche basate sulla teoria di Ball e Chew. Quattro eventi vengono usati per una determinazione accurata della massa dell'antiprotone, ricavando un valore $m_{\bar{p}} = (0.998 \pm 0.015)$ masse protoniche.

IL NUOVO CIMENTO Vol. XII, N. 6 16 Giugno 1959

Connections between Generalized Singular Functions and Bessel Functions.

E. Montaldi

Istituto di Scienze Fisiche dell'Università - Milano
Istituto Nazionale di Fisica Nucleare - Sezione di Milano

(ricevuto il 24 Febbraio 1959)

Summary. — After having introduced a suitable extension of the concept of « generalized singular function », a somewhat detailed mathematical investigation of the structure of the integrals involved is made. Among the main results, various integral relationships are obtained, which show the intimate connection between generalized singular functions and Bessel functions. A further elaboration of our formulae, leading to some new multiple integrals involving Bessel functions, will be given in a subsequent paper.

1. – In a recent paper (¹), Källén and Wilhelmsson have treated the so called « generalized singular functions », and have shown that the theory of these functions rests essentially on the consideration of the following integral:

$$
\begin{aligned}
(1.1)\qquad & F(x_1, \dots, x_4) = \\
& = \int \mathrm{d}^4 p_1 \mathrm{d}^4 p_2 \mathrm{d}^4 p_3 \mathrm{d}^4 p_4 \delta(p_1^2 + 1) \prod_{j=2}^{4} \delta(p_j^2 - 1) \prod_{h<k=1}^{4} \delta(p_h \cdot p_k) \theta(p_{14}) \exp\left[i \sum_{k=1}^{4} p_k \cdot x_k\right] ,
\end{aligned}
$$

(the symbols are explained below). Later (²) it was recognized that, under certain circumstances, it appears more convenient to study an integral which

(¹) G. Källén and H. Wilhelmsson: *Generalized Singular Functions* (Copenhagen, 1957).
(²) E. Montaldi: *Nuovo Cimento*, **11**, 149 (1959).

is formally analogous to (1.1), the difference lying in the fact that the integrations are now over the components of only three four vectors. In the present note, we start from a suitable generalization of (1.1) by introducing certain multiple integrals; successively, after having established their fundamental properties, we infer from these various formulae, in which the intimate connection between generalized singular functions and Bessel functions is made evident. We shall deal only with real quantities, but our final results hold —*mutatis mutandis*—in the complex case also. For simplicity's sake, we premise to the description of the main results an introductory section, devoted to the proof of some formulae which will be systematically used in the following.

2. – In this section, we shall be concerned with some preliminary results, on which all our later considerations will be based.

First of all, we prove the formula [3]:

$$\int \mathrm{d}^n \boldsymbol{u}\, \delta(\boldsymbol{u}^2 - \lambda) \prod_{r=1}^{m} \delta(\boldsymbol{u}\cdot\boldsymbol{x}_r - \mu_r) = \frac{\pi^{(n-m)/2}}{\Gamma((n-m)/2)\, D^{(n-m-1)/2}}\, A^{(n-m-2)/2}\theta(A)\,, \tag{2.1}$$

where: δ is the well-known Dirac's improper function;

$\boldsymbol{x}_1\ \boldsymbol{x}_2, \ldots, \boldsymbol{x}_m$ $(1 \leqslant m \leqslant n-1)$ are arbitrary vectors of S_n;

the quantities $\lambda_1, \mu_1, \ldots, \mu_m$ are some constants;

$$D = \mathrm{Det}\ |\boldsymbol{x}_r\cdot\boldsymbol{x}_s|\,; \qquad A = \left|\begin{array}{cccc} \lambda & \mu_1 & \ldots & \mu_m \\ \mu_1 & & & \\ \vdots & & D & \\ \mu_m & & & \end{array}\right|\,. \tag{2.2}$$

and, finally, θ is the step function defined by:

$$\theta(x) = \begin{cases} 1\,, & x > 0\,, \\ 0\,, & x < 0\,. \end{cases} \tag{2.3}$$

---

[3] The symbol $\int \mathrm{d}^n\boldsymbol{u}$ denotes, as usual, integration — between infinite limits — over the components of a vector belonging to a n-dimensional Euclidean space S_n; similarly, the symbol $\int \mathrm{d}^n u$ means integration – always between infinite limits — over the components of a vector belonging to a pseudoeuclidean space S'_n, with the metrics: $\mathrm{d}s^2 = \mathrm{d}x_1^2 + \ldots + \mathrm{d}x_{n-1}^2 - \mathrm{d}x_n^2$. The scalar products will be denoted by $\boldsymbol{u}\cdot\boldsymbol{v}$ $(=\sum_{r=1}^{n} u_r v_r)$, or by $u\cdot v$ $(=\sum_{r=1}^{n-1} u_r v_r - u_n v_n)$, respectively; in particular, $\boldsymbol{u}^2$ (u^2) will denote the square of a vector lying in S_n (S'_n).

[If, for $n=m+2$, the determinant A vanishes identically, we must put $\theta(A)=\frac{1}{2}$; this follows immediately from the formal relation $\int_0^\infty \delta(x)\,\mathrm{d}x = \frac{1}{2}\int_{-\infty}^{\infty}\delta(x)\,\mathrm{d}x=\frac{1}{2}$]. To prove (2.1), we shall apply an inductive procedure, starting from the simplest case ($m=1$) and passing successively to the values $m=2, 3, \ldots$. For $m=1$, we must consider the integral:

$$\int \mathrm{d}^n \boldsymbol{u}\,\delta(\boldsymbol{u}^2-\lambda)\,\delta(\boldsymbol{u}\cdot\boldsymbol{x}_1-\mu_1)\,; \tag{2.4}$$

since this—like (2.1)—is obviously invariant with respect to the rotation group in S_n, it is convenient to perform the calculation in the particular system —which we shall mark by an apex—where the vector $\boldsymbol{x}_1$ reduces to a single component—the n-th, say—not identically zero. Thus, we get:

$$\int \mathrm{d}^n \boldsymbol{u}\,\delta(\boldsymbol{u}^2-\lambda)\,\delta(\boldsymbol{u}\cdot\boldsymbol{x}_1-\mu_1) =$$
$$=\int \mathrm{d}^n \boldsymbol{u}\,\delta(\boldsymbol{u}^2-\lambda)\,\delta(u_n x'_{1,n}-\mu_1) = \frac{1}{|x'_{1,n}|}\int \mathrm{d}^{n-1}\boldsymbol{u}\,\delta\left(\boldsymbol{u}^2+\frac{\mu_1^2}{x'^2_{1,n}}-\lambda\right);$$

now, changing to polar variables, one sees immediately that [4]:

$$\int \mathrm{d}^n \boldsymbol{u}\,\delta(\boldsymbol{u}^2-\alpha) = 2\,\frac{\pi^{n/2}}{\Gamma(n/2)}\int_0^\infty u^{n-1}\,\delta(u^2-\alpha)\,\mathrm{d}u = \frac{\pi^{n/2}}{\Gamma(n/2)}\,\alpha^{(n/2)-1}\theta(\alpha)\,, \tag{2.5}$$

therefore, since obviously $x'^2_{1,n}=\boldsymbol{x}_1^2$, we have finally:

$$\int \mathrm{d}^n \boldsymbol{u}\,\delta(\boldsymbol{u}^2-\lambda)\,\delta(\boldsymbol{u}\cdot\boldsymbol{x}_1-\mu_1) = \frac{\pi^{(n-1)/2}}{\Gamma((n-1)/2)}\,\frac{(\lambda\boldsymbol{x}_1^2-\mu_1^2)^{(n-3)/2}}{|\boldsymbol{x}_1|^{n-2}}\,\theta(\lambda\boldsymbol{x}_1^2-\mu_1^2)\,, \tag{2.6}$$

(with $|\boldsymbol{x}_1|=(\boldsymbol{x}_1^2)^{\frac{1}{2}}$), which coincides with (2.1), specialized for $m=1$. Now, let $m=2$; in the system where $\boldsymbol{x}_2\equiv(0, 0, \ldots, x'_{2,n})$, we can write:

$$\int \mathrm{d}^n \boldsymbol{u}\,\delta(\boldsymbol{u}^2-\lambda)\,\delta(\boldsymbol{u}\cdot\boldsymbol{x}_1-\mu_1)\,\delta(\boldsymbol{u}\cdot\boldsymbol{x}_2-\mu_2) =$$
$$=\int \mathrm{d}^n \boldsymbol{u}\;\delta(\boldsymbol{u}^2-\lambda)\,\delta(\boldsymbol{u}\cdot\boldsymbol{x}'_1-\mu_1)\,\delta(u_n x'_{2,n}-\mu_2)\,,$$

[4] Here, use is made of the formula: $\delta(f(x))=\sum_r (1/|f'(x_r)|)\delta(x-x_r)$, the sum being over all real roots of the equation $f(x)=0$.

that is, denoting by $\boldsymbol{x}_1''$ the $(n-1)$ dimensional vector whose components are $(x'_{1,1}, \dots, x'_{1,n-1})$ (5):

$$\int d^n \boldsymbol{u}\,\delta(\boldsymbol{u}^2-\lambda)\,\delta(\boldsymbol{u}\cdot\boldsymbol{x}_1-\mu_1)\,\delta(\boldsymbol{u}\cdot\boldsymbol{x}_2-\mu_2) =$$

$$= \frac{1}{|x'_{2,n}|}\int d^{n-1}\boldsymbol{u}\,\delta\left(\boldsymbol{u}^2+\frac{\mu_2^2}{x'^2_{2,n}}-\lambda\right)\delta\left(\boldsymbol{u}\cdot\boldsymbol{x}_1''+\mu_2\frac{x'_{1,n}}{x'_{2,n}}-\mu_1\right);$$

if we now make use of (2.6) and then go back to the original system, we get (2.1), with $m=2$. The extension to the values $m=3, 4, \dots,$ is quite similar.

By the same technique, we shall now prove that:

$$\int d^n \boldsymbol{u}\,\delta(\boldsymbol{u}^2-1)\prod_{r=1}^{m}\delta(\boldsymbol{u}\cdot\boldsymbol{x}_r)\exp[\alpha\boldsymbol{u}\cdot\boldsymbol{y}] = \tag{2.7}$$

$$= \frac{\pi^{(n-m)/2}}{\sqrt{D}}\left(\frac{1}{2}\alpha\sqrt{\frac{B}{D}}\right)^{1-(n-m)/2} I_{((n-m)/2)-1}\left(\alpha\sqrt{\frac{B}{D}}\right),$$

$(1 \leqslant m \leqslant n-1)$, where D has still the form (2.2), while:

$$B = \begin{vmatrix} \boldsymbol{y}^2 & \boldsymbol{y}\cdot\boldsymbol{x}_1 & \dots & \boldsymbol{y}\cdot\boldsymbol{x}_m \\ \boldsymbol{y}\cdot\boldsymbol{x}_1 & & & \\ \vdots & & D & \\ \boldsymbol{y}\cdot\boldsymbol{x}_m & & & \end{vmatrix}, \tag{2.8}$$

and $I_k(x) = \exp[-\frac{1}{2}\pi i k]J_k(x\exp[\pi i/2])$ is the modified Bessel function of the first kind and of the k-th order. According to what we saw above, it will suffice to consider the simplest case $(m=1)$. Performing the calculation in the usual system, we have:

$$\int d^n\boldsymbol{u}\,\delta(\boldsymbol{u}^2-1)\,\delta(\boldsymbol{u}\cdot\boldsymbol{x}_1)\exp[\alpha\boldsymbol{u}\cdot\boldsymbol{y}] = \frac{1}{|x'_{1,n}|}\int d^{n-1}\boldsymbol{u}\,\delta(\boldsymbol{u}^2-1)\exp[\alpha\boldsymbol{u}\cdot\boldsymbol{y}''],$$

$\boldsymbol{y}''$ being the $(n-1)$-dimensional vector with components $(y'_1, \dots, y'_{n-1})$; that is, changing to polar variables, and then going back to the original system

(5) It will be observed that $x'^2_{2,n}=\boldsymbol{x}_2^2$, $x'_{1,n}x'_{2,n}=\boldsymbol{x}_1\cdot\boldsymbol{x}_2$ and, finally, $\boldsymbol{x}_1''^2+x'^2_{1,n}=\boldsymbol{x}_1^2$, whence:

$$\boldsymbol{x}_1''^2 = \boldsymbol{x}_1^2 - \frac{(\boldsymbol{x}_1\cdot\boldsymbol{x}_2)^2}{\boldsymbol{x}_2^2}.$$

(see footnote (5)):

$$(2.9)\quad \int \mathrm{d}^n \boldsymbol{u}\,\delta(\boldsymbol{u}^2-1)\,\delta(\boldsymbol{u}\cdot\boldsymbol{x}_1)\exp[\alpha\boldsymbol{u}\cdot\boldsymbol{y}] =$$

$$= \frac{1}{|\boldsymbol{x}_1|}\cdot 2\,\frac{\pi^{(n-2)/2}}{\Gamma((n-2)/2)}\int_0^\infty u^{n-2}\delta(u^2-1)\,\mathrm{d}u\int_0^\pi \exp\left[\alpha u\sqrt{\boldsymbol{y}^2-\frac{(\boldsymbol{x}_1\cdot\boldsymbol{y})^2}{\boldsymbol{x}_1^2}}\cos\theta\right](\sin\theta)^{n-3}\,\mathrm{d}\theta =$$

$$= \frac{1}{|\boldsymbol{x}_1|}\,\frac{\pi^{(n-2)/2}}{\Gamma((n-2)/2)}\int_0^\pi \exp\left[\alpha\sqrt{\boldsymbol{y}^2-\frac{(\boldsymbol{x}_1\cdot\boldsymbol{y})^2}{\boldsymbol{x}_1^2}}\cos\theta\right](\sin\theta)^{n-3}\,\mathrm{d}\theta =$$

$$= \frac{\pi^{(n-1)/2}}{|\boldsymbol{x}_1|^{(5-n)/2}}\left(\frac{1}{2}\alpha\sqrt{\boldsymbol{x}_1^2\boldsymbol{y}^2-(\boldsymbol{x}_1\cdot\boldsymbol{y})^2}\right)^{-(n-3)/2} I_{(n-3)/2}\left(\frac{\alpha}{|\boldsymbol{x}_1|}\sqrt{\boldsymbol{x}_1^2\boldsymbol{y}^2-(\boldsymbol{x}_1\cdot\boldsymbol{y})^2}\right),$$

and this is indeed (2.7), for $m=1$; here, use has been made of the well-known Poisson's integral formula (6):

$$(2.10)\qquad I_k(x) = \frac{1}{\sqrt{\pi}\,\Gamma(k+\frac{1}{2})}\left(\frac{1}{2}x\right)^k\int_0^\pi \exp[x\cos\theta](\sin\theta)^{2k}\,\mathrm{d}\theta\,.$$

In the Appendix, after having established a theorem on determinants, we shall show that it is possible to interpret the ratio B/D as the square of a vector (belonging to S_{n-m}), whose components will be given explicitly in terms of the quantities y_s and $x_{r,s}$. We now conclude this section giving a reduction formula for the integral:

$$(2.11)\quad C_{k,l}(\alpha,\beta,\gamma) =$$

$$= \int_0^\infty \frac{u^k\,\mathrm{d}u}{\sqrt{1+u^2}}\exp[-\alpha\sqrt{1+u^2}]\cosh(\beta u)\int_0^\pi \exp[\gamma u\cos\theta](\sin\theta)^l\,\mathrm{d}\theta\,,$$

and performing its explicit calculation for the case $k=2(m+1)$, $l=2m+1$

(6) We remark that the validity of (2.10) implies the condition $\mathrm{Re}\,k > -\frac{1}{2}$. The deduction of (2.9), therefore, presupposes $n \geqslant 3$; however, (2.9) holds for $n=2$ also, as one easily verifies by direct calculation. We note also that if $n=3$, the θ-integration has to be made between 0 and 2π; in this case, however, we must omit the factor 2 before the integral, which comes from the transformation of the volume element.

$(m = 0, 1, 2 \ldots)$ (7). From (2.11), it follows immediately that:

$$C_{k+2,\,l+2} = C_{k+2,\,l} - D_\gamma^2\, C_{k,\,l}\,, \qquad \left(D_\gamma = \frac{\partial}{\partial\gamma}\right),$$

whence, by iteration:

$$C_{k+2r,\,l+2r} = \sum_{j=0}^{r} (-1)^j \binom{r}{j} D_\gamma^{2j}\, C_{k+2r,\,2j,\,l}\,, \tag{2.12}$$

which is the reduction formula we wanted to obtain. Now consider:

$$C_{2m,1} = \int_0^\infty \frac{u^{2m}\,\mathrm{d}u}{\sqrt{1+u^2}} \exp\left[-\alpha\sqrt{1+u^2}\right]\cosh(\beta u)\int_0^\pi \exp\left[\gamma u \cos\theta\right]\sin\theta\,\mathrm{d}\theta =$$

$$= \frac{2}{\gamma}\int_0^\infty \frac{u^{2m-1}\,\mathrm{d}u}{\sqrt{1+u^2}}\exp\left[-\alpha\sqrt{1+u^2}\right]\cosh(\beta u)\sinh(\gamma u) =$$

$$= \frac{1}{\gamma} D_\gamma^{2m-1}\int_{-\infty}^{\infty} \frac{\mathrm{d}u}{\sqrt{1+u^2}} \exp\left[-\alpha\sqrt{1+u^2}\right]\cosh(\beta u)\cosh(\gamma u)\,; \qquad (m \geq 1).$$

Putting $u = \sinh t$, and noticing that:

$$\int_{-\infty}^{\infty} \exp\left[-\lambda\cosh t - \mu\sinh t\right]\mathrm{d}t = 2K_0\left(\sqrt{\lambda^2-\mu^2}\right), \qquad (\operatorname{Re}\lambda > |\operatorname{Re}\mu|), \tag{2.13}$$

where $K_0(x)$ is the modified Bessel function of the third kind and zeroth order (8), we get:

$$C_{2m,1} = \frac{1}{\gamma} D_\gamma^{2m-1}\left\{K_0\left(\sqrt{\alpha^2-(\beta+\gamma)^2}\right) + K_0\left(\sqrt{\alpha^2-(\beta-\gamma)^2}\right)\right\},$$

(7) In (2.11), the parameters α, β, γ, k and l may be real or complex; for convergence of the integral, it suffices that: $\operatorname{Re}\alpha > |\operatorname{Re}\beta| + |\operatorname{Re}\gamma|$, $\operatorname{Re} k > -1$, $\operatorname{Re} l > -1$.

(8) We follow here the definition given in ERDÉLYI, MAGNUS, OBERHETTINGER and TRICOMI: *Higher transcendental functions*, vol. 2, p. 5:

$$K_\mu(z) = \tfrac{1}{2}\pi \operatorname{cosec}(\pi\mu)\left\{I_{-\mu}(z) - I_\mu(z)\right\}.$$

(2.13) follows from the well-known integral formula:

$$K_\mu(z)\,\Gamma\left(\mu+\frac{1}{2}\right) = \sqrt{\pi}\left(\frac{1}{2}z\right)^\mu \cdot \int_0^\infty \exp\left[-z\cosh t\right]\cdot(\sinh t)^{2\mu}\,\mathrm{d}t \left(\operatorname{Re} z > 0,\ \operatorname{Re}\mu > -\frac{1}{2}\right).$$

writing: $\lambda\cosh t + \mu\sinh t = \sqrt{\lambda^2-\mu^2}\cosh(t+\omega)$, with $\omega = \cosh^{-1}\left(\lambda/\sqrt{\lambda^2-\mu^2}\right)$.

whence, by substitution into (2.12):

$$(2.14)\quad C_{2(m+1),2m+1}(\alpha,\beta,\gamma)=\sum_{j=0}^{m}(-1)^j\binom{m}{j}D_\gamma^{2j}\left\{\frac{1}{\gamma}D_\gamma^{2(m-j)+1}\left[K_0(\sqrt{A^{(+)}})+K_0(\sqrt{A^{(-)}})\right]\right\},$$

with:

$$(2.14a)\qquad A^{(\pm)}=\alpha^2-(\beta\pm\gamma)^2\,.$$

3. – After these introductory remarks, we now go over to define the integrals on which we shall base all our later consideration. Namely, we shall put:

$$(3.1)\quad I_n^{(r)}\left(\begin{array}{c|c}x_1 & x_2\,\dots\,x_r\\ \alpha_1 & \alpha_2\,\dots\,\alpha_r\end{array}\right)=$$

$$=\int\!\dots\!\int\prod_{i=1}^{r}\mathrm{d}^n u_i\,\delta(u_1^2+1)\prod_{j=2}^{r}\delta(u_j^2-1)\prod_{h<k=1}^{r}\delta(u_h\cdot u_k)\theta(u_{1,n})\exp\left[\sum_{s=1}^{r}\alpha_s u_s\cdot x_s\right],$$

($n\geq 2$, $r\leq n$); moreover, for simplicity's sake, we shall suppose ([9]) that:

α) The constants α_1, α_2, ..., α_r are all real and positive.

β) The vectors x_1, x_2, ..., x_r (whose components are also supposed to be all real) lie in the future of the « hypercone » of the space S'_n; that is they satisfy the conditions:

$$(3.2)\qquad x_{j}^2<0\,,\qquad x_{j,n}>0\qquad (1\leq j\leq r).$$

We shall not attempt here to perform the explicit calculation of the integrals (3.1) for arbitrary values of r; we shall rather make use of some simple properties of them to obtain various results (among these, in particular, a representation of the functions $K_n(x)$ — with n integer or half-integer — in terms of multiple integrals). We state now the relevant properties, and give their demonstration:

A) For $r=1$ we have the formula:

$$(3.3)\quad I_n^{(1)}\left(\begin{array}{c|c}x_1 & \\ \alpha_1 & \end{array}\right)=\int\mathrm{d}^n u\,\delta(u^2+1)\theta(u_n)\exp[\alpha_1 u\cdot x_1]=$$

$$=\pi^{(n/2)-1}\left(\frac{1}{2}\alpha_1\sqrt{-x_1^2}\right)^{1-(n/2)}K_{(n/2)-1}\left(\alpha_1\sqrt{-x_1^2}\right),$$

([9]) These hypotheses, which we introduce essentially to simplify the calculations, can be replaced, case by case, with less stringent assumptions, as will appear clearly from later developments. Noticing that (3.1) remains unchanged if the sign of one (or more) product $\alpha_k x_k$ ($2\leq k\leq r$) is inverted, we can also state conditions (α) and (β) as follows: α_1, α_2, ..., α_r real (with $\alpha_1>0$); x_1, x_2, ..., x_r inside the « hypercone » of the space S'_n (with $x_{1,n}>0$).

Indeed, by virtue of the above mentioned hypothesis, we can perform the calculation in the system where $x_1 \equiv (0, 0, ..., \sqrt{-x_1^2})$, obtaining:

$$\int d^n u\, \delta(u^2-1)\theta(u_n) \exp[\alpha_1 u \cdot x_1] = \int d^n u\, \delta(u^2-1)\theta(u_n) \exp[-\alpha_1 u_n \sqrt{-x_1^2}\,] =$$

$$= \frac{1}{2}\int \frac{d^{n-1}\boldsymbol{u}}{\sqrt{1+\boldsymbol{u}^2}} \exp[-\alpha_1 \sqrt{-x_1^2}\sqrt{1+\boldsymbol{u}^2}];$$

changing to polar variables, and then putting $|\boldsymbol{u}| = \sinh t$, we get—remembering foot-note ([8])—just (3.3). In this proof, use has been made of the obvious invariance property of the integrals (3.1) with respect to the transformations $L^{(\ )}$ which leave invariant the square of a vector of the space S'_n, without inverting the sign of the n-th component; moreover, we remark explicitly that the hypotheses $\alpha_1 > 0$, $x_{1.n} > 0$, $x_1^2 < 0$ are here essential; otherwise, the result would not converge ([10]).

B) For $r = 2$, the integral (3.1) can be worked out exactly only if $n = 4$; the case n even > 4 can be reduced to a single integration; in the remaining cases ($n = 2$, or n odd $\geqslant 3$) it is not possible to get a particularly simple result, so that we shall limit ourselves to consider only even values of $n \geqslant 4$. In other words, we shall study the integral:

$$(3.4)\quad I_n^{(2)}\begin{pmatrix} x_1 & | & x_2 \\ \alpha_1 & | & \alpha_2 \end{pmatrix} = \int d^n u\, d^n v\, \delta(u^2-1)\delta(v^2-1)\delta(u\cdot v)\theta(u_n) \exp[\alpha_1 u\cdot x_1 + \alpha_2 v \cdot x_2]\,,$$

assuming n to be of the form:

$$(3.5)\qquad n = 4 + 2m \qquad (m = 0, 1, 2, ...).$$

Noticing u — by virtue of the factor $\delta(u^2+1)\theta(u_n)$ — lies in the future of the hypercone — we can, first of all, perform the v — integration in the system were $u = (0, 0, ..., 1)$. In this way, we easily get the formula:

$$\int d^n v\, \delta(v^2-1)\delta(v\cdot u) \exp[\alpha_2 v\cdot x_2] = \int d^n v\, \delta(v^2-1)\,\delta(-v_n) \exp[\alpha_2 v \cdot y] =$$

$$= \int d^{n-1}\boldsymbol{v}\, \delta(\boldsymbol{v}^2-1) \exp[\alpha_2 \boldsymbol{v}\cdot\boldsymbol{y}]\,,$$

([10]) If $\alpha_1 < 0$, the result is still convergent, provided that also $x_{1.n} < 0$, and, obviously, with x_1 inside the hypercone. More generally, therefore, we can say that the convergence conditions of (3.3) — dealing always with real quantities — are $\alpha_1 x_{1.n} > 0$, $x_1^2 < 0$.

($y = (\boldsymbol{y}, y_n)$ being the vector x_2 in this system); thus, proceeding as in the deduction of (2.9):

$$\int \mathrm{d}^n v\,\delta(v^2-1)\,\delta(v\cdot u)\exp[\alpha_2 v\cdot x_2] = \pi^{(n-1)/2}\left(\frac{1}{2}\alpha_2|\boldsymbol{y}|\right)^{-(n-3)/2} I_{(n-3)/2}(\alpha_2|\boldsymbol{y}|)\,.$$

In order to go back to the original system, we make use of the relations $\boldsymbol{y}^2 - y_n^2 = y^2$, $-y_n = u\cdot x_2$, from which one obtains immediately:

$$|\boldsymbol{y}| = \sqrt{x_2^2 + (u\cdot x_2)^2}\,;$$

therefore, finally:

$$\text{(3.6)}\quad \int \mathrm{d}^n v\,\delta(v^2-1)\,\delta(v\cdot u)\exp[\alpha_2 v\cdot x_2] =$$
$$= \pi^{(n-1)/2}\left(\frac{1}{2}\alpha_2\sqrt{x_2^2+(u\cdot x_2)^2}\right)^{-(n-3)/2} I_{(n-3)/2}\left(\alpha_2\sqrt{x_2^2+(u\cdot x_2)^2}\right)\,.$$

By substitution in (3.4), we have:

$$\text{(3.7)}\quad I_n^{(2)}\begin{pmatrix} x_1 & x_2 \\ \alpha_1 & \alpha_2\end{pmatrix} = \pi^{(n-1)/2}\int \mathrm{d}^n u\,\delta(u^2+1)\,\theta(u_n)\exp[\alpha_1 u\cdot x_1]\cdot$$
$$\cdot\left(\frac{1}{2}\alpha_2\sqrt{x_2^2+(u\cdot x_2)^2}\right)^{-(n-3)/2} I_{(n-3)/2}\left(\alpha_2\sqrt{x_2^2+(u\cdot x_2)^2}\right)\,.$$

Now, making use of the assumption (β), we go over to the system—marked by an apex—where $x_2 = (0, 0, \ldots, \sqrt{-x_2^2})$. In this system, (3.7) becomes:

$$\text{(3.8)}\quad I_n^{(2)}\begin{pmatrix} x_1 & x_2 \\ \alpha_1 & \alpha_2\end{pmatrix} = \pi^{(n-1)/2}\int \mathrm{d}^n u\,\delta(u^2+1)\,\theta(u_n)\exp[\alpha_1 u\cdot x_1']\cdot$$
$$\cdot\left(\frac{1}{2}\alpha_2|\boldsymbol{u}|\sqrt{-x_2^2}\right)^{-(n-3)/2} I_{(n-3)/2}\left(\alpha_2|\boldsymbol{u}|\sqrt{-x_2^2}\right)\,;$$

remembering the integral formula (which easily follows from (2.10)):

$$\text{(3.9)}\qquad I_k(x) = \frac{1}{\sqrt{\pi}\,\Gamma(k+\frac{1}{2})}\left(\frac{1}{2}x\right)^k\int_{-1}^{1}(1-t^2)^{k-\frac{1}{2}}\cosh(xt)\,\mathrm{d}t\,.$$

(3.8) can be further worked out as follows:

$$I_n^{(2)}\begin{pmatrix} x_1 & x_2 \\ \alpha_1 & \alpha_2 \end{pmatrix} = \frac{1}{2}\frac{\pi^{(n-2)/2}}{\Gamma((n-2)/2)}\int_{-1}^{1}(1-t^2)^{(n-4)/2}\,\mathrm{d}t\,\cdot$$

$$\cdot\int \mathrm{d}^{n-1}\boldsymbol{u}(\boldsymbol{u}^2+1)^{-\frac{1}{2}}\exp[-\alpha_1 x'_{1,n}\sqrt{1+\boldsymbol{u}^2}+\alpha_1\boldsymbol{u}\cdot\boldsymbol{x}'_1]\cosh(\alpha_2 t|\boldsymbol{u}|\sqrt{-x_2^2}) =$$

$$=\left\{\frac{\pi^{(n-2)/2}}{\Gamma((n-2)/2)}\right\}^2\int_{-1}^{1}(1-t^2)^{(n-4)/2}\,\mathrm{d}t\,\cdot$$

$$\cdot\int_0^\infty \frac{u^{n-2}\,\mathrm{d}u}{\sqrt{1+u^2}}\exp[-\alpha_1 x'_{1,n}\sqrt{1+u^2}]\cosh(\alpha_2 t u\sqrt{-x_2^2})\int_0^\pi \exp[\alpha_1 u|\boldsymbol{x}'_1|\cos\theta](\sin\theta)^{n-3}\mathrm{d}\theta\,.$$

Finally, by virtue of (3.5):

$$(3.10)\qquad I_{2m+4}^{(2)}\begin{pmatrix} x_1 & x_2 \\ \alpha_1 & \alpha_2 \end{pmatrix} = \frac{\pi^{2(m+1)}}{(m!)^2}\int_1^1(1-t^2)^m\,\mathrm{d}t\,C_{2(m+1),\,2m+1}(\alpha_1 x'_{1,n},\,\alpha_2 t\sqrt{-x_2^2},\,\alpha_1|\boldsymbol{x}'_1|)\,,$$

the C function being defined in accordance with (2.14). The convergence condition—see foot-note (7)—is expressed by the inequality:

$$\alpha_1 x'_{1,n} > \alpha_2\sqrt{-x_2^2}+\alpha_1|\boldsymbol{x}'_1|\,,$$

which, written in the original system, becomes (11):

$$(3.11)\qquad \alpha_2^2x_2^2-\alpha_1^2x_1^2-2\alpha_1\alpha_2\sqrt{(x_1\cdot x_2)^2-x_1^2x_2^2}>0\,.$$

We must remark that, in our case, it is not possible to apply (2.14) as it stands; one has to make use of a small device, writing:

$$(3.12)\qquad C_{2m+2,2m+1}(\alpha_1 x'_{1,n},\,\alpha_2 t\sqrt{-x_2^2},\,\alpha_1|\boldsymbol{x}'_1|) =$$

$$=\sum_{j=0}^{m}(-1)^j\binom{m}{j}D_\gamma^{2j}\left\{\frac{1}{\gamma}D_\gamma^{2(m-j)+1}[K_0(\sqrt{M^{(+)}})+K_0(\sqrt{M^{(-)}})]\right\},$$

---

(11) More generally, if we restrict the hypotheses (α) and (β) to the reality condition only, the convergence of (3.4) is secured if the inequalities: $|\alpha_1||\boldsymbol{x}_1|+|\alpha_2||\boldsymbol{x}_2| < \alpha_1 x_{1,n}\pm\alpha_2 x_{2,n}$ hold, as can be seen from (3.7).

with:

$$M^{(\pm)} = \alpha_1^2 x'^2_{1,n} - (\alpha_2 t\sqrt{-x_2^2} \pm \gamma)^2 \tag{3.12a}$$

and replacing γ with $\alpha_1|\boldsymbol{x}_1'|$ once the indicated differentiations have been performed. Thus we have stated the following result: « The integral $I^{(2)}_{2m+4}\begin{pmatrix} x_1 & x_2 \\ \alpha_1 & \alpha_2\end{pmatrix}$, under the hypotheses ($\alpha$) and ($\beta$), can be expressed in terms of the quantities:

$$I_m^{(\pm)} = \int_{-1}^{1} (1-t^2)^m K_0\left(\sqrt{\alpha_1^2 x'^2_{1,n} - (\alpha_2 t\sqrt{-x_2^2} \pm \gamma)^2}\right) dt\,; \tag{3.13}$$

namely, one has:

$$I^{(2)}_{2m+4}\begin{pmatrix} x_1 \mid x_2 \\ \alpha_1 & \alpha_2\end{pmatrix} = \frac{\pi^{2(m+1)}}{(m!)^2}\sum_{j=0}^{m}(-1)^j\binom{m}{j} D_\gamma^{2j}\left\{\frac{1}{\gamma}\, D_\gamma^{2(m-j)+1}\left[I_m^{(+)} + I_m^{(-)}\right]\right\}, \tag{3.13a}$$

provided that, after having performed the differentiations, one replaces γ with $\alpha_1|\boldsymbol{x}_1'|$ ».

Going back from the « primed » system to the original one, the final result will hold also if we abandon the hypotheses (α) and (β), provided only that the convergence condition written in foot-note ([11]) is satisfied.

In particular, if $m = 0$, we have:

$$\begin{aligned} I_4^{(2)}\begin{pmatrix} x_1 \mid x_2 \\ \alpha_1 \mid \alpha_2\end{pmatrix} &= \frac{\pi^2}{\gamma}\frac{\partial}{\partial\gamma}\int_{-1}^{1}\Big\{K_0\left(\sqrt{\alpha_1^2 x'^2_{1,n} - (\alpha_2 t\sqrt{-x_2^2} + \gamma)^2}\right) + \\ &\quad + K_0\left(\sqrt{\alpha_1^2 x'^2_{1,n} - (\alpha_2 t\sqrt{-x_2^2} - \gamma)^2}\right)\Big\}_{\gamma\to\alpha_1|\boldsymbol{x}_1'|} dt = \\ &= \frac{\pi^2}{\alpha_1|\boldsymbol{x}_1'|}\frac{1}{\alpha_2\sqrt{-x_2^2}}\int_{-1}^{1}\frac{\partial}{\partial t}\Big\{K_0\left(\sqrt{\alpha_1^2 x'^2_{1,n} - (\alpha_2 t\sqrt{-x_2^2} + \alpha_1|\boldsymbol{x}_1'|)^2}\right) - \\ &\quad - K_0\left(\sqrt{\alpha_1^2 x'^2_{1,n} - (\alpha_2 t\sqrt{-x_2^2} - \alpha_1|\boldsymbol{x}_1'|)^2}\right)\Big\} dt = \frac{2\pi^2}{\alpha_1\alpha_2|\boldsymbol{x}_1'|\sqrt{-x_2^2}}\cdot \\ &\quad \cdot\Big\{K_0\left(\sqrt{\alpha_1^2 x'^2_{1,n} - (\alpha_2\sqrt{-x_2^2} + \alpha_1|\boldsymbol{x}_1'|)^2}\right) - K_0\left(\sqrt{\alpha_1^2 x'^2_{1,n} - (\alpha_2\sqrt{-x_2^2} - \alpha_1|\boldsymbol{x}_1'|)^2}\right)\Big\} \\ &= \frac{2\pi^2}{\alpha_1\alpha_2\sqrt{(x_1\cdot x_2)^2 - x_1^2x_2^2}}\Big\{K_0\left(\sqrt{\alpha_2^2x_2^2 - \alpha_1^2x_1^2 - 2\alpha_1\alpha_2\sqrt{(x_1\cdot x_2)^2 - x_1^2x_2^2}}\right) - \\ &\quad - K_0\left(\sqrt{\alpha_2^2x_2^2 - \alpha_1^2x_1^2 + 2\alpha_1\alpha_2\sqrt{(x_1\cdot x_2)^2 - x_1^2x_2^2}}\right)\Big\}. \end{aligned} \tag{3.14}$$

1493

A reduction formula as simple as this cannot be written if n is odd, since then one is led to the consideration of the integral:

$$C_{2m+1,0}(\alpha,\beta,\gamma)=\int_0^\infty \frac{u^{2m+1}\,\mathrm{d}u}{\sqrt{1+u^2}}\exp[-\alpha\sqrt{1+u^2}]\cosh(\beta u)\int_0^\pi \exp[\gamma u\cos\theta]\,\mathrm{d}\theta, \tag{3.15}$$

and the polar integration is no longer performable in an elementary way. The difficulty relevant to $n=2$ lies instead in the circumstance that the explicit calculation leads to the function:

$$F(\lambda,\mu)=\int_0^\infty \exp[-\lambda\cosh z-\mu\sinh z]\,\mathrm{d}z\,,$$

for which (since the inferior integration limit is zero, and not $-\infty$), a relation like (2.13) does not hold.

C) For $2<r\leqslant n$, we have the formula:

$$I_n^{(r)}\begin{pmatrix}x_1 & x_2 \dots x_r\\ \alpha_1 & \alpha_2 \dots \alpha_r\end{pmatrix}=\pi^{(n-r+1)/2}\int\dots\int\prod_{i=1}^{r-1}\mathrm{d}^n u_i\,\delta(u_1^2+1)\prod_{j=2}^{r-1}\delta(u_j^2-1)\cdot \tag{3.16}$$

$$\cdot\prod_{h<k=1}^{r-1}\delta(u_h\cdot u_k)\theta(u_{1,n})\exp[\sum_{s=1}^{r-1}\alpha_s u_s\cdot x]\left(\frac{1}{2}\alpha_r\sqrt{\Delta}\right)^{-(n-r-1)/2}I_{(n-r-1)/2}(\alpha_r\sqrt{\Delta})\,,$$

with:

$$\Delta=x_r^2+(u_1\cdot x_r)^2-\sum_{m=2}^{r-1}(u_m\cdot x_r)^2 \tag{3.16a}$$

which, in the particular case $r=n$, can also be written:

$$I_n^{(n)}\left(\begin{array}{c|c}x_1 & x_2 \dots x_n\\ \alpha_1 & \alpha_2 \dots \alpha_n\end{array}\right)=\frac{\pi}{2}\int\dots\int\prod_{i=1}^{n-2}\mathrm{d}^n u_i\,\delta(u_1^2+1)\prod_{j=2}^{n-2}\delta(u_j^2-1)\cdot \tag{3.17}$$

$$\cdot\prod_{h<k=1}^{n-2}\delta(u_h\cdot u_k)\theta(u_{1,n})\exp[\sum_{s=1}^{n-2}\alpha_s u_s\cdot x]\{I_0(\sqrt{\Delta^{(+)}})+I_0(\sqrt{\Delta^{(-)}})\},$$

with:

$$\Delta^{(\pm)}=\alpha_{n-1}^2\{x_{n-1}^2+(u_1\cdot x_{n-1})^2-\sum_{m=2}^{n-2}(u_m\cdot x_{n-1})^2\}+ \tag{3.17a}$$

$$+\alpha_n^2\{x_n^2+(u_1\cdot x_n)^2-\sum_{m=2}^{n-2}(u_m\cdot x_n)^2\}\pm 2\alpha_{n-1}\alpha_n\Gamma$$

1194

and

$$(3.17b)\qquad \Gamma = \begin{vmatrix} u_{1,1} & u_{1,2} & \dots & u_{1,n} \\ u_{2,1} & u_{2,2} & \dots & u_{2,n} \\ \cdot & \cdot & \cdot & \cdot \\ u_{n-2,1} & u_{n-2,2} & \dots & u_{n-2,n} \\ x_{n-1,1} & x_{n-1,2} & \dots & x_{n-1,n} \\ x_{n,1} & x_{n,2} & \dots & x_{n,n} \end{vmatrix} .$$

To prove (3.16), we consider the general formula (3.1), and perform the integration over u_r. This can be done immediately by means of (2.7): indeed, in the system where $(u_1 \equiv (0, 0, \dots, 1)$, we have:

$$\int \mathrm{d}^n u_r \delta(u_r^2 - 1) \prod_{m=1}^{r-1} \delta(u_r \cdot u_m) \exp[\alpha_r u_r \cdot x_r] = \int \mathrm{d}^{n-1} \boldsymbol{u}_r \delta(\boldsymbol{u}_r^2 - 1) \cdot$$

$$\cdot \prod_{m=2}^{r-1} \delta(\boldsymbol{u}_r \cdot \boldsymbol{u}'_m) \exp[\alpha_r \boldsymbol{u}_r \boldsymbol{x}'_r] = \pi^{(n-r+1)/2} D^{-\frac{1}{2}} \left(\frac{1}{2}\alpha_r \sqrt{\frac{B}{D}}\right)^{-(n-r-1)/2} I_{(n-r-1)/2}\left(\alpha_r \sqrt{\frac{B}{D}}\right),$$

with: $\boldsymbol{D} = \mathrm{Det}\,|\boldsymbol{u}'_i \cdot \boldsymbol{u}'_k|$ $(2 \leqslant i,\ k \leqslant r-1)$, and:

$$B = \begin{vmatrix} \boldsymbol{x}'^2_r & \boldsymbol{x}'_r \cdot \boldsymbol{u}'_2 & \dots & \boldsymbol{x}'_r \cdot \boldsymbol{u}'_{r-1} \\ \boldsymbol{x}'_r \cdot \boldsymbol{u}'_2 & & & \\ \vdots & & D & \\ \boldsymbol{x}'_r \cdot \boldsymbol{u}'_{r-1} & & & \end{vmatrix} .$$

Now, it is easily seen that the relations:

$$u_1^2 = -1\,, \qquad u_j^2 = 1 \qquad\qquad (2 \leqslant j \leqslant r-1),$$

$$u_i \cdot u_j = 0 \qquad\qquad (1 \leqslant i,\ j \leqslant r-1),$$

which are satisfied by the vectors u_k $(1 \leqslant k \leqslant r-1)$, written in the above mentioned system ,become: $\boldsymbol{u}'_i \cdot \boldsymbol{u}'_k = \delta_{ik}$ $(2 \leqslant i,\ k \leqslant r - 1)$; furthermore, $\boldsymbol{x}'^2_r = x_r^2 + (u_1 \cdot x_r)^2$, and $\boldsymbol{x}'_r \cdot \boldsymbol{u}'_s = x_r \cdot u_s$ $(2 \leqslant s \leqslant r-1)$. Therefore, we get:

$$D = 1, \quad B = \begin{vmatrix} x_r^2 + (u_1 \cdot x_r)^2 & x_r \cdot u_2 & \dots & x_r \cdot u_{r-1} \\ x_r \cdot u_2 & 1 & \dots & 0 \\ \cdot & \cdot & \cdot & \cdot \\ x_r \cdot u_{r-1} & 0 & \dots & 1 \end{vmatrix} = x_r^2 + (u_1 \cdot x_r)^2 - \sum_{m=2}^{r-1} (u_m \cdot x_r)^2\,,$$

and (3.16) is thus established. To obtain (3.17), we observe that, if $r=n$, the quantity Δ defined by (3.16a) equals the square of the following determinant:

$$\Delta'=\begin{vmatrix} x_{n,1} & x_{n,2} & \dots & x_{n,n} \\ u_{1,1} & u_{1,2} & \dots & u_{1,n} \\ u_{2,1} & u_{2,2} & \dots & u_{2,n} \\ \cdot & \cdot & \cdot & \cdot \\ u_{n-1,1} & u_{n-1,2} & \dots & u_{n-1,n} \end{vmatrix}; \tag{3.18}$$

indeed, denoting by Δ'' the determinant which one obtains from Δ' by multiplication of the elements of the last column by i, we have (performing the multiplication rows by rows):

$$\Delta'^2=-\Delta''^2=-\begin{vmatrix} x_n^2 & x_n\cdot u_1 & \dots & x_n\cdot u_{n-1} \\ x_n\cdot u_1 & -1 & \dots & 0 \\ \vdots & \vdots & & \vdots \\ x_n\cdot u_{n-1} & 0 & \dots & 1 \end{vmatrix} = x_n^2+(u_1\cdot x_n)^2 - \\ -\sum_{m=2}^{n-1}(u_m\cdot x_n)^2=\Delta\,, \qquad q.e.d.$$

Taking into account this property, and remembering that $I_{-\frac{1}{2}}(x)=\sqrt{(2/\pi x)}\cosh x$, we get then, putting $r=n$ in (3.16):

$$I_n^{(n)}\begin{pmatrix} x_1 & x_2 \dots x_n \\ \alpha_1 & \alpha_2 \dots \alpha_n\end{pmatrix}=\int\!\dots\!\int\prod_{i=1}^{n-1}\mathrm{d}^n u_i\,\delta(u_1^2+1)\prod_{j=2}^{n-1}\delta(u_j^2-1)\cdot \\ \cdot\prod_{h<k=1}^{n-1}\delta(u_h\cdot u_k)\theta(u_{1,n})\exp\big[\sum_{s=1}^{n-1}\alpha_s u_s\cdot x\big]\cosh(\alpha_n\Delta')\,.$$

The integration over u_{n-1} can be easily done if we adopt, once more, the device of performing the calculation in the system where $u_1=(0,0,\dots,1)$. In this system, the determinant Δ' — apart, possibly, from an inessential change of sign — becomes:

$$\Delta'\to R'=\begin{vmatrix} u'_{n-1,1} & u'_{n-1,2} & \dots & u'_{n-1,n-1} \\ x'_{n,1} & x'_{n,2} & \dots & x'_{n,n-1} \\ u'_{2,1} & u'_{2,2} & \dots & u'_{2,n-1} \\ \cdot & \cdot & \cdot & \cdot \\ u'_{n-2,1} & u'_{n-2,2} & \dots & u'_{n-2,n-1} \end{vmatrix} = \tag{3.19}$$

$$=\sum_{m=1}^{n-1}u'_{n-1,m}R'_m\,,\ \text{with:}\ R'_m=(-1)^{m+1}\begin{vmatrix} x'_{n,1} & \dots & x'_{n,m-1} & x'_{n,m+1} & \dots & x'_{n,n-1} \\ u'_{2,1} & \dots & u'_{2,m-1} & u'_{2,m+1} & \dots & u'_{2,n-1} \\ \cdot & \cdot & \cdot & \cdot & \cdot & \cdot \\ u'_{n-2,1} & \dots & u'_{n-2,m-1} & u'_{n-2,m+1} & \dots & u'_{n-2,n-1} \end{vmatrix}$$

In the Appendix, we shall show that:

$$
(3.20)\qquad \sum_{m=1}^{n-1} R'^2_m = \begin{vmatrix} x'^2_m & x'_n\cdot u'_2 & \dots & x'_n\cdot u'_{n-2} \\ x'_n\cdot u'_2 & 1 & \dots & 0 \\ \dots & \dots & \dots & \dots \\ x'_n\cdot u'_{n-2} & 0 & \dots & 1 \end{vmatrix} =
$$

$$
= x'^2_n - \sum_{m=2}^{n-2} (x'_n\cdot u'_m)^2 = x^2_m + (u_1\cdot x_n)^2 - \sum_{m=2}^{n-2} (u_m\cdot x_n)^2 ,
$$

moreover:

$$
(3.21)\qquad \sum_{m=1}^{n-1} u'_{j,m} R'_m = 0 \qquad\qquad (2 \leqslant j \leqslant n-2)
$$

(indeed, the sum at the r.h.s. gives the expansion of a determinant with two parallel rows equal), and, finally:

$$
(3.22)\qquad \Big(\sum_{m=1}^{n-1} x'_{n-1,m} R'_m\Big)^2 = -\begin{vmatrix} x'_{n-1,1} & x'_{n-1,2} & \dots & x'_{n-1,n-1} & i x'_{n-1,n} \\ x'_{n,1} & x'_{n,2} & \dots & x'_{n,n-1} & i x'_{n,n} \\ u'_{2,1} & u'_{2,2} & \dots & u'_{2,n-1} & 0 \\ \dots & \dots & \dots & \dots & \dots \\ u'_{n-2,1} & u'_{n-2,2} & \dots & u'_{n-2,n-1} & 0 \\ 0 & 0 & \dots & 0 & i \end{vmatrix}^2 =
$$

$$
= -\begin{vmatrix} x_{n-1,1} & x_{n-1,2} & \dots & x_{n-1,n-1} & i x_{n-1,n} \\ x_{n,1} & x_{n,2} & \dots & x_{n,n-1} & i x_{n,n} \\ u_{2,1} & u_{2,2} & \dots & u_{2,n-1} & i u_{2,n} \\ \dots & \dots & \dots & \dots & \dots \\ u_{n-2,1} & u_{n-2,2} & \dots & u_{n-2,n-1} & i u_{n-2,n} \\ u_{1,1} & u_{1,2} & \dots & u_{1,n-1} & i u_{1,n} \end{vmatrix}^2 = \Gamma^2 ,
$$

Γ being the determinant (3.17*b*). From this, it follows that:

$$
\int \mathrm{d}^n u_{n-1}\, \delta(u^2_{n-1} - 1) \prod_{h=1}^{n-2} \delta(u_{n-1}\cdot u_h) \exp[\chi_{n-1} u_{n-1}\cdot x_{n-1}] \cosh(\chi_n \Delta') =
$$

$$
= \frac{1}{2}\int \mathrm{d}^{n-1} \boldsymbol{u}_{n-1}\, \delta(\boldsymbol{u}^2_{n-1} - 1) \prod_{h=2}^{n-2} \delta(\boldsymbol{u}_{n-1}\cdot \boldsymbol{u}'_h) \exp[\chi_{n-1} \boldsymbol{u}_{n-1}\cdot \boldsymbol{x}'_{n-1}] \{\exp[\chi_n R'] + \exp[-\chi_n R']\};
$$

if we now make use of (2.7), and remember (3.20), (3.21) and (3.22), we get immediately (3.17). The possibility of performing two integrations with re-

spect to the u vectors, when $r=n$ depends essentially on the peculiar property — which does not hold any longer if $r<n$ — enjoyed in this case by the determinant Δ.

D) When the vectors $x_1, x_2, \ldots, x_r$ are not linearly independent, there exist reduction formulae, which allow a lowering of the value of the « index » r. We shall limit ourselves to considering here only two such formulae, namely:

$$(3.23)\qquad I_n^{(r)}\begin{pmatrix} x_1 & x_2 \ldots x_p \ldots x_{q-1}\; x_p\; x_{q+1} \ldots x_r \\ \alpha_1 & \alpha_2 \ldots \alpha_p \ldots \alpha_{q-1}\; \alpha_q\; \alpha_{q+1} \ldots \alpha_r \end{pmatrix} =$$

$$= \frac{\pi^{(n-r+1)/2}}{\Gamma((n-r+1)/2)}\, I_n^{(r-1)}\begin{pmatrix} x_1 & x_2 \ldots & x_p \ldots & x_{q-1}\; x_{q+1} \ldots x_r \\ \alpha_1 & \alpha_2 \ldots & \sqrt{\alpha_p^2+\alpha_q^2} \ldots & \alpha_{q-1}\; \alpha_{q+1} \ldots \alpha_r \end{pmatrix},$$

$$(3.24)\qquad I_n^{(r)}\begin{pmatrix} x_1 & x_2 \ldots x_{q-1}\; x_1\; x_{q+1} \ldots x_r \\ \alpha_1 & \alpha_2 \ldots \alpha_{q-1}\; \alpha_q\; \alpha_{q+1} \ldots \alpha_r \end{pmatrix} =$$

$$= \frac{\pi^{(n-r+1)/2}}{\Gamma((n-r+1)/2)}\, I_n^{(r-1)}\begin{pmatrix} x_1 & x_2 \ldots x_{q-1}\; x_{q+1} \ldots x_r \\ \sqrt{\alpha_1^2-\alpha_q^2} & \alpha_2 \ldots \alpha_{q-1}\; \alpha_{q+1} \ldots \alpha_r \end{pmatrix},$$

(the validity of (3.24) requires $\alpha_1 > \alpha_q$, the root being moreover given a plus sign). To prove (3.23), we change the integration variables as follows:

$$(3.25)\qquad u_q \to u_q\,, \qquad u_p \to \frac{1}{\alpha_p}\,(u_p - \alpha_q u_q)\,.$$

Then—introducing the symbol $\prod\limits_i^{(k)}$ to mean that the factor with $i=k$ must be ruled out from the product—we have, after some straightforward manipulations:

$$\prod_{j=2}^{r}\delta(u_j^2-1)\prod_{h<k=1}^{r}\delta(u_h\cdot u_k) \to (\alpha_p)^{r+1}\prod_{j=2}^{r}{}^{(p)}\delta(u_j^2-1)\,\delta(u_p^2-\alpha_p^2-\alpha_q^2)\cdot$$

$$\cdot\prod_{h<k=1}^{r}{}^{(p)}\delta(u_h\cdot u_k)\prod_{l=1}^{r}{}^{(p,q)}\delta(u_l\cdot u_p)\,\delta(u_p\cdot u_q-\alpha_q)\,,$$

introducing this into (3.1), and integrating over u_q [12]—which, by (3.25) no longer appears at the exponential—one gets (3.23). The justification of (3.24)

---

[12] The u_q-integration is of the form:

$$\int d^n u_q\,\delta(u_q^2-1)\prod_{j=1}^{r}{}^{(p,q)}\delta(u_q\cdot u_j)\,\delta\left(u_p\cdot u_q-\frac{\alpha_q}{\sqrt{\alpha_p^2+\alpha_q^2}}\right);$$

going to the system where $u_1\equiv(0, 0, \ldots, 1)$, it reduces immediately to (2.1).

is quite similar; it suffices to replace (3.25) with the analogous transformations:

$$u_1 \to u_1\,, \qquad u_q \to \frac{1}{\alpha_q}\,(u_q - \alpha_1 u_1)\,.$$

4. – After this work, we are now able to write down the formulae we have mentioned in the introduction. For the sake of simplicity, we shall limit ourselves to give an exhaustive exposition of our technique in a single case. By repeated application of (3.23), we see that:

$$(4.1)\quad I_n^{(r)}\begin{pmatrix} x_1 & x_2\; x_2 \dots x_2 \\ \alpha_1 & \alpha_2\; \alpha_3 \dots \alpha_r \end{pmatrix} = \frac{1}{S_{n,r}}\,\pi^{\frac14 (r-2)(2n-r-1)} I_n^{(2)}\begin{pmatrix} x_1 & x_2 \\ \alpha_1 & \sqrt{\alpha_2^2+\alpha_3^2+\dots+\alpha_r^2} \end{pmatrix}, \qquad (n \geqslant r \geqslant 3),$$

where we have put:

$$(4.2)\qquad S_{n,r} = \Gamma\left(\frac{n-r}{2}+\frac12\right)\Gamma\left(\frac{n-r}{2}+1\right)\Gamma\left(\frac{n-r}{2}+\frac32\right)\dots\Gamma\left(\frac{n}{2}-1\right).$$

On the other hand, by (3.16), one has:

$$(4.3)\quad I_n^{(r)}\begin{pmatrix} x_1 & x_2\; x_2 \dots x_2 \\ \alpha_1 & \alpha_2\; \alpha_3 \dots \alpha_r \end{pmatrix} = \pi^{(n-r+1)/2}\int\dots\int \prod_{i=1}^{r-1} \mathrm{d}^n u_i\, \delta(u_1^2+1)\prod_{j=2}^{r-1}\delta(u_j^2-1)\,\cdot$$
$$\cdot\prod_{h<k=1}^{r-1}\delta(u_h\cdot u_k)\,\theta(u_{1,n})\exp\Big[\alpha_1 u_1\cdot x_1 + \Big(\sum_{s=2}^{r-1}\alpha_s u_s\Big)\cdot x_2\Big]\left(\frac12\,\alpha_r\sqrt{\Delta}\right)^{-(n-r-1)/2} I_{(n-r-1)/2}(\alpha_r\sqrt{\Delta})\,,$$

with:

$$(4.4)\qquad \Delta = x_2^2 + (u_1\cdot x_2)^2 - \sum_{m=2}^{r-1}(u_m\cdot x_2)^2\,.$$

Combining (4.3) and (4.1), we thus get a first remarkable relationship, which becomes particularly simple when n is even $\geqslant 4$, because, in this case, the $2n$-ple integral $I_n^{(2)}$ can be reduced to a single integral, as we have seen in Section **3**, B). In the same way, we obtain the following formulae:

$$(4.5)\quad \pi^{(n-r+1)/2}\int\dots\int\Theta_{r-1}\exp\Big[\Big(\sum_{s=1}^{r-1}\alpha_s u_s\Big)\cdot x_1\Big]\left(\frac12\,\alpha_r\sqrt{\Delta_1^{(r)}}\right)^{-(n-r-1)/2} I_{(n-r-1)/2}(\alpha_r\sqrt{\Delta_1^{(r)}}) =$$
$$= \frac{1}{S_{n,r}}\,\pi^{\frac14(r-2)(2n-r-1)}\,\frac{\pi^{(n-1)/2}}{\Gamma((n-1)/2)}\, I_n^{(1)}\left(\frac{x_1}{\sqrt{\alpha_1^2-\sum_{j=2}^{r}\alpha_j^2}}\right);$$

$$(4.6)\quad \pi^{(n-r-1)/2}\int\dots\int\Theta_{r-1}\exp\Big[\Big(\sum_{s=1}^{m}\alpha_s u_s\Big)\cdot x_1+\Big(\sum_{s=m+1}^{r-1}\alpha_s u_s\Big)\cdot x_2\Big]\Big(\frac{1}{2}\,\alpha_r\sqrt{\Delta_2^{(r)}}\Big)^{-(n-r-1)/2}\cdot$$

$$\cdot I_{(n-r-1)/2}\big(\alpha_r\sqrt{\Delta_2^{(r)}}\big)=\frac{1}{S_{n,r}}\,\pi^{\frac{1}{2}(r-2)(2n-r-1)}\,I_n^{(2)}\left(\frac{x_1}{\sqrt{\alpha_1^2-\sum\limits_{j=2}^{m}\alpha_j^2}}\;\middle|\;\frac{x_2}{\sqrt{\sum\limits_{j=m+1}^{r}\alpha_j^2}}\right);$$

$$(4.7)\quad \pi\int\dots\int\Theta_{n-2}\exp\Big[\alpha_1 u_1\cdot x_1+\Big(\sum_{s=2}^{n-2}\alpha_s u_s\Big)\cdot x_2\Big]I_0\big(\sqrt{\alpha_{n-1}^2+\alpha_n^2}\sqrt{\Delta_2^{(n-1)}}\big)=$$

$$=\frac{1}{S_{n,n}}\,\pi^{\frac{1}{2}(n-2)(n-1)}\,I_n^{(2)}\left(\frac{x_1}{\alpha_1}\;\middle|\;\frac{x_2}{\sqrt{\sum\limits_{j=2}^{n}\alpha_j^2}}\right);$$

$$(4.8)\quad \pi\int\dots\int\Theta_{n-2}\exp\Big[\Big(\sum_{s=1}^{m}\alpha_s u_s\Big)\cdot x_1+\Big(\sum_{s=m+1}^{n-2}\alpha_s u_s\Big)\cdot x_2\Big]I_0\big(\sqrt{\alpha_{n-1}^2+\alpha_n^2}\sqrt{\Delta_2^{(n-1)}}\big)=$$

$$=\frac{1}{S_{n,n}}\,\pi^{\frac{1}{2}(n-2)(n-1)}\,I_n^{(2)}\left(\frac{x_1}{\sqrt{\alpha_1^2-\sum\limits_{j=2}^{m}\alpha_j^2}}\;\middle|\;\frac{x_2}{\sqrt{\sum\limits_{j=m+1}^{n}\alpha_j^2}}\right);$$

$$(4.9)\quad \pi\int\dots\int\Theta_{n-2}\exp\Big[\Big(\sum_{s=1}^{n-2}\alpha_s u_s\Big)\cdot x_1\Big]I_0\big(\sqrt{\alpha_{n-1}^2+\alpha_n^2}\sqrt{\Delta_1^{(n-1)}}\big)=$$

$$=\frac{1}{S_{n,n}}\,\pi^{\frac{1}{2}(n-2)(n-1)}\,\frac{\pi^{(n-1)/2}}{\Gamma((n-1)/2)}\,I_n^{(1)}\left(\frac{x_1}{\sqrt{\alpha_1^2-\sum\limits_{j=2}^{n}\alpha_j^2}}\;\middle|\;\right);$$

$$(4.10)\quad \pi\int\dots\int\Theta_{n-2}\exp\Big[\alpha_1 u_1\cdot x_1+\Big(\sum_{s=2}^{m}\alpha_s u_s\Big)\cdot x_2+\Big(\sum_{s=m+1}^{n-2}\alpha_s u_s\Big)\cdot x_1\Big]\cdot$$

$$\cdot I_0\big(\sqrt{\alpha_{n-1}^2+\alpha_n^2}\sqrt{\Delta_1^{(n-1)}}\big)=\frac{1}{S_{n,n}}\,\pi^{\frac{1}{2}(n-2)(n-1)}\,I_n^{(2)}\left(\frac{x_1}{\sqrt{\alpha_1^2-\sum\limits_{j=m+1}^{n}\alpha_j^2}}\;\middle|\;\frac{x_2}{\sqrt{\sum\limits_{j=2}^{m}\alpha_j^2}}\right);$$

$$(4.11)\quad \frac{\pi}{2}\int\dots\int\Theta_{n-2}\exp\Big[\Big(\sum_{s=1}^{m}\alpha_s u_s\Big)\cdot x_1+\Big(\sum_{s=m+1}^{n-2}\alpha_s u_s\Big)\cdot x_2\Big]\big\{I_0(\sqrt{\Delta^{(+)}})+I_0(\sqrt{\Delta^{(-)}})\big\}=$$

$$=\frac{1}{S_{n,n}}\,\pi^{\frac{1}{2}(n-2)(n-1)}\,I_n^{(2)}\left(\frac{x_1}{\sqrt{\alpha_1^2-\sum\limits_{j=2}^{m}\alpha_j^2-\alpha_{n-1}^2}}\;\middle|\;\frac{x_2}{\sqrt{\sum\limits_{j=m+1}^{n-2}\alpha_j^2+\alpha_n^2}}\right);$$

with:

$$(4.12)\qquad \Theta_p=\prod_{i=1}^{p}\mathrm{d}^n u_i\,\delta(u_1^2+1)\prod_{j=2}^{p}\delta(u_j^2-1)\prod_{h<k=1}^{p}\delta(u_h\cdot u_k)\,\theta(u_{1,n})\,,$$

$$(4.13)\qquad \Delta_\lambda^{(j)}=x_\lambda^2+(u_1\cdot x_\lambda)^2-\sum_{m=2}^{j-1}(u_m\cdot x_\lambda)^2\,,$$

1560

$$\Delta^{(\pm)} = \alpha_{n-1}^2 \Delta_1^{(n-1)} + \alpha_n^2 \Delta_2^{(n-1)} \pm 2\alpha_{n-1}\alpha_n \begin{vmatrix} u_{1,1} & u_{1,2} & \dots & u_{1,n} \\ u_{2,1} & u_{2,2} & \dots & u_{2,n} \\ \cdot & \cdot & \cdot & \cdot \\ u_{n-2,1} & u_{n-2,2} & \dots & u_{n-2,n} \\ x_{1,1} & x_{1,2} & \dots & x_{1,n} \\ x_{2,1} & x_{2,2} & \dots & x_{2,n} \end{vmatrix}; \tag{4.14}$$

to these, we can add the analogous results which follow from the obvious invariance property of the integrals (3.1) with respect to an arbitrary permutation of the vectors $x_2, \dots, x_r$ (and of the pertaining constants $\alpha_2, \dots, \alpha_r$). In the form written above, our formulae throw light essentially on the unexpected structural simplicity of integrals of the form (3.16), when the vectors x_j satisfy certain conditions; however, their interest is not limited to this fact, since, by further work, it is possible to deduce from them various other integral formulae, as will be shown in a subsequent paper.

Appendix

Given $m \leqslant n-1$ vectors of the space S_n, consider the determinant D of their scalar products:

$$D = \operatorname{Det}|\boldsymbol{x}_r \cdot \boldsymbol{x}_s|, \tag{A.1}$$

and put:

$$D' = \operatorname{Det}|x_{r,s}|, \qquad (1 \leqslant r,\ s \leqslant m), \tag{A.2}$$

$D'_{j,r}$ — determinant obtained from D' by replacement of the r-th column $(1 \leqslant r \leqslant m)$ with $x_{1,j}, x_{2,j}, \dots, x_{m,j}$ $(m+1 \leqslant j \leqslant n)$;

$$a_{rs} = \delta_{rs} + \frac{1}{D'^2} \sum_{j=1}^{m} D'_{j,r} D'_{j,s}, \qquad (m+1 \leqslant r,\ s \leqslant n), \tag{A.3}$$

and, finally:

$$R = \operatorname{Det}|a_{rs}| = \begin{vmatrix} a_{m+1,m+1} & a_{m+1,m+2} & \dots & a_{m+1,n} \\ a_{m+1,m+2} & a_{m+2,m+2} & \dots & a_{m+2,n} \\ \cdot & \cdot & \cdot & \cdot \\ a_{m+1,n} & a_{m+2,n} & \dots & a_{n,n} \end{vmatrix}. \tag{A.4}$$

Then, we have the formula:

$$D = D'^2 R, \tag{A.5}$$

which generalizes a well-known property enjoyed by the determinant D when $m = n$. To prove (A.5), we shall evaluate in two different ways the integral

$$I = \int \mathrm{d}^n \boldsymbol{u}\, \delta(\boldsymbol{u}^2 - 1) \prod_{r=1}^{m} \delta(\boldsymbol{u}\cdot\boldsymbol{x}_r)\,,$$

and then we shall make a comparison of the two results.

Applying (2.1), one has immediately:

$$\text{(A.6)} \qquad I = \frac{\pi^{(n-m)/2}}{\Gamma((n-m)/2)}\, D^{-\frac{1}{2}}\,;$$

(the factor $\theta(D)$ can be omitted, since — as is easily verified — D is always $\geqslant 0$). On the other hand, the product $\prod_{r=1}^{m} \delta(\boldsymbol{u}\cdot\boldsymbol{x}_r)$ implies the relations:

$$\sum_{j=1}^{m} u_j x_{r,j} = - \sum_{k=m+1}^{n} u_k x_{r,k}\,, \qquad (r = 1, 2, \ldots, m),$$

which, solved with respect to $u_j' s$ $(1 \leqslant j \leqslant m)$, give:

$$u_j = -\frac{1}{D'} \sum_{k=m+1}^{n} u_k D'_{j,k}\,. \qquad (1 \leqslant j \leqslant m).$$

Therefore, putting $A_r = \sum_{k=m+1}^{n} u_k x_{r,k}$, we can write:

$$I = \int \mathrm{d}u_{m+1} \ldots \mathrm{d}u_n\, \delta\left(u_{m+1}^2 + \ldots + u_n^2 + \frac{1}{D'^2} \sum_{j=1}^{m} \sum_{k,l=m+1}^{n} u_k u_l D'_{j,k} D'_{j,l} - 1\right) \cdot$$

$$\cdot \int \mathrm{d}u_1 \ldots \mathrm{d}u_m \prod_{r=1}^{m} \delta\big(\sum_{j=1}^{m} u_j x_{r,j} + A_r\big) =$$

$$= \int \mathrm{d}u_{m+1} \ldots \mathrm{d}u_n\, \delta\big(\sum_{r,s=m+1}^{n} a_{rs} u_r u_s - 1\big) \int \mathrm{d}u_1 \ldots \mathrm{d}u_m \prod_{r=1}^{m} \delta\big(\sum_{j=1}^{m} u_j x_{r,j} + A_r\big)\,.$$

The integrations over the first m components, changing to the new variables:

$$u_r' = \sum_{j=1}^{m} u_j x_{r,j}\,, \qquad (1 \leqslant r \leqslant m),$$

give:

$$\frac{1}{|D'|} \int \mathrm{d}u_1' \ldots \mathrm{d}u_m' \prod_{r=1}^{m} \delta(u_r' + A_r) = \frac{1}{|D'|}\,;$$

to perform the remaining integrations, it is convenient to diagonalize the quadratic form $\sum_{r,s} a_{rs} u_r u_s$, and then introduce polar coordinates. In this way,

one easily gets:

$$I = \frac{\pi^{(n-m)/2} R^{-\frac{1}{2}}}{\Gamma((n-m)/2) \cdot |D'|}, \tag{A.7}$$

whence, by comparison with (A.6), (A.5) follows, *q.e.d.*

In particular, if $m = n-1$, (A.5) becomes:

$$D = D'^2 + \sum_{r=1}^{n-1} D_r'^2, \tag{A.8}$$

D'_r being the determinant one obtains from D' by replacement of the r-th column with $x_{1.n}, \ldots, x_{n-1.n}$; this property has been invoked in the proof of (3.20). As a further application of (A.5), we shall now evaluate in another way the integral (2.7), thus gaining a « geometrical » interpretation of the ratio B/D. Proceeding as before, we have:

$$\int \mathrm{d}^n \boldsymbol{u}\, \delta(\boldsymbol{u}^2 - 1) \prod_{r=1}^{m} \delta(\boldsymbol{u} \cdot \boldsymbol{x}_r) \exp[\alpha \boldsymbol{u} \cdot \boldsymbol{y}] = \tag{A.9}$$

$$= \frac{1}{|D'|} \int \mathrm{d}u_{m+1} \ldots \mathrm{d}u_n \delta\Big(\sum_{r,s=m+1}^{n} a_{rs} u_r u_s - 1\Big) \exp\left[\alpha \sum_{k=m+1}^{n} u_k \left(y_k - \frac{1}{D'} \sum_{r=1}^{m} y_r D'_{r,k}\right)\right].$$

Now, let Λ be the matrix which diagonalizes the quadratic form $\sum_{r,s} a_{rs} u_r u_s$,(13) denoting by r_j $(j = 1, 2, \ldots, n-m)$ the roots of the secular equation, and putting (with symbolic notation):

$$\boldsymbol{\eta} = \Lambda^{-1} \boldsymbol{\xi}, \tag{A.10}$$

where $\boldsymbol{\xi}$ is the $(n-m)$-dimensional vector whose components are

$$y_k - \frac{1}{D'} \sum_{r=}^{m} y_r D'_{r,k}, \qquad (k = m+1, \ldots, n),$$

(A.9) becomes:

$$\int \mathrm{d}^n \boldsymbol{u}\, \delta(\boldsymbol{u}^2 - 1) \prod_{r=1}^{m} \delta(\boldsymbol{u} \cdot \boldsymbol{x}_r) \exp[\alpha \boldsymbol{u} \cdot \boldsymbol{y}] = \tag{A.11}$$

$$= \frac{1}{|D'|} \int \mathrm{d}^{n-m} \boldsymbol{v}\, \delta\Big(\sum_{j=1}^{n-m} r_j v_j^2 - 1\Big) \exp[\alpha \boldsymbol{v} \cdot \boldsymbol{\eta}] = \frac{1}{|D'| \sqrt{r_1 r_2 \ldots r_{n-m}}} \cdot$$

$$\cdot \int \mathrm{d}^{n-m} \boldsymbol{v}\, \delta(\boldsymbol{v}^2 - 1) \exp[\alpha \boldsymbol{v} \cdot \boldsymbol{\eta}'] = \frac{1}{|D'| \sqrt{R}} \pi^{(n-m)/2} \left(\frac{1}{2} \alpha |\boldsymbol{\eta}'|\right)^{1-(n-m)/2} I_{((n-m)/2)-1}(\alpha |\boldsymbol{\eta}'|).$$

---

(13) This matrix, moreover, will be subjected to the condition $\Lambda^T \Lambda = 1$, which leaves unchanged the form of the volume element in the space S_{n-m}.

Finally, taking in account (A.5), we can write:

$$\text{(A.12)}\qquad \int \mathrm{d}^n \boldsymbol{u}\, \delta(\boldsymbol{u}^2-1) \prod_{r=1}^{m} \delta(\boldsymbol{u}\cdot \boldsymbol{x}_r) \exp[\alpha \boldsymbol{u}\cdot \boldsymbol{y}] = $$

$$= \frac{1}{\sqrt{D}}\, \pi^{(n-m)/2} \left(\frac{1}{2}\,\alpha\,|\boldsymbol{\eta}'|\right)^{1-(n-m)/2} I_{((n-m)/2)-1}\,(\alpha\,|\boldsymbol{\eta}'|)\,;$$

by comparison with (2.7), we see that the ratio B/D equals the square of the $(n-m)$-dimensional vector $\boldsymbol{\eta}'$, whose components are:

$$\text{(A.13)}\qquad \eta_h' = \frac{1}{\sqrt{r_h}}\,\eta_h\,, \qquad (h=1, 2, \dots, n-m)\,.$$

This proof, however, is of merely formal interest; for practical purposes, it is convenient to make use of (2.7), which we have done in the text.

RIASSUNTO

Dopo aver opportunamente esteso il concetto di « funzione singolare generalizzata », si studia in dettaglio, da un punto di vista matematico, la struttura degli integrali che vi compaiono. Fra i principali risultati figurano varie relazioni integrali, che mettono in luce l'intima connessione tra le funzioni singolari generalizzate e le funzioni di Bessel. Una ulteriore elaborazione di queste formule porta a taluni nuovi integrali multipli coinvolgenti funzioni di Bessel, e verrà discussa in un successivo lavoro.

1504

IL NUOVO CIMENTO Vol. XII, N. 6 16 Giugno 1959

On the Dirac Equation for Baryons.

N. Dallaporta and T. Toyoda (*)

Istituto di Fisica dell'Università - Padova
Istituto Nazionale di Fisica Nucleare - Sezione di Padova

(ricevuto il 26 Febbraio 1959)

Summary. — Making use of physical considerations, possible forms of direct interaction between baryons and other fields in Gürsey's equation have been investigated, and a new interpretation of the eight-component spinors as representing for example (p-Ξ^-) or (Σ^+-Σ^-) is proposed. It enables us to relate the boson conjugation and the spinor conjugation proposed by Budini, Dallaporta and Fonda in an organic way with the single fundamental equation. The most important conservation laws of electric current and baryon number are automatically guaranteed in our formalism, independently from each other.

It has been shown some time ago by Gürsey [1] that the reducible 8-component Dirac equation for baryon states

$$(1)\qquad \begin{pmatrix} \gamma^\mu \dfrac{\partial}{\partial x^\mu} & im\gamma_5 \\ -im\gamma_5 & \gamma^\mu \dfrac{\partial}{\partial x^{\mu}} \end{pmatrix} \begin{pmatrix} \chi \\ \tilde{\chi} \end{pmatrix} = 0\,,$$

is invariant both for the γ_5-gauge transformation [2]

$$(2)\qquad \chi' = \exp[i\gamma_5\theta]\chi\,, \qquad \tilde{\chi}' = \exp[-i\gamma_5\theta]\tilde{\chi}$$

(*) On leave of absence from Rikkyo University, Tokyo.

(1) F. Gürsey: *Nuovo Cimento*, **7**, 411 (1958).

(2) B. Touschek: *Nuovo Cimento*, **5**, 1281 (1957).

and for the Pauli transformation ([3])

$$\chi' = a\chi + b\gamma_5\chi^c\,, \qquad \tilde{\chi}' = a\tilde{\chi} - b\gamma_5\tilde{\chi}^c\,, \tag{3}$$

where θ is a real parameter and a and b are parameters satisfying

$$|a|^2 + |b|^2 = 1\,. \tag{4}$$

The first one may be understood as a special case of the more general Toyoda transformation ([4]),

$$\begin{pmatrix}\chi\\ \tilde{\chi}\end{pmatrix}' = \begin{pmatrix}\exp[i\{\varepsilon + (1-\varepsilon)\gamma_5\}\vartheta] & 0\\ 0 & \exp[i\{\varepsilon - (1-\varepsilon)\gamma_5\}\vartheta]\end{pmatrix}\begin{pmatrix}\chi\\ \tilde{\chi}\end{pmatrix}, \tag{5}$$

under which equation (1) is also invariant. In general $\partial/\partial x^\mu$ appearing in Eq. (1) should be replaced by $\partial_{|\mu}$ and $\tilde{\partial}_{|\mu}$ respectively, since the generalized gauge transformation (5) involves a real function ϑ (see ref. ([4])). The detailed structure of the Dirac equation in the general case shall be discussed in a forthcoming paper ([5]).

For the later convenience we shall rewrite Eq. (1) as

$$\left\{\Gamma^\mu \frac{\partial}{\partial x^\mu} + im\Gamma_5\right\} X = 0\,, \tag{6}$$

with

$$X = \begin{pmatrix}\chi\\ \tilde{\chi}\end{pmatrix}, \qquad \Gamma^\mu = \begin{pmatrix}0 & \gamma^\mu\\ \gamma^\mu & 0\end{pmatrix}, \qquad \Gamma_5 = \begin{pmatrix}-\gamma_5 & 0\\ 0 & \gamma_5\end{pmatrix}, \qquad \Gamma^\mu\Gamma_5 = \Gamma_5\Gamma^\mu\,. \tag{7}$$

It is evident that Eq. (6) can be reduced into two ordinary 4-component Dirac equations, since the two matrices in Eq. (6) are commutable. In fact a unitary transformation

$$\begin{pmatrix}\chi\\ \tilde{\chi}\end{pmatrix} = \begin{pmatrix}\beta & \alpha\\ \alpha & -\beta\end{pmatrix}\begin{pmatrix}\psi\\ \tilde{\psi}\end{pmatrix}, \tag{8}$$

where

$$\alpha = \tfrac{1}{2}(1+\gamma_5)\,, \qquad \beta = \tfrac{1}{2}(1-\gamma_5) \tag{9}$$

([3]) W. Pauli: *Nuovo Cimento*, **6**, 204 (1957).
([4]) T. Toyoda: *Nucl. Phys.*, **8**, 661 (1958).
([5]) C. Ceolin and T. Toyoda: to be published in the *Nuovo Cimento*.

gives us the separation (*). Then the two Dirac equations are quite independent from each other, so the transformed functions may be rewritten as:

$$\begin{pmatrix}\psi\\ \tilde{\psi}\end{pmatrix} \equiv \begin{pmatrix}\psi_{p}\\ i\tilde{\psi}_{n}^{c}\end{pmatrix}. \tag{10}$$

This special choice corresponds to Gürsey's transformation [1].

Being led by the two facts, that is, the reducibility of Eq. (1) or Eq. (6), and the isomorphism of the Pauli transformation group to the unimodular group, GÜRSEY interpreted ψ_p and $\tilde{\psi}_n$ states as representing the proton and the neutron respectively. One may remark, however, that such an interpretation is not the only possible and that other ones may appear to be more suited in order to introduce in the most simple way the electromagnetic interaction term into Gürsey's equation. In fact, as we shall show later, there are only two independent possibilities for the introduction of electromagnetic interaction into Eq. (1) or Eq. (6), if we want to maintain the reducibility of the equation according to the physical standpoint. And the most simple choice for these two cases corresponds either to the same electric charge or to opposite charges for the two states.

From another side, the electromagnetic interaction appears to be of fundamental importance as soon as one tries to understand not only the behaviour of a single baryon state but of the whole baryon scheme. In this respect, a recent paper of BUDINI, DALLAPORTA and FONDA [5] has stressed the point that the existence of different baryon states may be related to the existence of two kinds of conjugation, into which the ordinary charge conjugation may be decomposed, the boson conjugation B which reverses the sign of the electric charge (or of the hypercharge) but not the sign of energy, and the spinor conjugation S which reverses the sign of energy but not the sign of the electric charge (or of the hypercharge). The product of the two operations obviously reverses the sign of both energy and charge and is the ordinary charge conjugation.

(*)
$$T=\begin{pmatrix}\beta & \alpha\\ \alpha & -\beta\end{pmatrix}, \qquad T^{-1}=\begin{pmatrix}\beta & \alpha\\ \alpha & -\beta\end{pmatrix},$$

$$T^{-1}\begin{pmatrix}0 & \gamma^{\mu}\\ \gamma^{\mu} & 0\end{pmatrix}T=\begin{pmatrix}\gamma^{\mu} & 0\\ 0 & -\gamma^{\mu}\end{pmatrix}, \qquad T^{-1}\begin{pmatrix}-\gamma_5 & 0\\ 0 & \gamma_5\end{pmatrix}T=\begin{pmatrix}I & 0\\ 0 & -I\end{pmatrix}.$$

The following formula will be used later

$$T^{-1}\begin{pmatrix}0 & \gamma^{\mu}\gamma_5\\ -\gamma^{\mu}\gamma_5 & 0\end{pmatrix}T=\begin{pmatrix}\gamma^{\mu} & 0\\ 0 & \gamma^{\mu}\end{pmatrix}.$$

[5] P. BUDINI, N. DALLAPORTA and L. FONDA: *Nuovo Cimento*, **9**, 316 (1958).

Thus, if we disregard the mass differences between all baryons, the Ξ states are obtained from the nucleons by applying to them the boson conjugation while the anti Ξ states by applying the spinor conjugation, and the anti-nucleons by ordinary charge conjugation. From such an example one may understand that the distinction between the different baryon states should be intimately correlated to all possible fields to which these states may be coupled and that a complete baryon wave equation should contain implicitly all baryon states in their true relation with the fields with which they are able to interact.

As a preliminary step in this direction, we have tried to discuss the behaviour of Gürsey's equation in connection with the electromagnetic interaction. As already stated, the two most simple independent ways to introduce a vector field interaction like the electromagnetic one into Eq. (6), due to the requirement for reducibility of the equation (*) lead us to the following two types:

$$\left\{\Gamma^\mu \frac{\partial}{\partial x^\mu} - ie\Gamma^\mu\Gamma_5 A_\mu + im\Gamma_5\right\} X = 0\,, \tag{11}$$

$$\left\{\Gamma_\mu \frac{\partial}{\partial x^\mu} - ie\Gamma^\mu A_\mu + im\Gamma_5\right\} X = 0\,. \tag{12}$$

Although the above two equations look quite different from each other, they are essentially equivalent, as it is shown in the following, if we confine ourselves to one kind of vector field.

Applying the transformation (8) to both (11) and (12) respectively, we obtain for case (11)

$$\left|\begin{aligned} &\left\{\gamma^\mu\left(\frac{\partial}{\partial x^\mu} - ieA_\mu\right) + im\right\}\psi = 0\,, \\ &\left\{\gamma^\mu\left(\frac{\partial}{\partial x^\mu} + ieA_\mu\right) + im\right\}\tilde{\psi} = 0\,, \end{aligned}\right. \tag{13}$$

(*) All other types (vector coupling) (7)

$$\begin{pmatrix} 0 & \gamma^\mu \\ -\gamma^\mu & 0 \end{pmatrix}, \quad \begin{pmatrix} \gamma^\mu & 0 \\ 0 & \gamma^\mu \end{pmatrix}, \quad \begin{pmatrix} \gamma^\mu & 0 \\ 0 & -\gamma^\mu \end{pmatrix},$$

$$\begin{pmatrix} 0 & \gamma^\mu\gamma_5 \\ \gamma^\mu\gamma_5 & 0 \end{pmatrix}, \quad \begin{pmatrix} \gamma^\mu\gamma_5 & 0 \\ 0 & \gamma^\mu\gamma_5 \end{pmatrix} \text{ and } \begin{pmatrix} \gamma^\mu\gamma_5 & 0 \\ 0 & -\gamma^\mu\gamma_5 \end{pmatrix},$$

form an irreducible algebra with

$$\begin{pmatrix} 0 & \gamma^\mu \\ \gamma^\mu & 0 \end{pmatrix} \text{ and } \begin{pmatrix} -\gamma_5 & 0 \\ 0 & \gamma_5 \end{pmatrix}.$$

The invariance condition under (2) is always assumed.

(7) L. BIEDENHARN: *Phys. Rev.*, **82**, 100 (1951).

for case (12):

$$(14)\qquad \left|\begin{array}{l} \left\{\gamma^{\mu}\left(\dfrac{\partial}{\partial x^{\mu}} - ieA_{\mu}\right) + im\right\}\psi = 0\,, \\ \left\{\gamma^{\mu}\left(\dfrac{\partial}{\partial x^{\mu}} - ieA_{\mu}\right) + im\right\}\tilde{\psi} = 0\,. \end{array}\right.$$

It may be of some interest to point out that γ_5 disappears in both cases. Furthermore, since ψ and $\tilde{\psi}$ are completely independent from each other, it is also possible to replace $\tilde{\psi}$ by $\tilde{\psi}^c$ in (14)

$$(14')\qquad \left|\begin{array}{l} \left\{\gamma^{\mu}\left(\dfrac{\partial}{\partial x^{\mu}} - ieA_{\mu}\right) + im\right\}\psi = 0\,, \\ \left\{\gamma^{\mu}\left(\dfrac{\partial}{\partial x^{\mu}} - ieA_{\mu}\right) + im\right\}\tilde{\psi}^c = 0\,. \end{array}\right.$$

It is now evident from the sign of the electromagnetic term that in both cases ψ and $\tilde{\psi}$ are to be interpreted as representing particles with opposite charge. In addition Eq. (11) (or Eq. (12) with an adequate interchange of operators discussed later) is invariant with respect to the boson conjugation and also the spinor conjugation as we shall show soon. These properties enable us to make an adequate interpretation for the states ψ and $\tilde{\psi}$ as either Σ^+ and Σ^-, or proton and Ξ^-.

Owing to the symmetry existing between the electric charge states and the hypercharge states of the mesons and baryons as is apparently seen in some elementary particle schemes ([8-10]), one could presumably infer that, should we have introduced instead of the electromagnetic interaction a corresponding suitable hypercharge interaction into Eq. (6), we could have also interpreted the pair of states ψ and $\tilde{\psi}$ as representing neutron and Ξ^0.

It is rather straigthforward to show that Eq. (11) is invariant with respect to the boson conjugation and also to the spinor conjugation. Let us first define the operator

$$(15)\qquad X^B = \begin{pmatrix} 0 & \gamma_5 \\ \gamma_5 & 0 \end{pmatrix} X \equiv BX\,.$$

If we interpret this operation by means of the reduced states ψ and $\tilde{\psi}$, it is exactly equivalent to the interchange of ψ with $\tilde{\psi}$ and therefore is equivalent to the boson conjugation of B.D.F. In fact, under this operation Eq. (11) transforms into

$$(16)\qquad \left\{\Gamma^{\mu}\frac{\partial}{\partial x^{\mu}} + ie\Gamma^{\mu}\Gamma_5 A_{\mu} + im\Gamma_5\right\} X^B = 0\,.$$

([8]) N. Dallaporta: *Nuovo Cimento*, **7**, 200 (1958); **11**, 142 (1959).
([9]) J. Schwinger: *Phys. Rev.*, **104**, 1164 (1956).
([10]) J. Tiomno: *Nuovo Cimento*, **6**, 69 (1957).

It is then apparent that Eq. (11) is invariant under the operation B, if the sign of the electromagnetic interaction is reversed, that is, if we change e into $-e$. It may be of some interest to see a similarity (*) between the operation B and the so-called mass reversal [11] in the case of non-electromagnetic interaction, although the latter has been used in the frame of the ordinary 4-component Dirac equation.

To proceed to the discussion about the spinor conjugation, let us define the « adjoint » of X by

$$\overline{X} = X^\dagger \begin{pmatrix} 0 & \gamma^4 \\ \gamma^4 & 0 \end{pmatrix}, \tag{17}$$

where † means to take Hermitic conjugate. Then we have:

$$(\overline{X}X) = (\bar{\tilde{\chi}}, \bar{\chi}) \begin{pmatrix} \chi \\ \tilde{\chi} \end{pmatrix} = (\bar{\tilde{\chi}}\chi) + (\bar{\chi}\tilde{\chi}), \tag{18}$$

where the adjoints of 4-component spinors are given as usual,

$$\bar{\chi} = \chi^\dagger \gamma^4, \qquad \bar{\tilde{\chi}} = \tilde{\chi}^\dagger \gamma^4. \tag{19}$$

Let us take antihermitic representation for γ^1, γ^2, γ^3 and Hermitic representation for γ^4 and γ_5 as usual. Taking Hermitic conjugate of Eq. (11) and multiplying by (Γ^4) from the right hand side we obtain the adjoint equation,

$$\overline{X}\left\{\frac{\partial}{\partial x^\mu}\Gamma^\mu + ieA_\mu\Gamma^\mu\Gamma_5 - im\Gamma_5\right\} = 0. \tag{20}$$

Then it is possible to introduce another conjugation defined as

$$X^S = \begin{pmatrix} 0 & \gamma_5 C \\ \gamma_5 C & 0 \end{pmatrix} \overline{X}^T \equiv S\overline{X}^T, \tag{21}$$

where C is the ordinary 4×4 charge conjugation matrix defined by:

$$C^{-1}\gamma^\mu C = -\gamma^{\mu T}, \qquad C^{-1}\gamma_5 C = \gamma_5^T, \tag{22}$$

charge conjugate of $A_\mu = A_\mu$.

(*) $$B = \gamma_5 \begin{pmatrix} 0 & I \\ I & 0 \end{pmatrix}.$$

The mass reversal is defined by multiplication of γ_5 and change the sign in front of m.

[11] J. J. Sakurai: *Nuovo Cimento*, 7, 649 (1958).

Taking the usual charge conjugate of both sides in Eq. (8),

$$(8^c)\qquad \begin{pmatrix}\chi^c\\ \tilde{\chi}^c\end{pmatrix}=\begin{pmatrix}\alpha & \beta\\ \beta & -\alpha\end{pmatrix}\begin{pmatrix}\psi^c\\ \tilde{\psi}^c\end{pmatrix},$$

we can see that the conjugation (21) is equivalent to interchange of ψ with $-\tilde{\psi}^c$ and $\tilde{\psi}$ with ψ^c and therefore it corresponds to the spinor conjugation of B.D.F. Under this operation Eq. (11) transforms into:

$$(23)\qquad \left\{\Gamma^\mu\frac{\partial}{\partial x^\mu}-ie\Gamma^\mu\Gamma_5A_\mu+im\Gamma_5\right\}X^s=0\,.$$

Without change of the sign of the electromagnetic term Eq. (11) is invariant under this transformation. Therefore this operation is equivalent to the change of the sign of the energy with no change of the sign of the electric charge.

Finally, if we apply both conjugations successively, we obtain

$$(24)\qquad X^c=BS\overline{X}^T=\begin{pmatrix}C & 0\\ 0 & C\end{pmatrix}\begin{pmatrix}\bar{\tilde{\chi}}^T\\ \bar{\chi}^T\end{pmatrix},$$

which is the ordinary charge conjugation of ψ and $\tilde{\psi}$ ($\psi\to\psi^c$, $\tilde{\psi}\to-\tilde{\psi}^c$).

It is evident that the two B and S conjugations are commutable between each other.

Concerning Eq. (12) exactly the same argument can be given just by interchanging the roles of $\tilde{\psi}$ and $\tilde{\psi}^c$ and of the boson and the spinor conjugations. Namely for Eq. (12)

$$(25)\qquad S=\begin{pmatrix}0 & \gamma_5\\ \gamma_5 & 0\end{pmatrix},\quad B=\begin{pmatrix}0 & \gamma_5C\\ C\gamma_5 & 0\end{pmatrix},\quad X^s=SX\,,\quad X^B=B\overline{X}^T.$$

The physical significance of the two conjugations into which the charge conjugation has been decomposed may become even clearer if we introduce another vector field interaction into Eq. (11). As mentioned above, if we try to introduce some vector fields interacting with baryons, there are only two independent types which are compatible with the reducibility and invariance under (2). These two types are equivalent as far as only one kind of field is concerned However, when we introduce two different fields into Eq. (11), the two types of coupling behave in quite different ways. Taking the first type which appeared in Eq. (11) for an electromagnetic interaction, we can try to assume the second type which is seen in Eq. (12), with no aim to explaining its real nature, for baryonic interaction. If we denote the latter vector field by Φ_μ,

we obtain

$$\left\{\Gamma^\mu\left(\frac{\partial}{\partial x^\mu}-ig\Phi_\mu\right)-ie\Gamma^\mu\Gamma_5A_\mu+im\Gamma_5\right\}X=0\,. \tag{26}$$

The transformation (8) applied to the above equation gives us the two separate equations:

$$\left|\begin{aligned}&\left\{\gamma^\mu\left(\frac{\partial}{\partial x^\mu}-ig\Phi_\mu-ieA_\mu\right)+im\right\}\psi=0\,,\\&\left\{\gamma^\mu\left(\frac{\partial}{\partial x^\mu}-ig\Phi_\mu+ieA_\mu\right)+im\right\}\tilde{\psi}=0\,.\end{aligned}\right. \tag{27}$$

We shall write down the applications of the three conjugations (15), (21) and (24) to Eq. (26) with the assumption: charge conjugate of $\Phi_\mu=\Phi_\mu$

$$\left|\begin{aligned}&\left\{\Gamma^\mu\left(\frac{\partial}{\partial x^\mu}-ig\Phi_\mu\right)+ie\Gamma^\mu\Gamma_5A_\mu+im\Gamma_5\right\}X^B=0\,,\\&\left\{\Gamma^\mu\left(\frac{\partial}{\partial x^\mu}+ig\Phi_\mu\right)-ie\Gamma^\mu\Gamma_5A_\mu+im\Gamma_5\right\}X^S=0\,,\\&\left\{\Gamma^\mu\left(\frac{\partial}{\partial x^\mu}+ig\Phi_\mu\right)+ie\Gamma^\mu\Gamma_5A_\mu+im\Gamma_5\right\}X^c=0\,,\end{aligned}\right. \tag{28}$$

which show clearly that the boson conjugation changes the sign of e and not of g, the spinor conjugation changes the sign of g and not of e, and the charge conjugation changes the signs of both e and g.

This behaviour of the baryon wave equation with respect to transformations in which the signs of e and g are changed independently should necessarily be completed by the existence of two independent conservation laws expressing the independent conservation of the e and the g coupling constants. In fact, this can be shown in the following way.

Let us first write the Lagrangian leading to Eq. (11)

$$\begin{aligned}\mathcal{L}=\frac{i}{2}\Big\{&\bar{X}\left[\Gamma^\mu\left(\frac{\partial}{\partial x^\mu}-ig\Phi_\mu\right)-ie\Gamma^\mu\Gamma_5A_\mu+im\Gamma_5\right]X-\\&-\bar{X}\left[\left(\frac{\partial}{\partial x^\mu}+ig\Phi\right)\Gamma^\mu+ieA_\mu\Gamma^\mu\Gamma_5-im\Gamma_5\right]X\Big\}\,,\end{aligned} \tag{29}$$

and one easily verifies that Eq. (11) and its «adjoint» (20) can be deduced from it.

Next, we define the following two independent four vector currents:

$$S_b^\mu = -ig\left(\frac{\partial\mathcal{L}}{\partial(\partial X/\partial x^\mu)}X - \bar{X}\frac{\partial\mathcal{L}}{\partial(\partial\bar{X}/\partial x^\mu)}\right) = g\bar{X}\Gamma^\mu X\,, \tag{30}$$

$$S_e^\mu = -ie\left(\frac{\partial\mathcal{L}}{\partial(\partial X/\partial x^\mu)}\Gamma_5 X - \bar{X}\Gamma_5\frac{\partial\mathcal{L}}{\partial(\partial\bar{X}/\partial x^\mu)}\right) = e\bar{X}\Gamma^\mu\Gamma_5 X\,,$$

and one immediately verifies that their four divergence is zero in both cases:

$$\frac{\partial S_b^\mu}{\partial x^\mu} = 0\,, \qquad \frac{\partial S_e^\mu}{\partial x^\mu} = 0\,. \tag{31}$$

By comparison with (29) one sees immediately that the first condition expresses the conservation of g, and the second one the conservation of e. The physical meaning of these expressions turns out to be clearer if, by use of (8) we express the χ spinors through the ψ spinors of the separated equations. One then obtains:

$$S_b^\mu = g[\bar{\psi}\gamma^\mu\psi + \bar{\tilde{\psi}}\gamma^\mu\tilde{\psi}]\,, \qquad S_e^\mu = e[\bar{\psi}\gamma^\mu\psi - \bar{\tilde{\psi}}\gamma\tilde{\psi}]\,. \tag{32}$$

The sense of these expressions is quite clear if we remind that ψ represents the proton and $\tilde{\psi}$ the Ξ^-, or other similar pairs.

One may conclude from this derivation that, should in fact a neutral vector field Φ_μ interact directly with baryons, the conservation of the charge g of this field could be made responsible for the conservation of baryonic number. Consequently two fundamental conservation laws, that of baryonic number conservation and of electric charge conservation may be derived independently and on a parallel footing from a single fundamental equation.

RIASSUNTO

In base a considerazioni fisiche, sono state esaminate le forme possibili per le interazioni tra barioni e campi nell'equazione di Gürsey, e viene invece proposta una nuova interpretazione per gli spinori ad otto componenti come coppie di stati del tipo protone-Ξ^- e Σ^+-Σ^-. Ciò permette di collegare in modo organico le operazioni di coniugazione bosonica e coniugazione spinoriale proposte da BUDINI, DALLAPORTA e FONDA coll'equazione di Gürsey. Le leggi di conservazione della carica elettrica e del numero barionico sono automaticamente garantite dal presente formalismo in modo indipendente l'una dall'altra.

1513

Nucleon Structure and Pion-Pion Interaction.

D. I. Blohinčev, V. S. Barašenkov and B. M. Barbašov
Joint Institute for Nuclear Research - Dubna

(ricevuto il 23 Marzo 1959)

Summary. — The density of a meson cloud in a nucleon is calculated on the basis of the extended source theory. The nucleon periphery is determined as a region of the applicability of the one-meson state. The pion-pion interaction cross section is estimated. The coefficient of pion absorption in a nucleon found experimentally is compared with that calculated by the optical model.

1. – Introduction.

Some years ago the analysis of energy losses and of multiple production of mesons in nucleon collisions led us to the conclusion that it is reasonable to distinguish three types of nucleon collisions: a core with a core (KK), a pion cloud with a core (Kπ), and finally, the collisions of pion clouds ($\pi\pi$) [1,2]. It was also meant that the collisions of the first type (KK) should be considered by the methods of the Fermi statistical theory, the collisions of the second type (Kπ) using the method of the parameter of collision and the meson theory.

The contribution of the collisions of type ($\pi\pi$) is very likely small (see, further Section **4**, as well as [2]). It would have been possible to develop the theory of periphery collisions (πK) only according to the pion cloud theory of a nucleon. The theory of this cloud was developed in papers by G. Chew [3], G. Salzman *et al.* [4].

---

(1) D. I. Blohinčev: *Journ. Exp. Theor. Phys.*, **29**, 33 (1955).
(2) D. I. Blohinčev: *CERN Symposium*, **2**, 155 (1956).
(3) G. F. Chew: *Phys. Rev.*, **94**, 1748 (1954); **95**, 1669 (1954).
(4) G. Salzman: *Phys. Rev.*, **99**, 973 (1955); **105**, 1076 (1957).

Later on, however, in Hofstadter's experiments (see [5,6]) on the study of the charge and magnetic moment distribution in the nucleons serious doubts were cast on the correctness of the classical picture of the pion cloud in the real nucleons.

There was found an essential discrepancy between the great magnitude of the proton electric radius and the small magnitude of this quantity for a neutron. These difficulties gave rise to quite different points of view on the nucleon structure [7,8] and even to doubts concerning the applicability of electrodynamics at distances of the order of 10^{-13} cm [6-9].

Meanwhile all these doubts seem to be based on an insufficiently clear understanding that the usual interpretation of R. HOSTANDER's experiments

$$F_{1p}(q) = F_{2p}(q) \quad F_{2n}(q)\,; \qquad F_{1n}(q) = 0\,.$$

(Here F_{1p}, F_{1n} are electrical and F_{2p}, F_{2n} magnetic form-factors for a proton and neutron) is, indeed, neither unique nor exact, but only possible.

The contradiction which arises between the density distribution law of the meson charge according to Yukawa theory $\sim \exp[-\alpha r]/r^2$ and the charge distribution $\sim \exp[-\beta r]$ obtained experimentally is also of no practical importance since the regions of the applicability of these expressions are quite different.

All this made us analyse the *spatial* picture of the charge and magnetic moment density distribution in the nucleon, which results from the extended source theory, and compare it with experimental data. Sections **2**, **3** are concerned with this.

Section **4** deals with the application of the pion cloud theory in the nucleons to the estimate of the $(\pi\pi)$ interaction cross-section.

2. – Nucleon core and pion cloud.

We shall suppose that the first approximation is not a bare, point nucleon but that distributed over the region $a \simeq \hbar/Mc$ (M is the nucleon mass).

([5]) R. HOFSTADTER, F. BUMILLER and M. YEARIAN: *Rev. Mod. Phys.*, **30**, 482 (1958).

([6]) W. PANOFSKY: *Annual Intern. Conf. on High Energy Physics, CERN* (Geneva, 1958), p. 3.

([7]) I. E. TAMM: *Journ. Exp. Theor. Phys.*, **32**, 178 (1957).

([8]) Discussion, *Annual Intern. Conf. on High Energy Physics, CERN* (Geneva, 1958), p. 33.

([9]) S. DRELL: *Annual Intern. Conf. on High Energy Physics, CERN* (Geneva, 1958), p. 27.

This distribution is due to virtual nucleons, antinucleons and strange particles. At the same time it is a pion cloud source in a nucleon (*).

If $v(k)$ is the Fourier component of this extended source, then the expressions for the charge density ϱ_π and for the density of the magnetic moment in this cloud $\boldsymbol{m}_\pi$ yield (see paper (6)):

$$\varrho_\pi(r) = -e\mu^3\tau_3 \frac{4f^2}{(2\pi)^5}\int \frac{v(k)v(k')}{\omega\omega'(\omega+\omega')}(\boldsymbol{kk'})\exp[i(\bar{k}-\bar{k}')\boldsymbol{r}]\,\mathrm{d}^3(kk')\,, \tag{1}$$

$$\overline{m}_\pi(r) = -e\mu^3 c\tau_3 \frac{2if^2}{(2\pi)^5}\int \frac{v(k)v(k')}{\omega^2\omega'^2}\bar{k}(\bar{\sigma}[\bar{r}[\bar{k}\bar{k}']])\exp[i(\bar{k}-\bar{k}')\bar{r}]\,\mathrm{d}^3(kk')\,. \tag{2}$$

All the lengths in these formulae are measured in units $1/\mu = 1.4\cdot10^{-13}$ cm, the pion mass is put equal to a unit; σ is the Pauli matrix; τ_3 is the matrix of the isotopic spin.

Expressions (1) and (2) are the first approximations which take into account the contribution of only one-pion-state.

The total density of charge and of magnetic moment in the nucleon is equal to

$$\varrho(r) = \varrho_\pi(r) + \varrho_k(r)\,; \qquad \overline{m}(r) = \overline{m}_\pi(r) + \overline{m}_k(r)\,, \tag{3}$$

where the densities of electric charge and magnetic moment are designated in terms of $\varrho_k(r)$ and $\overline{m}_k(r)$. These densities are concentrated in the central part of the nucleon and are due to nucleon and antinucleon pairs and to strange particles (charge and magnetic moment of a nucleon core), as well as to two-three and other higher pion states. At present we know very little about these states and for the time being shall consider them as components of the nucleon core.

Expression (1) can be easily reduced to the form

$$\varrho_\pi(r) = e\mu^3\tau_3 \frac{4f^2}{(2\pi)^5}\int\limits_0^\infty \mathrm{d}\xi \left(\frac{\mathrm{d}I}{\mathrm{d}r}\right)^2, \tag{4}$$

where

$$I(r) = \int \frac{v(k)}{\omega}\exp[i\bar{k}\bar{r} - \xi\omega]\,\mathrm{d}^3k\,, \tag{5}$$

whereas ξ is an auxiliary variable.

(*) It may be said that Tamm's model (loc. cit.) is applied not to a nucleon as a whole, but only to its central region.

Making the integration over angles and taking $v(k)=V(\omega)$ we obtain

$$I(r)=\frac{2\pi}{ir}V\left(-\frac{\mathrm{d}}{\mathrm{d}\xi}\right)Q(\xi,r)+\text{c. c.}\,, \tag{6}$$

$$Q(\xi,r)=\int_1^\infty \exp\left[-\xi\omega+ir(\omega^2-1)^{\frac12}\right]\mathrm{d}\omega\,. \tag{7}$$

Supposing further $\omega=\cosh t$ and introducing $\varrho=\sqrt{\xi^2+r^2}$ we obtain

$$I(r)=-\frac{4\pi}{r}V\left(-\frac{\mathrm{d}}{\mathrm{d}\xi}\right)\frac{\mathrm{d}K_0(\varrho)}{\mathrm{d}r}\,, \tag{8}$$

where $K_0(\varrho)$ is an well-known Bessel function.

The function $v(k)=V(\omega)$ serves as a cut-off factor. We choose it in the form

$$V(\omega)=\exp\left[-\beta(\omega-1)\right]\,, \tag{9}$$

where $1/\beta$ is a cut-off frequency.

Only in such a choice of $V(\omega)$ the operation $V(-\mathrm{d}/\mathrm{d}\xi)$ has a simple meaning of displacement $\xi\to\xi+\beta$.

Using now (4) and (8) one may easily obtain

$$\varrho_\pi(r)=e\mu^3\tau_3\frac{2f^2}{\pi^3}\exp\left[2\beta\right]r^2\int_{\sqrt{r^2+\beta^2}}^\infty\frac{\mathrm{d}\varrho}{\varrho^3\sqrt{\varrho^2-r^2}}K_2^2(\varrho)\,. \tag{10}$$

Here $K_2(\varrho)$ is the Bessel function. Just in a similar way the magnetic moment distribution may be calculated:

$$\overline{m}_\pi(r)=e\mu^3c\tau_3\frac{f^2}{2(2\pi)^3}\exp\left[2\beta\right]\left[\overline{r}[\overline{\sigma}\overline{r}]\right]\left\{\int_{\sqrt{r^2+\beta^2}}^\infty\frac{\mathrm{d}\varrho K_2(\varrho)}{\varrho\sqrt{\varrho^2-r^2}}\right\}^2. \tag{11}$$

The asymptotic expressions for these magnitudes are independent of the form of the cut-off function; they are as follows:

$$\varrho_\mu(r)=e\mu^3\tau_3\frac{f^2}{2\pi^{\frac32}}\frac{\exp\left[-2r\right]}{r^{\frac52}}+\dots\,, \tag{12}$$

$$\overline{m}_\pi(r)=e\mu^3c\tau_3\frac{f^2}{16\pi}\left[r[\sigma r]\right]\frac{\exp\left[-2r\right]}{r^4}+\dots\,. \tag{13}$$

1517

3. – Numerical results.

In general the quantities $\varrho_\pi(r)$ and $\bar{m}_\pi(r)$ essentially depend upon the form-factor of the source $V(\omega)$, in our choice of $V(\omega)$ they depend upon the quantity β.

We have chosen the quantity β so that the calculated phase shift of the P-wave for pion scattering on a nucleon would be in best agreement with experiment in the low energy region. The calculations have shown that $\beta = \frac{1}{7}$. This choise corresponds also to the form-factor accepted in papers [1,10].

The r.m.s. electric and magnetic radii appear to be equal to $\langle r_e^2\rangle_\pi = 0.19$ and $\langle r_m^2\rangle_\pi = 0.40$.

For the charge of the pion cloud eQ_π and for the pion magnetic moment $M_\pi e\hbar/Mc$ we obtain: $Q_\pi = 0.76$ and $M_\pi = 1.25$.

Now we shall be concerned with a more detailed consideration of the nucleon electric radius. According to the definition this radius is equal to:

$$\langle r_e^2\rangle = \frac{1}{e}\int r^2\varrho(r)\,\mathrm{d}^3r\,, \tag{14}$$

where ϱ is the total density of the pion cloud and nucleon core charges.

Put $\varrho_k = Q_k\varrho_c$ where Q_k is the total charge of a core and designate

$$\langle r_e^2\rangle_c = \frac{1}{e}\int r^2\varrho_c(r)\,\mathrm{d}^3r\,. \tag{15}$$

Expanding now the charge of a core Q_k in the scalar and vector parts Q_k^s and Q_k^v respectively we may write (14) as follows:

$$\langle r_e^2\rangle = \tau_3\langle r_e^2\rangle_\pi + (Q_k^s - \tau_3 Q_k^v)\langle r_e^2\rangle_c\,. \tag{16}$$

The isotopic symmetry of this expression is evident. Since for a neutron $Q_\pi + Q_k = 0$ and $Q_s + 0.5$ then $Q_k^v = 0.26$.

It is well-known experimentally that the root-mean-square radius of a neutron is $\langle r_e^2\rangle_n \simeq 0$. Therefore, it follows from (16):

$$\langle r_e^2\rangle_c = \langle r_e^2\rangle_\pi/(Q_k^s + Q_k^v) \tag{17}$$

and

$$\langle r_e^2\rangle_p = \langle r_e^2\rangle_c\,. \tag{18}$$

(10) G. SALZMAN and F. SALZMAN: *Phys. Rev.*, **108**, 1619 (1957).

Taking into account the values mentioned above Q_k and $\langle r_e^2\rangle_\pi$ we find that $\langle r_e^2\rangle_c = (0.5)^2 \simeq (0.7\cdot 10^{-13}\ \text{cm})^2$.

Thus, assuming the electric radius of a neutron equal to zero we obtain a reasonable value for the proton radius. The form of the charge distribution in the core is arbitrary enough (since only the value Q_k is known and $\langle r_e^2\rangle_c$). We choose $\varrho_c(r)$ as follows:

$$\varrho_c(r) = \frac{e}{8\pi a^3}\exp[-r/a]\,. \tag{19}$$

At this

$$\langle r_e^2\rangle_c = 12a^2\,. \tag{20}$$

Now in order to obtain $\langle r_e^2\rangle_c = 0.25$ it is necessary to take

$$a = \tfrac{1}{7} \simeq \hbar/Mc = 2\cdot 10^{-14}\ \text{cm}\,.$$

Thus, (19) is an example of a core which is characterized by a *small* length $a \sim \hbar/Mc$. At the same time it has a great root-mean-square radius.

Table I presents the values of the densities of an electric charge in the spherical layer $d_\pi(r) = 4\pi r^2\varrho_\pi(r)$ (*). In Fig. 1*a* and 1*b* are given the charge density distributions in a proton and neutron and in their cores.

TABLE I.

$r\cdot(m_\pi c/\hbar)$	0	0.05	0.075	0.1	0.125
$d_\pi(r)(\hbar/m_\pi c)(1/e)$	0	0.17	0.58	1.13	1.6
$r\cdot(m_\pi c/\hbar)$	0.15	0.2	0.3	0.4	0.5
$d_\pi(r)(\hbar/m_\pi c)(1/e)$	1.95	2.05	1.46	0.9	0.55
$r\cdot(m_\pi c/\hbar)$	0.6	0.7	1.0	1.5	20
$d_\pi(r)(\hbar/m_\pi c)(1/e)$	0.35	—	0.146	0.082	0.0145

(*) The values $\varrho_\pi(r)$ we calculated differ from those given in (11). However, as it is shown (12), the numerical data of paper (11) are not correct.

(11) F. ZACHARIASEN: *Phys. Rev.*, **402**, 295 (1956).

(12) D. R. YENNIE, M. M. LEVY and D. RAVENHALL: *Rev. Mod. Phys.*, **29**, 144 (1957).

The curve for a proton coincides practically with that given in HOFSTADTER's paper ([5]). As for the charge density in a neutron it is seen that it oscillates near zero. This accounts for a small electric radius of a neutron. In Fig. 1*a* and 1*b* the region of the one pion « atmosphere » of a nucleon is separated from the region where the core charges are essentially mixed by a vertical line.

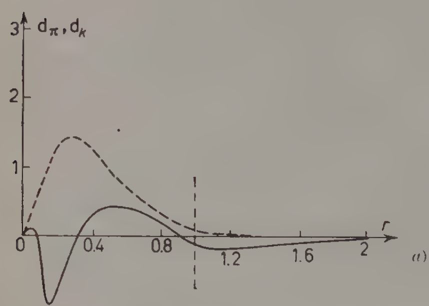

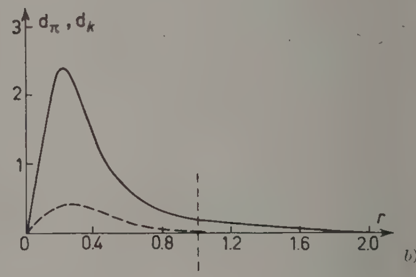

Fig. 1. – Electromagnetic structure of a nucleon. *a*) the structure of a proton; *b*) the structure of a neutron. The solid curve shows the distribution of an electric charge in a proton and neutron; the dashed line shows the corresponding distribution of an electric charge in cores of a proton and neutron. r in units of $\hbar/m_\pi c = 1.4\cdot 10^{-13}$ cm. $d(r)$ and $dk(r)$ in units $e(m_\pi c/\hbar)$.

As is seen in the region of an « atmosphere » $r > 1.4\cdot 10^{-13}$ cm. The region where the asymptotic expansions (12) and (13) are correct line even further. This is, so to say, the nucleon « stratosphere ».

The number of mesons containing in this region is extremely small.

One may analogously consider the magnetic structure of a nucleon. Choosing the distribution of the magnetic moment of a nucleon core in the form

$$m_c(r) = \frac{\mu}{8\pi a^3} \exp\left[-r/a\right] , \tag{21}$$

and putting $a = \frac{1}{7}$, from the condition $m = \tau_3 \cdot 1.85(e\hbar/2Mc)$ we obtain for the root-mean-square magnetic radii of a proton and neutron

$$\langle r_m^2\rangle_n = \langle r_m^2\rangle_p = (0.7\cdot 10^{-13}\ \text{cm})^2 .$$

Thus, the main results of the P. HOFSTADTER group:

$$\langle r_e^2\rangle_n \simeq 0 ; \qquad \langle r_e^2\rangle_p \simeq \langle r_m^2\rangle_p \simeq \langle r_m^2\rangle_n \simeq (0.8\cdot 10^{-13}\ \text{cm})^2$$

may be put in agreement with the concepts of the modern meson theory. At the same time the distribution of an electric charge and magnetic moment of a core is defined by a small length $a=\hbar/Mc\ll\hbar/m_\pi c$.

4. – Pion cloud and pion-pion interaction.

In pion scattering on nucleons with the parameter of the collision $b>\hbar/m_\pi c$ one may consider the scattering to be entirely due to the interaction of virtual pions of a nucleon with an incoming pion.

Now we shall draw our attention to the calculation of the pion absorption coefficient in this region.

First of all we evaluate the cross-section of the pion-pion interaction. Pions may be considered as particles consisting of virtual nucleon-antinucleon pairs (cf. ([13])). At this

$$\pi^+ = \mathrm{p}\cdot\tilde{\mathrm{n}}\,;\qquad \pi^- = \tilde{\mathrm{p}}\cdot\mathrm{n}\,;\qquad \pi^0 = 2^{-\frac{1}{2}}(\mathrm{p}\cdot\mathrm{n}+\tilde{\mathrm{p}}\tilde{\mathrm{n}})$$

and the hypotetic pion $\pi_0^0=2^{-\frac{1}{2}}(\mathrm{p}\cdot\mathrm{n}-\tilde{\mathrm{p}}\cdot\tilde{\mathrm{n}})$ (cf. ([14])). Here p, n are a proton and neutron whereas $\tilde{\mathrm{p}}$, $\tilde{\mathrm{n}}$ are an antiproton and antineutron.

This interpretation of a pion as a compound particle makes it possible to consider the dimensions of a pion a as a distance between the particles and antiparticles into which a pion virtually dissociates. Due to strong nucleon interaction the cross-section of the pion-pion interaction would be of the order

$$\sigma_{\pi\pi}\simeq\pi a^2\,. \tag{22}$$

The distance a may be estimated from the mass difference of $\pi^\pm$ and π^0 mesons. It is $9\,m_0$ (m_0 is an electron mass). At the same time it is a difference between the electromagnetic energies of a charged and neutral pion. It equals

$$\Delta E=\alpha\frac{e^2}{a}+\beta\left(\frac{e\hbar}{2Mc}\right)^2\frac{m^2}{a^3}\,. \tag{23}$$

Here the first term is an electrostatic energy, the second one is a magnetic energy, the numbers α, β are of the order of a unit, m is the total magnetic

([13]) E. Fermi and C. N. Yang: *Phys. Rev.*, **76**, 1739 (1949); M. A. Markov: *Hyperons and K-mesons*, CTI (1958).

([14]) A. M. Baldin: *Nuovo Cimento*, **8**, 569 (1958).

([15]) D. I. Blohinčev, V. S. Barašenkov and V. G. Grišin: *Nuovo Cimento*, **9**, 249 (1958).

1521

moment of a nucleon ($m' \simeq 2$). Putting $\Delta E = 9m_0c^2$ we find $a \simeq 2h/Mc$, therefore, $\sigma_{\pi\pi} \geqslant 5\cdot 10^{-27}$ cm².

The coefficient of the pion absorption $k(r)$ may be approximately written

$$k(r) \simeq \sigma_{\pi\pi}\cdot n(r)\,, \tag{24}$$

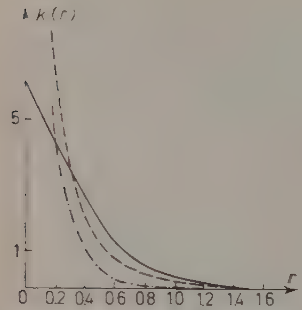

Fig. 2. – The solid curve shows the mean coefficient of pion absorption in a nucleon $K=k(r)$ for $E=1.3$ GeV. Dashed curve: the same for $E=5$ GeV. The point-dash line shows the values $K=k(r)$ calculated starting from $\varrho(r)-\varrho_\pi(r)-\varrho_k(r)$. r in units of 10^{-13}; $k(r)$ in the units of 10^{13} cm.

where $n(r)$ is the pion density in the nucleon « atmosphere ». In the region of the one pion state $n(r) \simeq (1/e)\frac{3}{2}\varrho(r)$ (the factor $\frac{3}{2}$ takes into account the presence of neutral mesons).

The curve $k(r)$ calculated by the data of Table I is plotted in Fig. 2. At this we put $\sigma_{\pi\pi} = 5\cdot 10^{-27}$ cm².

The curve $k(r)$ calculated by the experimental data for pions with an energy $E = 1.3$ GeV and $E = 5$ GeV according to the optical model (cf. ([5])) is also plotted there.

As is seen the agreement is rough.

However, one could hardly expect a better agreement since in the region $r = 0.2 \div 1$ the composition of the nucleon « atmosphere » is not reduced to the one pion state whereas the exact composition $\varrho_k(r)$ is not known. In the region $r \geqslant 1$ the values $k(r)$ obtained by the optical model are very doubtful.

Therefore, for the determination of pion-pion interaction the exact measurements of the diffractional pion scattering on nucleons at small angles seem to be very important and promising.

RIASSUNTO (*)

Si calcola la densità della nube mesonica in un nucleone, in base alla teoria della sorgente estesa. Si riconosce che la periferia del nucleone è regione di applicabilità dello stato monomesonico. Si stima la sezione d'urto dell'interazione pione-pione. Si confronta il coefficiente d'assorbimento dei pioni nel nucleone trovato sperimentalmente con quello calcolato dal modello ottico.

(*) *Traduzione a cura della Redazione.*

Un separatore di masse a focalizzazione magnetica del 2° ordine.

B. ARCIPIANI, G. BARSANTI, M. FUMELLI, L. MUSUMECI e N. TALINI
C.A.M.E.N., Laboratorio di Fisica - Livorno

(ricevuto il 16 Febbraio 1959)

Riassunto. — Viene descritto un separatore d'isotopi elettromagnetico con un magnete analizzatore di 90°, di raggio 40 cm e focalizzazione magnetica del secondo ordine. Vengono presentati i primi risultati sperimentali con una sorgente di ioni a bassa potenza. Il dispositivo è destinato alla produzione di campioni isotopici puri per scopi di ricerca.

Introduzione.

Un separatore elettromagnetico è stato recentemente costruito nel Laboratorio di Fisica Nucleare del CAMEN di Livorno. L'impianto che è destinato alla produzione di campioni isotopici ad alto grado di purezza per scopi di ricerca, è stato realizzato sullo schema teorico precedentemente studiato da uno degli autori [1,2] e EWALD [3].

Le sue caratteristiche principali sono: settore magnetico uniforme di 90°; raggio di curvatura delle traiettorie 40 cm; sorgente e collettore in posizione

(1) L. MUSUMECI: *Nuovo Cimento*, **7**, 351 (1950).
(2) L. MUSUMECI: *Nuovo Cimento*, **9**, 429 (1952).
(3) EWALD e HINTENBERGER: *Methoden und Andwendungen der Massenspektroskopie*, (1953), pp. 52 e segg.

simmetrica rispetto al settore magnetico; focalizzazione del 2° ordine; apertura iniziale del fascio di ioni all'uscita della sorgente circa 12°.

L'insieme del dispositivo è schematicamente indicato in Fig. 1.

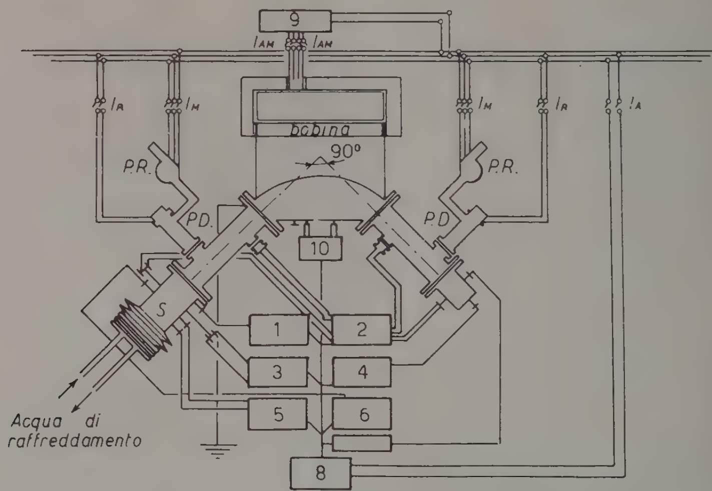

Fig. 1. – Schema generale. S.) Sorgente di ioni; P.R.) Pompa rotativa; P.D.) Pompa a diffusione; 1) Sistema elettrostatico; 2) Misura vuoto; 3) Termocoppia; 4) Collettore; 5) Resistenza di riscaldamento; 6) Alimentazione sorgente; 7) Alimentazione collettore; 8) Alimentazione generale; 9) Alimentatore stabilizzato magnete; 10) Misura campo magnetico.

2. – Settore magnetico.

Il campo magnetico è ottenuto mediante un elettromagnete di acciaio dolce (circa 2000 kg) eccitato da due bobine (40000 spire, circa 400 kg di rame) indipendenti e collegabili in serie od in parallelo. Le espansioni polari sono ricavate da un cilindro circolare retto il cui raggio (40 cm) è uguale a quello di curvatura delle traiettorie. Ne risulta un profilo circolare dei bordi di entrata e di uscita del settore magnetico tale da soddisfare le condizioni teoriche per una focalizzazione geometrica del 2° ordine.

Nel caso particolare considerato, la corrente di eccitazione del magnete è fornita da due alimentatori stabilizzati a circa $1/10^4$ mentre l'intensità e l'uniformità del campo sono controllate mediante un flussometro a risonanza nucleare (approssimazione $1/10^5$).

La buona stabilizzazione della tensione acceleratrice degli ioni e l'esatta misura del campo magnetico hanno consentito di individuare le varie masse isotopiche fin dall'inizio del funzionamento, semplificando l'operazione di messa a punto del dispositivo. Tale operazione risulta inoltre facilitata dal particolare profilo adottato per il contorno del campo. Infatti, in virtù del

contorno circolare, tutte le traiettorie entranti in direzione normale ne escono pure in direzione normale e quindi gli eventuali errori trasversali di aggiustamento della sorgente e del collettore non influiscono nè sulla aberrazione dovuta al flusso disperso nè sulla distanza focale e vengono automaticamente compensati con una piccola variazione di intensità del campo magnetico deflettore o della tensione acceleratrice.

Il traferro è di 8 cm e le superfici delle espansioni polari giacciono in piani orizzontali. L'impiego della macchina è attualmente previsto fino a valori di induzione di circa 0.5 Wb/m². Entro questo limite il diagramma di magnetizzazione è praticamente lineare ed il flusso disperso dal magnete è trascurabile.

La scelta del settore magnetico di 90° è stata suggerita da varie circostanze; principalmente: 1) esso consente di ottenere, per un dato raggio di curvatura R delle traiettorie, lo stesso valore massimo della dispersione $D = R\,\Delta M/M$, che si otterrebbe con una deflessione di 180°; 2) il predetto risultato si ottiene, nel caso del settore di 90°, con una superficie di espansioni polari inferiore a quella che sarebbe richiesta per una deflessione di 180°; 3) la possibilità di collocare la sorgente di ioni ed il collettore in posizione esterna al campo magnetico principale elimina ogni limitazione di carattere fisico o geometrico nella costruzione di tali parti. Limitazioni di questa natura esistono invece nel caso del settore di 180° che impone di operare con la sorgente ed il collettore immersi nel campo magnetico.

3. – Camera a vuoto.

La camera a vuoto è in ottone saldato. Il corpo centrale, inserito nel traferro del magnete, porta lungo una parete laterale dei fori attraverso i quali è possibile introdurre, a tenuta di vuoto, la sonda del flussometro a risonanza nucleare o altri elementi di osservazione e controllo. Agli estremi, in corrispondenza dei bordi di entrata e di uscita del settore magnetico, sono saldate due flangie alle quali si applicano i tubi cilindrici che portano la sorgente ed il collettore.

Il diametro interno di questi tubi è 10 cm. A ciascuno di essi è saldata nella parte inferiore una flangia per il fissaggio di una pompa a diffusione e nella parte superiore una flangia normalizzata per l'applicazione della testa sensibile di un vacuometro.

La lunghezza della camera, esclusa la sorgente ed il collettore, è di 143 cm e la sua superficie interna è circa 10600 cm².

4. – Sistema a vuoto.

È costituito da due gruppi di pompaggio ciascuno dei quali consiste di una pompa a diffusione da 300 l/s e di una rotativa da 15 m³/h. Il vuoto finale di lavoro è di circa 10^{-5} mm Hg.

Una ulteriore pompa a diffusione da 100 l/s può essere applicata direttamente alla sorgente. Le pompe a diffusione sono del tipo a vapori d'olio a due stadi, refrigerate ad acqua.

1525

Le rotative assicurano un vuoto preliminare limite di circa 10^{-3} mm Hg. Il sistema è munito di dispositivi automatici di sicurezza. Il controllo del vuoto è effettuato mediante vacuometri tipo Penning.

5. – Sorgente di ioni.

L'impianto completo prevede l'impiego di una sorgente a forte intensità di tipo classico per sostanze gassose o evaporabili. Altri tipi di sorgenti sono in corso di studio.

Fra queste ne è stata realizzata una del tipo ad emissione termica ([4-7]) per la produzione di ioni litio.

Varie esperienze sono state eseguite con impiego di platino, tungsteno e molibdeno come supporti del preparato emittente.

I risultati finora raggiunti non sono definitivi ma si possono considerare qualitativamente soddisfacenti in rapporto al dispositivo sperimentale usato.

Per la preparazione e la deposizione del materiale emittente è stato seguito in ogni caso il procedimento indicato da I. CORNIDES *et al.* ([5]).

Una miscela di Li_2O, Al_2O_3 e SiO_2 rispettivamente nelle proporzioni 15.2%, 14.8% e 70%, viene fusa e vetrificata. Successivamente viene ridotta in polvere e la sua sospensione in amil-acetato, con collodio, spalmata sulla superficie metallica. L'intensità di emissione ionica nel caso del Pt riscaldato indirettamente a 1500° può raggiungere il valore di 0.1 mA/cm².

Le prove attualmente in corso tendono a determinare le condizioni di massimo rendimento effettivo della sorgente in relazione al dispositivo geometrico ed alla temperatura di funzionamento. In particolare è stato sperimentato il riscaldamento diretto della superficie emittente con buoni risultati.

Una sorgente termica del tipo descritto di piccola potenza (inferiore a 100 W), è stata utilizzata per le prove generali di funzionamento del separatore. La corrente ionica utile raccolta sul collettore in queste condizioni è stata di circa 10 μA per il ^{7}Li e di circa 1 μA per il ^{6}Li. Per il normale funzionamento dell'impianto, la potenza assorbita può essere elevata fino a circa 1000 W con un corrispondente aumento della superficie emittente.

Il riscaldamento di questa è in c.a. fornita da un trasformatore il cui secondario è ad alto isolamento ed è mantenuto al potenziale di accelerazione degli ioni.

La fenditura di ingresso usata per il litio è di 6×0.5 cm. La sua larghezza può essere però variata in relazione alle masse isotopiche da separare in modo da ottenere la massima intensità di emissione compatibile con il necessario potere risolutivo.

([4]) EWALD e HINTENBERGER: *Methoden und Anwendungen der Massenspektroskopie*, (1953), pp. 42 e segg.

([5]) I. CORNIDES, I. ROOSR e A. SIEGLER: *Nucl. Instr.*, **1**, 94 (1957).

([6]) G. H. PALMER: *Journ. Nucl. Ener.*, **7**, 1 (1958).

([7]) M. INGHRAM e W. A. CHUPKA: *Rev. Sci. Instr.*, **24**, 518 (1953).

6. – Collettore.

È costituito da un pozzo di Faraday isolato e munito di schermo soppressore per l'eliminazione degli elettroni secondari.

La fenditura di uscita ha l'altezza di 6 cm, mentre la larghezza può essere variata in relazione alla massa degli ioni da raccogliere, alla stabilizzazione del fascio ed alla larghezza della fenditura di entrata della sorgente.

L'attuale collettore, costruito a scopo sperimentale, ha un'unica fenditura di uscita che consente quindi di raccogliere un solo isotopo per volta. Esso sarà successivamente sostituito con un dispositivo multiplo.

La corrente ionica è rivelata da uno strumento di misura inserito fra il collettore e la massa.

7. – Conclusioni.

Le prove sino ad oggi effettuate hanno dimostrato la funzionalità dello strumento per la separazione di quantità ponderabili di isotopi. Tuttavia ulteriori esperienze sono in corso per determinare: 1) la massima intensità di corrente ionica ottenibile in relazione ai vari tipi di sorgente ed alle condizioni di focalizzazione elettrostatica; 2) l'effettivo vantaggio pratico della focalizzazione magnetica del 2° ordine del tipo descritto nella separazione di isotopi ontigui ad alto numero di massa.

* * *

Gli autori ringraziano il Prof. T. Franzini per i suggerimenti durante lo studio e l'esecuzione del progetto e l'Ing. M. Camerini (Capo Sala Progetti del CAMEN) per la sua collaborazione tecnica nella costruzione dell'impianto.

SUMMARY

An electromagnetic isotope separator with a 90° analyzing magnet, radius 40 cm and second-order magnetic focusing is described. The first experimental results obtained with a low power ion source are presented. The device is designed for the production of very pure isotopic samples for research purposes.

IL NUOVO CIMENTO Vol. XII, N. 6 16 Giugno 1959

On the Pumping Speed of Oil Diffusion Pumps.

S. Petralia and U. Valdrè

Istituto di Fisica dell'Università - Bologna
Istituto Nazionale di Fisica Nucleare - Sezione di Bologna

(ricevuto il 31 Marzo 1959)

Summary. — The measurements of the jet breakdown pressure of an oil diffusion pump have been taken in respect of the heat input, and those of the pumping speed S have been taken both in relation to heat input and forepressure, both for air and for hydrogen. It was found that: 1) the breakdown pressure of the jet is the same for air and hydrogen and increases when the heat input increases; 2) the pumping speed both for air and hydrogen is independent of the forepressure; 3) the pumping speed for air is nearly constant in relation to heat input, while for hydrogen it has a distinct maximum for which the ratio $S(H_2)/S(A)$ is equal to 1.34. Such a value agrees with the calculations which may be made using the theory of R. Jaeckel. At the end, the plan for the apparatus for measuring the pumping speed of a diffusion pump has been referred to.

Several authors [1-7] have studied the behaviour of diffusion pumps when different gases are pumped, and in particular hydrogen, in view of its use in proton accelerators.

They have found, contrary to theoretical expectations, a noticeable lowering of the pumping speed, when air is replaced by a lighter gas.

This phenomenon has been explained by means of the larger back diffusion which, through the jet of vapour, the lighter molecules have in relation to air.

(1) R. J. Gibson jr.: *Rev. Sci. Instr.*, **19**, 276 (1948).
(2) R. B. Setlow: *Rev. Sci. Instr.*, **19**, 533 (1948).
(3) D. Fluke: *Rev. Sci. Instr.*, **19**, 665 (1948).
(4) B. B. Dayton: *Rev. Sci. Instr.*, **19**, 793 (1948).
(5) J. Blears and R. W. Hill: *Rev. Sci. Instr.*, **19**, 847 (1948).
(6) R. Jaeckel: *Kleinste Drucke ihre Messung und Erzeugung* (Berlin, 1950), p. 145.
(7) L. Riddiford and R. F. Coe: *Journ. Sci. Instr.*, **31**, 33 (1954).

The suggestions which can be drawn from the above mentioned work in order to increase the pumping speed for gases lighter than air, are:

1) to reduce the forepressure of the pump adding, for example, a second diffusion pump;
2) to increase the heat input of the pump so as to create a denser vapour jet.

These facts were taken into consideration when the vacuum system of the Cockcroft and Walton 500 keV accelerator was designed for the Institute of Physics of Bologna. Afterwards, during the running tests, certain indications made us think that the pump used did not give the above mentioned results, as yielded by some pumps made in U.S.A. Above all, the pumping speed for hydrogen was, starting from the breakdown pressure, independent of the forepressure.

It was decided, therefore, to carry out a series of tests on the behaviour of the diffusion pump in our plant when pumping air and hydrogen (*). Some of the tests concerned the breakdown of the vapour jet which takes place when the forepressure is increased. To this purpose, air or hydrogen was introduced by means of a needle valve between the rotary pump and the diffusion pump and the pressure variations on the high vacuum side were observed.

A test was made with under-heated, normally heated and over-heated pump. In Fig. 1 are shown in the two most interesting cases the pressure values existing on the high vacuum side as function of the pressure existing on the low vacuum side.

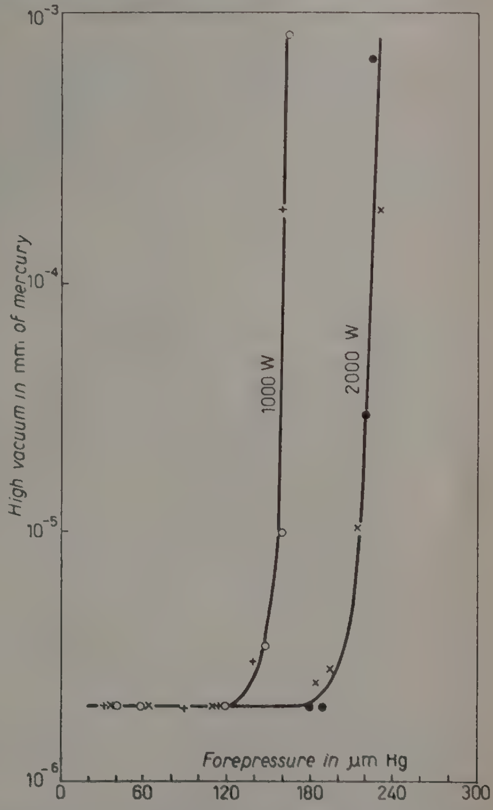

Fig. 1. – Back-diffusion of air and hydrogen through oil vacuum pump. ○, ● Air; +, × Hydrogen. Meker power input 2250 W.

It will be seen that the breakdown pressure is the same for the two gases and increases with increasing heat input of the diffusion pump. The

(*) The pump used was a Edwards 903B with three stages, the first of which is an ejector stage.

measuring of the forepressure was carried out at a point intermediate between the diffusion pump and the rotary pump. The real breakdown pressure is higher than that shown in the graph because of the resistance of the vacuum line.

The pumping speed of the diffusion pump was then measured both with hydrogen and air using the oil manometer method ([8]) and taking into account the suggestions given by A. GUTHRIE and R. K. WAKERLING ([9]).

To calculate the pumping speed S, the following formula is used

$$S = \frac{p_0}{p}\frac{A\cdot h}{t}\left[1+2\frac{h}{p_0}\frac{\varrho_0}{\varrho}\left(\frac{V_0}{A\cdot h}-1\right)\right], \tag{1}$$

where p_0 indicates the atmospheric pressure, p the pressure in the high vacuum side, measured with a ion gauge, h the change of level in a branch of the oil manometer, whose cross-section is A, V_0 the initial volume delimited between the needle valve and the oil level, ϱ and ϱ_0 respectively the density of mercury and oil, t the time taken to arrive at the height h. In our case the term

$$2\frac{h}{p_0}\frac{\varrho_0}{\varrho}\left(\frac{V_0}{A\cdot h}-1\right),$$

is not negligible as people usually consider, but gives the major contribution to the value of the pumping speed.

The pumping speed was measured with varying forepressure, up to a forepressure of 10^{-4} mm Hg, with the result that the functioning of the pump is completely independent of the value of the forepressure. This is shown in Table I.

TABLE I.

Gas	Power input (W)	High vacuum pressure (mm Hg)	Forepressure (mm Hg)	Pumping speed (l/s)
Air	2000	$7.8\cdot10^{-5}$	0.075	955 ± 48
	2000	$7.9\cdot10^{-5}$	$1\cdot10^{-4}$	933 ± 46
Hydrogen	2000	$7.3\cdot10^{-5}$	0.035	1220 ± 106
	2000	$7.6\cdot10^{-5}$	$1\cdot10^{-4}$	1228 ± 109

SETLOW ([2]) and BLEARS and HILL ([5]) found instead, that for pumps whose pumping speed is of the order of 100 l/s, the pumping speed depends considerably on the forepressure.

([8]) S. DUSHMAN: *Scientific Foundations of Vacuum Technique* (London, 1955), p. 160.

([9]) A. GUTHRIE and R. K. WAKERLING: *Vacuum Equipment and Techniques* (New York, 1949), p. 93.

Afterwards the pumping speed of the pump was measured for air and hydrogen as function of the heat input.

Some of the results are shown together in Fig. 2 in which the pumping speeds are expressed in litres per second and each series of experimental points refers to a certain high vacuum value.

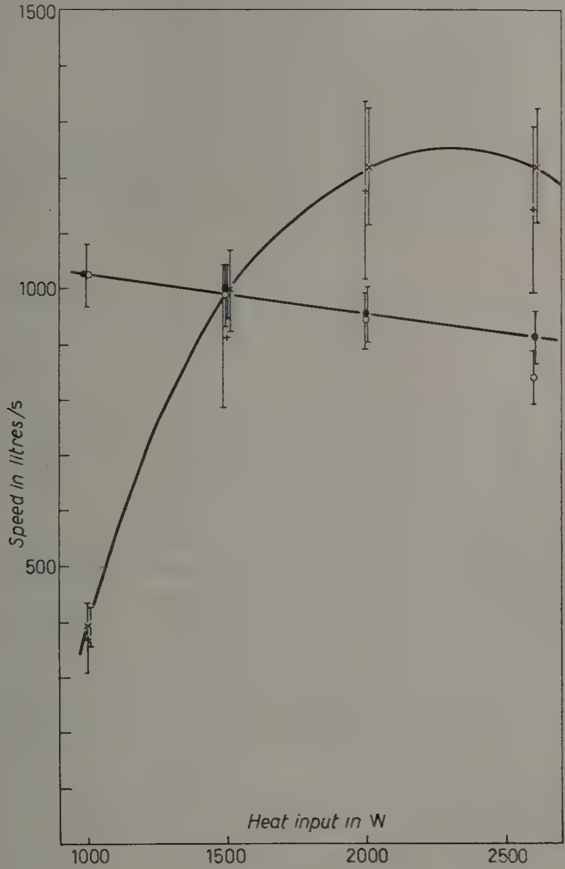

Fig. 2. – Pumping speed versus heating input of 903 oil diffusion pump for air and hydrogen. Room temperature: 21 °C. Fine side pressure for air: ∘) $3.9 \cdot 10^{-5}$ mm Hg; •) $7.9 \cdot 10^{-5}$ mm Hg. Fine side pressure for hydrogen: +) $2.6 \cdot 10^{-5}$ mm Hg; x) $7.5 \cdot 10^{-5}$ mm Hg.

From the graph it appears that the pumping speed for air is practically constant for a large range of the heater's power. In the case of hydrogen the pumping speed is much less than that of air at low heat input, increases rapidly with the heat input and reaches a maximum higher than the pumping

speed for air. The position of the maximum roughly corresponds to a heat input of 2250 W which is the value fixed by the manufacturer.

If we consider the ratio between the maximum pumping speed for hydrogen and the corresponding one for air, it is lower than 3.8 which we should have if the law of inverse proportionality with the square root of molecular weight M were valid. It is 1.34.

In Table II are shown the values of the ratios $S(H_2)/S(A)$ given in literature together with other features of middle and high pumping speed pumps.

When possible we have deduced the value of such a ratio both by the heat input for which we have the maximum value $S(A)_{max}$ of the pumping speed for air, and by the heat input for which we have the maximum value $S(H_2)_{max}$ of the pumping speed for hydrogen. The ratio has the value 3.45, which is close to the theoretical value 3.8, in one case only; in the other cases it is between 1 and 2.5. The inverse $(M)^{\frac{1}{2}}$ value is obtained by BLEARS and HILL overheating a one stage low speed oil diffusion pump.

TABLE II.

Authors	$\frac{S(H_2)}{S(A)_{max}}$	Power input (W)	$\frac{S(H_2)_{max}}{S(A)}$	Power input (W)	no. of stages	Oil	Makers indicated speed for air (l/s)
SETLOW (1948)	0.93	—	1.50	—	3	Amoil S	275
DAYTON (1948)	—	—	1.88	1000	3	Octoil	500
	1.66	2100	3.5	2840	—	Octoil	1400
BLEARS and HILL (1948)	—	—	1.0	makers' Ratings	3	—	(8 in.) diam.)
JAECKEL (1950)	—	—	2.1	—	—	Apiezon E	2400
RIDDIFORD and COE (1954)	0.65	1000	2.5	1520	3	—	700
Present work (1957)	0.39	1125	1.34	2300	3	Silicone 703	1500

We should take into account, however, that the law of inverse proportionality, on which the pumping speed depends, is complicated by factors which depend on the features of the pump: this law can give only approximate values.

Various formulae have been proposed which give the pumping speed of a diffusion pump. R. JAECKEL [5] gives for the maximum of the specific pumping speed s, the formula:

$$s = \frac{1}{4}\,\frac{\bar{c}}{1+\frac{1}{4}(\bar{c}/w)}\,, \tag{2}$$

where $\bar{c}$ is the mean speed of the gas molecule and w the speed of the vapour molecule.

If we write (2) both for air and for hydrogen and eliminate the speed w of the vapour, we obtain:

$$\frac{1}{s(A)} - \frac{1}{s(H_2)} = 6.31\cdot 10^{-5}\ \text{s/cm}$$

at the room temperature of 21 °C, corresponding to that of our measurements.

Our pump having a mouth cross-section of 334.5 cm², we obtain in our case the value $(7.1 \pm 1.4)\cdot 10^{-5}$ s/cm. As will be seen, the agreement between the experimental and theoretical data which is derived from (2) is fairly good, especially if we consider that (2) refers to the maximum theoretical value of the pumping speed.

On the basis of our experiments we conclude, therefore, that no advantage is obtained by inserting another diffusion pump and over-heating the pump in our plant. Probably this fact is to be ascribed to the particular feeding of the final stage of the pump which reduces the back diffusion for hydrogen. We note also that the first ejector stage will allow the pump to work with a high forepressure.

During the calibration of the measuring device a graph was made. It is related to the equation (1) and allowed us to find the value V_0 of the vacuum tank to be inserted in the apparatus, after having fixed the range of the product $p\cdot S$ of the pressure p on the high vacuum side times the pumping speed S.

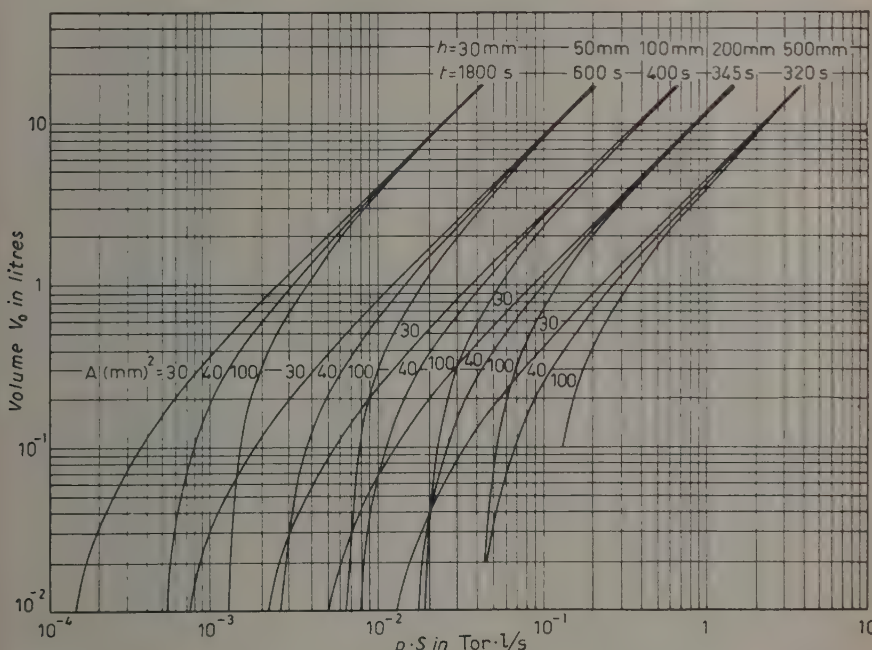

Fig. 3. – Diagram for the design of the experimental apparatus for measuring the pumping speed by the oil manometer method and to make the measurements having a fixed error percentage on the sum $\Delta t/t + \Delta h/h$.

We think it useful to reproduce such a graph in Fig. 3 both because it is generally valid and also because we have not found in the literature any indication of a better way of constructing the measuring apparatus.

In the figure every group of three curves refers to a certain value of the height h, which corresponds to a time t for making the measurement and has, as a variable, the cross-section A of the manometric tube. For A we chose the values 30, 40 and 100 mm²,

The graph has been plotted assuming that the relative error in the measurements of h and t is 1 %. We have assumed an absolute error of 2 s for t and an absolute error of 0.25 mm for h; to the latter we have added the error which may be made because of the speed at which the oil rises, computed proportionally to the said speed by means of a coefficient $k = 1$ s.

The calculations have been made assuming the value of 760 mm Hg for the atmospheric pressure and an average value of 0.95 g/cm³ for the oil density.

If a precision of ε % is required instead of 1 % on the sum of $(\Delta h/h) + (\Delta t/t)$, it is sufficient to multiply the value of V_0 deduced from the graph by the quantity $(0.01 \cdot \varepsilon \cdot h - 0.25)/(0.01 \cdot h - 0.25)$; this is the same as moving the curves in the direction of the axis of the abscissa.

RIASSUNTO

Su una pompa a diffusione ad olio sono state eseguite misure di rottura del getto, sia per l'aria che per l'idrogeno, in funzione della potenza riscaldante e misure della velocità di aspirazione S sia in funzione della potenza che del vuoto preparatorio. Si è trovato che: 1) la pressione di rottura del getto è la stessa per l'aria e per l'idrogeno e cresce col crescere della potenza riscaldante; 2) la velocità di aspirazione sia per l'aria che per l'idrogeno è indipendente dal prevuoto; 3) la velocità di aspirazione per l'aria è pressochè costante con la potenza riscaldante, mentre per l'idrogeno passa per un massimo netto in corrispondenza del quale il rapporto $S(H_2)/S(A)$ vale 1.34. Tale valore è in accordo con i calcoli che si possono fare in base alla teoria di R. Jaeckel. Si fanno inoltre considerazioni sulla progettazione del dispositivo di misura della velocità di aspirazione di una pompa a diffusione.

IL NUOVO CIMENTO Vol. XII, N. 6 16 Giugno 1959

On Fixing Solutions for Nuclear Emulsions.

D. Heughebaert and J. Heughebaert
Istituto Nazionale di Fisica Nucleare - Sezione di Milano

(ricevuto il 22 Aprile 1959)

Summary. — Clearing time, swelling, transparence and corrosion of Ilford K-5 emulsion in fixing solutions of 3 different compositions have been studied, and a solution chosen which, while reducing the clearing time and the danger of corrosion, does not increase the opacity, nor, to any appreciable extent, the swelling of the emulsion.

The aim of this work was to find a formula for the fixing bath such as to minimize both corrosion and distortion due to swelling of the emulsion.

Among the various fixing formulae in the literature, we have chosen three in common use for nuclear emulsions:

1) « Neutral » hypo (without additions)

i.e. sodium thiosulphate ($Na_2S_2O_3 \cdot 5H_2O$ commercial)	400 g
tap water	1 l

2) Hypo with bisulphite

i.e. sodium thiosulphate ($Na_2S_2O_3 \cdot 5H_2O$ commercial)	400 g
sodium metabisulphite ($Na_2S_2O_5$ anh.)	14 g
tap water	1 l

3) Buffered hypo solution with sodium sulphite and acetic acid

i.e. sodium thiosulphate ($Na_2S_2O_3 \cdot 5H_2O$ commercial)	400 g
sodium sulphite (Na_2SO_3 anh.)	12.5 g
acetic acid (pure)	10 cm^3
tap water	1 l

The pH of the freshly prepared solutions were, respectively, 7.5 for formula (1), and 4.8 for formulae (2) and (3).

The emulsions employed were Ilford K-5, 600 μm thick, developed by the normal temperature cycle. In order to compare the corrosive effects of the baths, these first trials were carried out with a silver concentration so low as to afford little protection. The solutions were stirred and maintained at 4 °C. Dilution was started after 80 hours of fixing. The plates were washed in running water at a temperature of 15 °C.

During fixing, the pH of the solutions was measured at regular intervals with a pH meter sensitive to 0.05 pH, and the variation in thickness of the emulsion determined by a micro comparator sensitive to 1 μm. As a test of the corrosion, gap counting was made on the ends of recoil protons from neutrons from the reaction $d + {}^3H \rightarrow n + {}^4He$ (*). This simple parameter was found to be reproducible and adequate for this comparison.

The results of these measurements are given in Table I and Fig. 1. Only one, the third of these solutions, maintained a stable pH. The other two tend to become more alkaline. In the interval of pH and in the conditions of the experiment the swelling of the emulsions is greater and the clearing time shorter, for the more alkaline solutions.

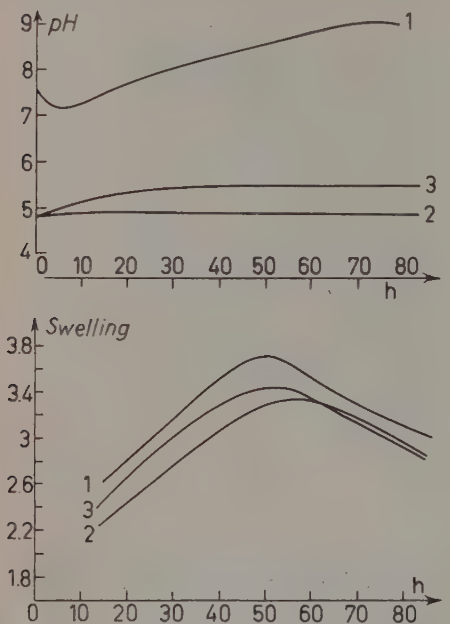

Fig. 1. – pH of solutions and swelling of emulsions in the fixing baths: 1) « Neutral » hypo. 2) Hypo with bisulphite. 3) Buffered hypo solution with sodium sulphite and acetic acid. At the beginning of fixing: 0 g/l of AgBr. At the end of fixing: 6 g/l of AgBr.

TABLE I.

Solution	Clearing time	Thickness at max. swelling / Thickness before processing	No. of gaps in proton ends (last 40 μm) (**)
« Neutral » hypo	45 h	3.75	8.7 ± 0.5
Hypo with bisulphite	52 h	3.38	12.9 ± 0.5
Buffered hypo	54 h	3.30	14.2 ± 0.5

(**) Mean of 120 tracks.

(*) We wish to thank Dr. MICHELETTI of the Institute of Physics of Milan who made the exposures.

1536

Note that the acid solutions remained colourless and without signs of precipitation, whereas the « neutral » (unbuffered) solution was yellowish at the end of the fixing. This is possibly due to the precipitation of silver salts, encouraged by alkaline solutions. The emulsion was also more stained than those fixed in acid baths. This may probably be due in part to this precipitation. This point will have to be investigated more fully.

Corrosion is definitely greater in the acid than in the « neutral » solution (average pH 8) and probably a little greater in the buffered solutions with sulphite (average pH 4.8) than in that with bisulphite (average pH 5.3).

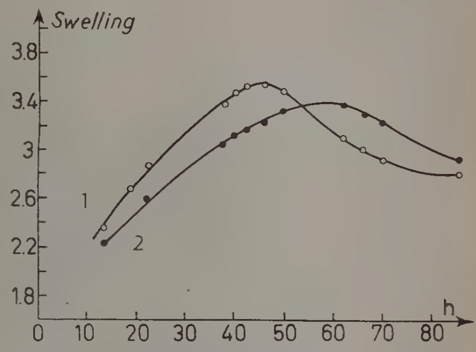

Fig. 2. – Swelling of emulsions in the fixing baths: 1) Buffered hypo solution with sodium sulphite and acetic acid (pH 6.8). 2) Buffered hypo solution with sodium sulphite and acetic acid (pH 4.8). At the beginning of fixing: 0 g/l of AgBr. At the end of fixing: 2 g/l of AgBr.

On the basis of these results, it was decided to try a fixing solution with sodium sulphite and acetic acid at a pH greater than 4.8 but still less than neutral. A second group of emulsions was fixed therefore in two solutions, solution (3) at pH 4.8 and a solution (4) at a pH of 6.8 composed of:

sodium thiosulphate ($Na_2S_2O_3 \cdot 5H_2O$ commercial)	400	g
sodium sulphite (Na_2SO_3 anh.)	12.5	g
acetic acid (10% solution)	12	cm^3
tap water	1	l

The pH of both solutions was found to be stable to $\pm$ 0.1 pH during all the time of operation.

In these trials, three different baths were used for each solution with increasing concentration of AgBr, in order to determine the quantity of silver necessary to afford sufficient protection against corrosion. The results are given in Fig. 2 and Table II.

It can be seen that the addition of AgBr does not lengthen appreciably the clearing time.

That full protection against corrosion can be obtained with less AgBr in the solution at pH 6.8 than in that at pH 4.8 is obvious from Table II. The smallest quantity of AgBr necessary to afford protection cannot however be determined from these results since the statistical weight of the measurements and the number of trials with different quantities of AgBr are too few. A more extended series of tests is required to obtain this figure.

(*) *The Nuclear Handbook - Nuclear Emulsions* (London, 1958), p. 12.

TABLE II.

	pH	Quantity of AgBr		Clearing time	Thickness at max. swelling / Thickness before processing	No. of gaps in protons ends (last 40 μm) (**)
		at the beginning	at the end			
a)	6.8	0 g/l	2 g/l	45 h	3.54	10.5 ± 1
	4.8	0 g/l	2 g/l	52 h	3.41	15 ± 1
b)	6.8	10 g/l	12 g/l	47 h	3.55	9 ± 1
	4.8	10 g/l	12 g/l	52 h	3.40	12 ± 1
c)	6.8	18 g/l	20 g/l	48 h	3.50	9 ± 1
	4.8	18 g/l	20 g/l	53 h	3.30	9 ± 1

(**) Mean of [illegible]0 tracks.

In conclusion, among the fixing solutions considered here, the buffered solution with acetic acid and sulphite is to be preferred to the « neutral » and bisulphite solutions, since the latter are unstable in pH. An adjustment of the pH of the buffered solution to pH 6.8 is preferable, in that a more satisfactory protection against corrosion is obtained than at pH 4.8, the clearing time is shorter by 10% while the increased swelling is not more than 5%.

This work has been presented in a more extended form at the « Colloque International de Photographie Corpusculaire » of Montréal.

* * *

We are grateful to Prof. P. CALDIROLA who, as Director of the Section of Milan of the Istituto Nazionale di Fisica Nucleare, made possible our stay in Milan.

We wish to thank, for their continual help and criticism, Prof. A. BONETTI, Mrs. C. DILWORTH and Prof. G. P. S. OCCHIALINI.

RIASSUNTO (*)

Si sono studiati il tempo di schiarimento, la trasparenza e la corrosione dell'emulsione Ilford K-5 in 3 differenti soluzioni di fissaggio e si è scelta una soluzione che, mentre riduce il tempo di schiarimento e il pericolo di corrosione, non aumenta l'opacità ne in modo apprezzabile il rigonfiamento dell'emulsione.

(*) *Traduzione a cura della Redazione.*

On the Elastic Scattering of Low Energy K⁻ on Protons.

D. AMATI (*)

Istituto di Fisica dell'Università - Roma
Istituto Nazionale di Fisica Nucleare - Sezione di Roma

E. GALZENATI and B. VITALE (*)

Istituto di Fisica Teorica dell'Università - Napoli
Scuola di Perfezionamento in Fisica Teorica e Nucleare del C.N.R.N. - Napoli

(ricevuto il 25 Novembre 1958)

Recent experimental data on the elastic K^--p scattering in the low energy region (1) show a significant increase of the elastic cross section $\sigma^{el}_-(\omega)$ with energy when the kinetic energy goes from zero to about 30 MeV. This increase is followed by a continuous decrease which brings $\sigma^{el}_-(\omega)$ from its maximum value of 65 mb at 25 MeV to about 27 mb at 95 MeV. At first sight such an energy dependence for an interaction which takes place essentially in an s-wave, would seem rather peculiar. We shall see, hewever, that it can be well understood on the basis of a simple linear behaviour of the scattering amplitude as suggested by dispersion relations.

By making use of the optical theorem and of the fact that at low energy the scattering is isotropic, we find

$$\sigma^{el}_-(\omega) = 4\pi\left(\frac{k_c}{k}\right)^2\left(D^2_-(\omega) + \frac{k^2}{(4\pi)^2}\,\sigma^2_-(\omega)\right), \tag{1}$$

where k and k_c are the K^- momenta in the Lab. system and in the C.M. system respectively, $D_-(\omega)$ the real part of the scattering amplitude and σ_- the total K^--p cross-section.

In the following we shall find a dispersion expression, depending on the relative K-Λ and K-Σ parities, that will relate $D_-(\omega)$ to integrals over the total cross-

(*) Present adress: CERN, Geneva.

(1) M. F. KAPLON: *Report at Geneva Conference* (1958).

sections of K^- and K^+ on protons (σ_- and σ_+). In such a way, from the knowledge of the total cross-sections in a range of energy, we should be able to find $D_-(\omega)$ and then, using (1), $\sigma^{el}_-(\omega)$ for every combination of relative parities. It will be shown in such a way that the requirement that the two terms in the bracket of (1) combine so to give the energy behaviour of $\sigma^{el}(\omega)$ previously discussed can be well satisfied if the K-meson is pseudoscalar with respect to either Λ and Σ.

We shall start from the relativistic dispersion relations for D_+ and D_- which have been derived in a previous paper (2). From them it is easy to obtain a subtracted dispersion relation which is especially suitable for our problem, namely:

$$D_-(\omega) = D_+(\overline{\omega}) + \sum_H P_{\mathrm{KH}} g_H^2 X(H) \frac{\omega + \overline{\omega}}{(\omega_H - \omega)(\omega_H + \overline{\omega})} + \tag{2}$$

$$+ \frac{(\omega + \overline{\omega})}{4\pi^2} \int_K^\infty k' \left[\frac{\sigma_-(\omega')}{(\omega' - \omega)(\omega' + \overline{\omega})} - \frac{\sigma_+(\omega')}{(\omega' + \omega)(\omega' - \overline{\omega})} \right] \mathrm{d}\omega' + \frac{(\omega + \overline{\omega})}{\pi} \int_{\omega_0}^K \frac{A_-(\omega')\, \mathrm{d}\omega'}{(\omega' - \omega)(\omega' + \overline{\omega})},$$

where P_{KH} indicates the relative K-H parity, $\omega_0 = 234$ MeV, $\omega_\Lambda = 64$ MeV and $\omega_\Sigma = 156$ MeV. The expressions for $X(H)$ are as follows:

$$P_{\mathrm{KH}} = +1: \quad X(H) = \frac{(H + N)^2 - K^2}{4NH}; \qquad P_{\mathrm{KH}} = -1: \quad X(H) = \frac{K^2 - (H - N)^2}{4NH}, \tag{3}$$

where K, N and H stand for the masses of the respective particles.

The dispersion relation (2) requires as little experimental information as possible for a subtracted dispersion relation; besides σ_+ and σ_-, indeed, only the knowledge of the sign of $D_+(\overline{\omega})$ at one energy is required. We can therefore choose $\overline{\omega}$ as that energy where $D_+(\omega)$ is known with the greatest accuracy and its sign is correctly given by the Coulomb interference. There is now no doubt about the sign of D_+ being negative, because of the observed constructive interference of the nuclear scattering with the Coulomb scattering in the low energy region.

We have used, in calculating $D_-(\omega)$ by means of (2), the most recent experimental information given at the Geneva Conference and summarized by KAPLON (1). We have put $\overline{\omega} = 554$ MeV (60 MeV kinetic energy in the Lab. system). We have estimated the contribution coming from the unphysical region by integrating also over it and by taking in the unphysical range an analytic continuation for A_-.

For s-s or ps-ps K-meson the results are sensitive only to the sum of the squares of the coupling constants, so that their relative value does not enter essentially in the problem. For the s-s case no value of the coupling constants can be chosen so to find agreement with the energy behaviour of $\sigma^{el}(\omega)$. For ps-ps the results thus obtained are given in Fig. 1, where the theoretical values of σ^{el} are compared with the experimental values. Some of the experimental errors are shown therein. The theoretical curve is normalized in such a way as to give agreement with experiment at 589 MeV.

---

(2) D. AMATI and B. VITALE: *Nuovo Cimento*, **7**, 190 (1958).

We see from Fig. 1 that the qualitative behaviour of σ^{el} is rather well described by the dispersion relation (2). It is important to note, however, that some of the errors introduced by our approximations cannot be estimated in a reliable way. In particular, our way of dealing with the unphysical range contribution, which very probably overestimates the unphysical region term in (2), has no theoretical justification. The calculation of σ^{el}_- through D_-, as indicated by (1), is also strongly dependent on the behaviour of the total cross section, mainly in the high energy region. Our expressions therefore cannot be used in order to establish the numerical value of the coupling constants by the normalization of σ^{el}_- to its experimental value at one or two energies. We note besides that also the choice of the cut-off (which we took as in the integrals appearing in (2)) can slightly influence the quantitative results for σ^{el}.

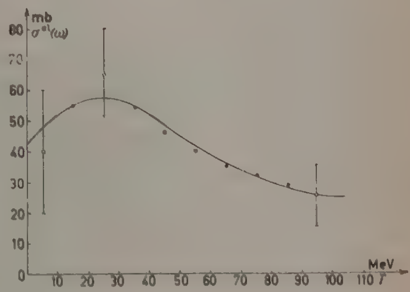

Fig. 1.

The s-ps and ps-s cases are a little more tricky, but it can be safely stated that only a very high g^2_{ps}/g^2_s ratio could lead to a rather poor agreement with experiment.

A similar result can be obtained by considering an effective range expression rather similar to that used previously for K^+p (3). Relating the sign of the effective range and that of the scattering length (as obtained in previous calculations (4,5)) to the parity values, one finds that both are probably negative for the s-s case while the effective range is negative and $D(k) > 0$ for the ps-ps case. This would mean a monotonically increasing value for $D^2(\omega)$ for the s-s case and a decreasing one for ps-ps. By observing the experimental values, one sees that $k_2\sigma^2(\omega)$ has an increasing trend, so that a decreasing $D^2(\omega)$ is needed in order to find the maximum for σ^{el}_- from (1), favouring then the ps-ps case.

We conclude then, that if K is pseudoscalar with respect to Λ and Σ (as predicted in the preceding analysis (3,5)) the characteristic behaviour of $\sigma^{el}(\omega)$ should be expected without imposing any new feature to K^-p interaction (as the presence of a resonance). Or, reversing the argument, we can take this as a further evidence for the pseudoscalarity of heavy mesons.

(3) D. Amati: *Phys. Rev.*, in press.
(4) P. T. Matthews and A. Salam: *Phys. Rev.*, **110**, 569 (1958).
(5) E. Galzenati and B. Vitale: *Phys. Rev.*, in press.

On the Elasticity in the High Energy Jet Events.

J. Iwadare
Research Institute for Fundamental Physics Kyoto University - Kyoto

(ricevuto il 5 Marzo 1959)

Recent experiments on jets have confirmed the fact that a high proportion, $(1-K)$, of the primary energy is emitted within a cone of very narrow angle in the laboratory system. The quantity $(1-K)$ is called elasticity.

Air shower experiments suggest that this ratio lies between 0.3 and 0.8 [1,2]. Bristol data [3] have shown that about 78% of the total energy is carried away by a relatively small number of particles ($\sim 1/8$ of the total number of secondary particles) emitted in a narrow cone in the forward direction of nucleon-nucleon collisions.

As is well known, two types of model have been used so far to explain the observed high elasticity [2]. In the first type, it is assumed that only a small part of the field energy of the actual nucleons contributes to the emission of secondary particles, the remainder being retained by the incident nucleons. The pre-existing field model of Lewis, Oppenheimer and Wouthuysen (L.O.W.), the Heisenberg-Bhabha model and the excited nucleon models of Takagi and Kraushaar-Marks belong to this type.

In the second type theories, which include the hydrodynamical model of Landau, the entire nucleon is considered to take part in the emission process. In this case the elasticity can be explained as follows. Consider a nucleon-nucleon collision in the centre of mass system. The total field energy of the two nucleons spreads away in the forward and backward directions according to the laws of relativistic hydrodynamics, and is then emitted as secondary particles. In the emission process an appreciable amount of the energy is concentrated in a few secondary particles to produce the high elasticity of the event. Amai and others [4] have estimated the proportion of the energy which is carried away by the first two particles of the greatest energy as shown in Table I.

In the following, we shall call these two types of model the kinematical and the dynamical models of the elasticity.

In the present note, we shall examine the two models in the context of the

(1) Discussions at the Symposium on Extremely High Energy Phenomena held in Kyoto in Feb. 1956. See reference (2).

(2) Z. Koba: *Prog. Theor. Phys.*, **17**, 288 (1957). Further references are found in the paper.

(3) B. Edwards, J. Losty, D. H. Perkins, K. Pinkau and J. Reynolds: *Phil. Mag.*, **3**, 237 (1958).

(4) S. Amai, H. Fukuda, C. Iso and M. Sato: *Prog. Theor. Phys.*, **17**, 241 (1957).

TABLE I. – *The fraction of the total energy of collision carried away by the first two particles of the greatest energy predicted by Landau's theory* [4].

Incident energy in the laboratory system (GeV)		10^3	10^5	10^7	10^9
nucleon-nucleon collision	the first particle	58%	45	33	25
	the next particle	22%	19	15	11
nucleon-nucleus collision	the first particle	49%	37	28	22
(effective number of the target nucleons = 2)	the next particle	16%	14	12	10

recent Bristol data obtained from photographic emulsions. The following two features of jets are particularly interesting.

1. – The total energy carried by π-mesons.

If the elasticity is of kinematical nature, that is, if the main part of the energy is to be carried away by the incident nucleons, the proportion of the energy carried away by π-mesons should be very small ($\leqslant K$). On thee ontrary, in the dynamical model, this proportion is not connected directly with the value of K, because in this model the high energy particles in the narrow cones may be π-mesons.

Recently an analysis of the angular distribution of charged secondary particles was performed by the Bristol group on the primary jets of energy > 1000 GeV. It shows that the average proportion of the energy which is carried away by π-mesons is likely to lie between 0.22 ± 0.05 and 0.40 ± 0.07. The analysis, however, is based on the assumption of the constancy of transverse momenta of π-mesons, and also depends on a very accurate determination of the smallest angles of emission which is hardly attainable. Here we shall try to infer the magnitude of the quantity in question more directly from the observed data and to compare it with the more or less independent estimate quoted above.

A tentative estimate is obtained as follows. K. PINKAU [8] has measured the energy of the electromagnetic cascades associated with jets of energy > 1000 GeV. From the measured values, we can estimate the total energy of π's emitted, correcting for the pairs which materialize outside the scanned volume, and then the total energy of π's (charged and neutral) using the assumption of charge independence. The results are given in Table II. E_0 is the primary energy of a jet estimated from the angular distribution of the secondary particles; $\sum E_{\text{pair}}$ is the sum of the energies of the electron pairs which materialize in the narrow cone within 2 cm from the jet origin; $\sum E_\pi/E_0$ is the fraction of the energy carried away by π's.

The mean value of $\sum E_\pi/E_0$ is found

[8] K. PINKAU: private communication.

TABLE II. – *The fraction of the total energy of collision carried away by pions. E_0: the primary energy of the collision; $\sum E_{\text{pair}}$: the total energy of the observed electron pairs; $\sum E_\pi$: the estimated total energy of the secondary pions.*

event	E_0 (GeV)	$\sum E_{\text{pair}}$ (GeV)	$\sum E_\pi/E_0$
P2	13000	78	0.044
P5	9000	276	0.224
P7	1640	81	0.363
P9	3000	263	0.640
P10	2000	293	1.070
P13	2000	353	1.295
P15	1800	160	0.650
P16	4200	75	0.131
P19	1800	20	0.081
P20	40000	5030	0.920
P24	25000	1000	0.293
P25	67000	390	0.047
P26	5000	1000	1.464
mean			0.56 ± 0.13

to be 0.56 ± 0.13. It is a little larger than those found by other methods. Although there may be some bias against lower values of $\sum E_{\text{pair}}$ due to the scanning efficiency for the primary jets, we do not think that it is significant for jets with energy >1000 GeV. If we assume that the remaining part of the energy is carried away by particles other than π's which constitute $\sim 27\%$ of secondary particles ([3]), (X-particles in ref. ([3])), then the ratio of the mean energies becomes

$$\overline{E}_\pi/\overline{E}_X \sim 1/2.1\,. \tag{1}$$

On the other hand the observed ratio

$$\overline{p}_{T\pi}/\overline{p}_{TX} \sim 1/2.7\,. \tag{2}$$

These figures are consistent with an assumption that π's and X's have similar angular distributions.

In connection with the predictions in Table I, a test for Landau's theory has been proposed ([1]). The test consists in searching for γ-rays of extremely high energies produced by the decay of π^0 in the narrow cone, which is expected in Landau's theory. In the jet events quoted in Table II, only one electron pair with an energy more than 10% of the primary energy has been observed (*). But the statistics are too poor to decide anything about the point.

2. – Angular distribution of the emitted particles produced by π-nucleon collisions.

Another interesting feature is the angular distribution of the secondary particles produced by π-nucleon collisions. If the nucleon core plays a special role in the collisions, as the kinematic models of elasticity suggest, the pion-nucleon collisions are expected to show different features from those of nucleon-nucleon collisions, since there is only one nucleon to play the special role in the collisions. For example, Bhabha's model, which is based on the assumption that the nucleon core and pion cloud evaporate secondary particles independently, will predict a complex angular distribution of secondary particles for the pion-nucleon collisions. In the L.O.W. and Kraushaar-Marks model, the emission will occur nearly isotropi-

(*) Lately an article has been published by ZHDANOV and others. (G. B. ZHDANOV, E. A. ZAMČALOVA, M. I. TRET'IAKOVA and M. N. ŠČERBAKOVA: *Journ. Exp. Theor. Phys.*, **34**, 582 (1958). In this article the authors describe an event of type $1 + 12n$ which was found in G-5 emulsions flown in Italy. The primary energy is estimated to be $E_0 = 250^{+250}_{-125}$ GeV. There is one π^0-meson carrying the energy of about 200 GeV. The lower limit of the total energy of the soft cascades was estimated as 150 GeV, about 30% of the primary energy.

The present author would like to express his thanks to Prof. Z. KOBA who has attracted his attention to the article.

cally in the rest system of the final nucleon. On the other hand, in Landau's theory the emission is expected to occur symmetrically with forward and backward peaks in the centre of momentum system of the nucleon and pion.

To check the point, we can make use of the angular distribution of shower particles produced in the secondary jets. The incident particle can be regarded as a pion in most of these events. The angular distributions measured by the Bristol group are shown in Fig. 1 *a*, *b*. That for the primary jets >1000 GeV is shown in Fig. 1 *c* for the sake of comparison. Dashed curves are those predicted by Landau's theory for the median energy of the jets, and solid

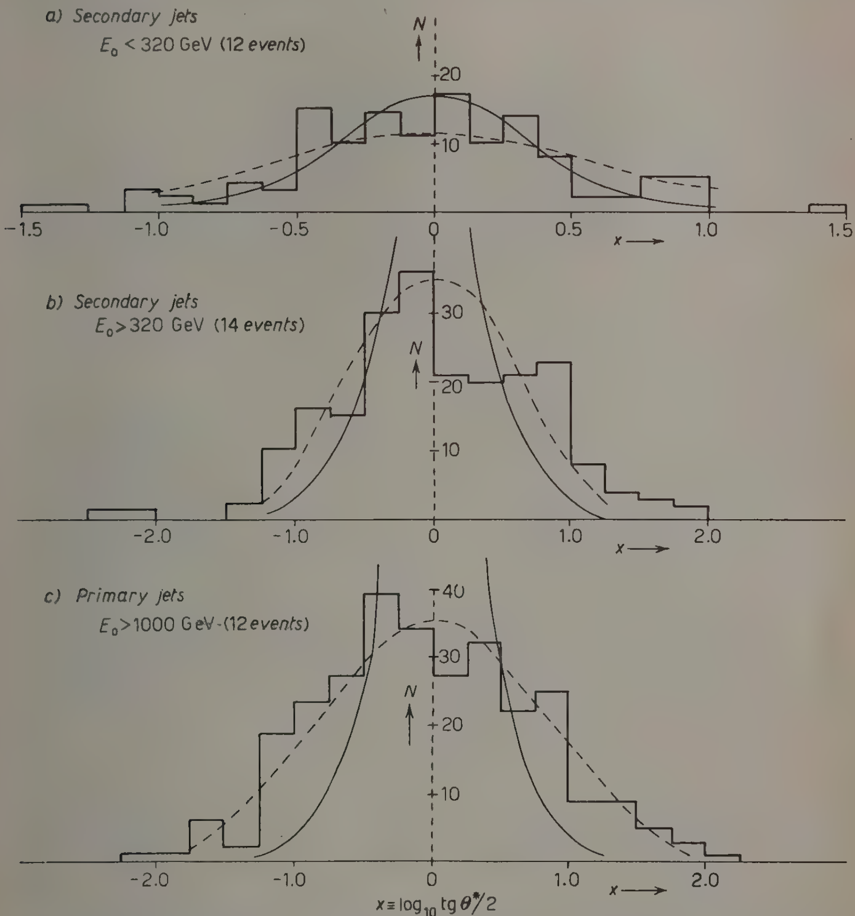

Fig. 1. – Angular distribution of the secondary particles. *a*) Secondary jets, $E_0 < 320$ GeV (12 events); *b*) Secondary jets, $E_0 > 320$ GeV (14 events); *c*) Primary jets, $E_0 > 1000$ GeV (12 events). Ordinate is $x = \log_{10} \mathrm{tg}\,(\theta^*/2)$. Dashed curves are due to Landau's theory. Solid curves correspond to the isotropic distribution.

curves are for the isotropic distribution. The angles θ^* are evaluated in the system for which the Lorentz transformation factor is given by

$$(3) \qquad \gamma = \frac{1}{[\operatorname{tg} \theta_{\text{lab}}]_{\text{geometrical mean}}},$$

where θ_{lab}'s are the angles of emitted particles in the laboratory system. The distribution for the low energy group < 320 GeV shown in Fig. 1 *a* seems to have a simple structure which is symmetrical with respect to forward and backward directions, and is consistent with the distribution given by Landau's theory. The distribution for the high energy group > 320 GeV in Fig. 1 *b* is somehow skewed but still not inconsistent with a symmetric distribution.

In ref. [3] the average value of the transverse momentum of the secondary pions in the primary jets is determined to be 0.52 GeV/c from the analysis of the electron pairs due to π^0 decay. On this basis, one can estimate the energy of the primary particle of the secondary jet measuring the emitted angle of the particle with respect to the direction of the parent particle. Then one can deduce the γ-factor of the centre of momentum system of the pion-nucleon collision. The values of the γ-factor thus determined are in good agreement with those defined by (3). The circumstance shows it quite plausible that the secondary particles are emitted symmetrically in the centre of momentum system of collision.

Although it seems that the data quoted above are in favour of Landau's view, yet they are not sufficiently strong to reject the kinematical model of elasticity. We hope that the accumulation of further data will decide the point, to throw some light on the nature of the nucleon-nucleon interactions at high energies.

* * *

The present analysis is mainly based on the unpublished data obtained by the Bristol group and performed during the author's stay in Bristol. The author would like to express his sincere thanks to the members of the group for their kindness in making their data available prior to publication.

The author is also very grateful to Prof. Z. Koba, Dr. K. Pinkau and Dr. J. Losty who have read the manuscript very carefully and given him many helpful suggestions.

IL NUOVO CIMENTO Vol. XII, N. 6 16 Giugno 1959

An Analysis of Hyperfragments Originated in K^--Stars.

S. Mora and I. Ortalli
Istituto di Fisica dell'Università - Parma

(ricevuto il 2 Aprile 1959)

The purpose of the present note is to give a short description of 17 mesonic hyperfragments originated in K^- stars; it is hoped to increase the statistics and to give a more complete discussion in the future.

As an introduction to the subject we refer to the papers of Franzinetti and Morpurgo (1), Filipkowski *et al.* (2), Slater (3), and Levi Setti, Slater, Telegdi (4). Our analysis closely follows in many points that of Slater (3).

A total of 4346 K^- stars (excluding zero prong stars and stars with only one thin prong), found in an emulsion stack exposed to the K^- beam of the Bevatron, has been explored following all the black and grey prongs; in addition the prongs of Σ^- stars have been followed.

We have found 27 mesonic hyperfragments of which 9 have been rejected owing to impossibility of following the π^- track and 1 owing to confusion in the decay point. The experimental characteristics of the remaining 17 events have been reported in the following Table I.

The notation used is indicated at the bottom of the Table.

Events 1 and 2 are clearly two body decays. Events 4 to 9 are three body decays of the kind $\pi^- + {}^1H + F'$ as may be seen from the coplanarity, momentum balance and Q value. Event no. 3 appears only consistent with a three body decay in which a neutron is emitted.

The remaining events (10 to 17) cannot be uniquely identified. From the characteristics of the track of the hyperfragment, when sufficiently long, near the decay point, the above decay events should be at rest; this is further confirmed, particularly for the uniquely identified events, by the momentum balance. The interpretation of the events is given in Tables II and III.

Table II contains the uniquely identified events, Table III the remaining ones.

The first column in these Tables contains the number of the event corresponding to that in Table I; the second column the proposed identification; the third the Q value the of reaction, that

(1) C. Franzinetti and G. Morpurgo: *Suppl. Nuovo Cimento*, **6**, 780 (1957).

(2) A. Filipkowski, J. Gierula and P. Zielinski: *Acta Phys. Pol.*, **16**, 141 (1956).

(3) W. E. Slater: *Suppl. Nuovo Cimento*, **10**, 1 (1958).

(4) R. Levi Setti, W. E. Slater and V. L. Telegdi: *Suppl. Nuovo Cimento*, **10**, 68 (1958).

TABLE I.

No.	Track	Range (μm)	ϑ (°)	φ (°)
1	F	1325		
	π^-	24100	—	−36.3
	r_0	7.6	180	+32
2	F	480		
	π^-	40370	—	+16.2
	r_0	7.8	180	−12
3	F	15		
	π^-	15550	—	−6.5
	r_0	7.0	146.7	−0
4	F	95		
	π^-	10370	—	−40
	^{1}H	245	−25.5	−30.8
	r_0	37	+166.7	+37
5	F	4.5		
	π^-	15450	—	−14.7
	^{1}H	67	+65.8	+31.8
	r_0	7.2	−153.3	−0
6	F	6.3		
	π^-	16850	—	+48.8
	^{1}H	17.7	−20	−42.7
	r_0	5.7	+176	−25
7	F	190		
	π^-	16150	—	+10
	^{1}H	20	+25.5	+26.7
	r_0	9.8	−177	−16
8	F	69		
	π^-	16200	—	0
	^{1}H	31	+25.5	−32
	r_0	10.5	−168	+20
9	F	84		
	π^-	5430	—	+39.7
	^{1}H	680	+6.7	+21.8
	r_0	8.5	−177.2	−24

No.	Track	Range (μm)	ϑ (°)	φ (°)
10	F	540		
(*)	π^-	17370	—	+2,8
	^{1}H	255	180	−32
	r_0	0	—	—
11	F	2070		
(*)	π^-	16480	—	+22.7
(**)	^{1}H	266	180	−33.5
	r_0	1.4	—	—
12	F	37		
(*•*)	π^-	13100	—	−8.5
	^{1}H	338	−156.7	−10.7
	r_0	2.2	+42	—
13	F	11		
	π^-	17410	—	−10.2
	^{1}H	58	+167	0
	r_0	1.3	−140	—
14	F	1210		
(*)	π^-	11480	—	+34.8
	^{1}H	614	178	−33.5
	r_0	2.0	0	—
15	F	21		
	π^-	15380	—	+34.5
	^{1}H	86	−115	−11.5
	r_0	3.3	+120	—
16	F	21		
	π^-	11940	—	−11.3
	^{1}H	395	171.7	0
	r_0	0	—	—
17	F	29		
	π^-	7950	—	−9.5
	^{1}H	340	−11.7	−6.3
	r_0	6.5	+169.8	−0

Notation used in the Table I: F is the hyperfragment, r_0 the recoil, ϑ the azimuthal angle of the track with respect to the π^- direction at the decay point, φ the dip angle of the track with respect to the horizontal plane.

(*) In these events measurements of δ-rays have been made on the track of hyperfragment and charge 1 for 10, 11, charge 2 for 14 has been found.

(**) In this case scattering-range measurements have been made on the hyperfragment track and a value of (4200 ∓ 1500) MeV has been found for the mass.

(*•*) Here ^{1}H suffers an elastic proton-proton scattering. Its energy at the decay point has been deduced from energy balance at the scattering point.

1548

TABLE II.

No.	Decay scheme	Q (MeV)	B_Λ (MeV)	ε (MeV)	P (MeV/c)	r_i (μm)	r_0 (μm)	δ (°)	$\theta_{\pi\Lambda}$ (°)
1	${}^{3}\mathrm{H} \to {}^{3}\mathrm{He}+\pi^-$	41,3	1,4	0,7					
2	${}^{4}\mathrm{H} \to {}^{4}\mathrm{He}+\pi^-$	56,1	0,9	1,0					
3	${}^{4}\mathrm{H} \to {}^{3}\mathrm{He}+\mathrm{n}+\pi^-$	34,1	2,4	0,6					
4	${}^{4}\mathrm{He} \to {}^{3}\mathrm{He}+{}^{1}\mathrm{H}+\pi^-$	36,1	1,1	0,7	188	38	37	1	19
5	${}^{5}\mathrm{He} \to {}^{4}\mathrm{He}+{}^{1}\mathrm{H}+\pi^-$	35.0	2.2	0.7	132	8.0	7.2	5	40
6	${}^{5}\mathrm{He} \to {}^{4}\mathrm{He}+{}^{1}\mathrm{H}+\pi^-$	34.3	2.9	0.6	107	5.5	5.7	6	31
7	${}^{5}\mathrm{He} \to {}^{4}\mathrm{He}+{}^{1}\mathrm{H}+\pi^-$	34.7	2.5	0.6	141	9.4	9.8	5	13
8	${}^{5}\mathrm{He} \to {}^{4}\mathrm{He}+{}^{1}\mathrm{H}+\pi^-$	35.4	1.8	0.7	146	10.2	10.5	7	19
9	${}^{7}\mathrm{Li} \to {}^{6}\mathrm{Li}+{}^{1}\mathrm{H}+\pi^-$	31.6	5.6	0.5	213	8.8	8.5	4	22

TABLE III.

No.	Decay scheme	Q (MeV)	B_Λ (MeV)	ε (MeV)	P (MeV/c)	r_i (μm)	r_0 (μm)	δ (°)	$\theta_{\pi\Lambda}$ (°)
10	${}^{2,3,4}\mathrm{H} \to {}^{1,2,3}\mathrm{H}+{}^{1}\mathrm{H}+\pi^-$	38.3	−1.1	0.7	9				170
11	${}^{3,4}\mathrm{H} \to {}^{2,3}\mathrm{H}+{}^{1}\mathrm{H}+\pi^-$	37.7	−0.5	0.7	23	1	1.4		124
12	${}^{4}\mathrm{He} \to {}^{3}\mathrm{He}+{}^{1}\mathrm{H}+\pi^-$	35.1	2.1	0.7	51	1.9	2.2		131
	${}^{5}\mathrm{He} \to {}^{4}\mathrm{He}+{}^{1}\mathrm{H}+\pi^-$	35.0	2.2	0.7	51	1.8	2.2		
13	${}^{4}\mathrm{He} \to {}^{3}\mathrm{He}+{}^{1}\mathrm{H}+\pi^-$	34.9	2.3	0.7	40	1.4	1.3		32
	${}^{5}\mathrm{He} \to {}^{4}\mathrm{He}+{}^{1}\mathrm{H}+\pi^-$	34.8	2.4	0.7	40	1.4	1.3		
14	${}^{4}\mathrm{He} \to {}^{3}\mathrm{He}+{}^{1}\mathrm{H}+\pi^-$	36.1	1.1	0.7	53	2.1	2.0		177
	${}^{5}\mathrm{He} \to {}^{4}\mathrm{He}+{}^{1}\mathrm{H}+\pi^-$	36.0	1.2	0.7	53	2.0	2.0		
15	${}^{3}\mathrm{H} \to {}^{1}\mathrm{H}+{}^{1}\mathrm{H}+\mathrm{n}+\pi^-$	34.7	0.3	0.7					
	${}^{5}\mathrm{He} \to {}^{4}\mathrm{He}+{}^{1}\mathrm{H}+\pi^-$	33.0	4.2	0.6	91	4.2	3.3		57
	${}^{7}\mathrm{He} \to {}^{6}\mathrm{He}+{}^{1}\mathrm{H}+\pi^-$	32.6	4.6	0.6	91	3.5	3.3		
16	${}^{4}\mathrm{H} \to {}^{1}\mathrm{H}+{}^{1}\mathrm{H}+\mathrm{n}+\pi^-$	34.8	0.2	0.8					
	${}^{4}\mathrm{He} \to {}^{3}\mathrm{He}+{}^{1}\mathrm{H}+\pi^-$	34.1	3.1	0.7	43	1.4	0		148
	${}^{5}\mathrm{He} \to {}^{4}\mathrm{He}+{}^{1}\mathrm{H}+\pi^-$	34.0	3.2	0.7	43	1.3	0		
	${}^{7}\mathrm{He} \to {}^{6}\mathrm{He}+{}^{1}\mathrm{H}+\pi^-$	34.0	3.2	0.7	43	1	0		
17	${}^{7}\mathrm{Li} \to {}^{6}\mathrm{Li}+{}^{1}\mathrm{H}+\pi^-$	31.1	6.1	0.5	195	7.5	6.5	6	11
	${}^{8}\mathrm{Li} \to {}^{7}\mathrm{Li}+{}^{1}\mathrm{H}+\mathrm{d}\ \pi^-$	30.6	6.6	0.5	195	5.7	6.5		

is the sum od the kinetic energies of the products; in this determination use has been made of the range-energy relations given by BARKAS *et al.* [5], for particles of unit charge and of the curves given in ref. [4] for the other particles.

It should be pointed out that in our case the density of the emulsion is unknown; this has been taken into account in the determination of the error, as we shall say in a moment. Column 4 gives the binding energy B_Λ, having assumed a Q value for the Λ of $(37{,}2 \mp 0{,}2)$ MeV.

The statistical error ε as defined in ref. [3] is reported in column 5: to this error one has to add a systematic error due to the uncertainty in the range-energy relations, which is taken to be, according to ref. [4], $6\cdot 10^{-3}\,Q$ MeV and a similar error due to the fact that the density of emulsion is unknown. In addition one has to keep in mind the error in the assumed Q value for the Λ.

Column 6 gives the resultant momentum P of the π^-, ^{1}H system, for three body decays. Column 7 gives the range r_i of the recoil inferred from the momentum given in column 6. Column 8 gives the measured range r_0 of the recoil; in several cases of Table III the dip of the recoil was deduced from that of $\boldsymbol{P}$.

Column 9 gives the angle δ between the resultant $\boldsymbol{P}$ and the momentum of the recoil. Column 10 gives the angle $\theta_{\pi\Lambda}$ of emission of the pion with respect to the direction of P in the reference system in which $P = 0$.

([5]) W. H. BARKAS, P. H. BARRETT, P. CÜER, H. H. HECKMAN, F. M. SMITH and H. K. TICHO: *Nuovo Cimento*, **8**, 185 (1958).

In the Table III attention should be particularly given to the events n. 10 and 11 which show characteristics very similar to 5 events already existing [3,6]; in particular:

1) The pion and proton are nearly colinear;

2) The binding energy is negative. In the event no. 10 there is no visible recoil, while in the event no. 11 a short recoil (1,4 μm) is present. In the event no. 11, in addition the mass of the hyperfragment can be directly measured due to the long range; it is *not* consistent with that of an hyperdeuteron.

In conclusion we may say that the general agreement between the results of the present and previous works is good; we wish howerer to stress again the importance of clarifying through an increased statistics the questions raised by the events 10 and 11 and by the other 5 similar events now existing in the world [3,4,6].

* * *

We are greatly indebted to Prof. G. MORPURGO for having suggested this work and for having constantly followed it.

To Prof. G. DASCOLA we are grateful for assistance in several occasions.

Finally we wish to acknowledge the help received from the Bologna emulsion group during the early phases of this work.

([6]) C. GROTE: *Nuovo Cimento*, **10**, 652 (1958).

A Decrease in the Intensity of the Cosmic Radiation Observed Underground, at Sea Level and at Mountain Altitude.

P. Chaloupka and P. Mokrý

Institute for Physics of the Czechoslovakian Academy of Sciences - Praha

T. Kowalski

Institute for Nuclear Research of the Polish Academy of Sciences - Kraków

T. Sándor, A. Somogyi and F. Telbisz

Central Research Institute for Physics of the Hungarian Academy of Sciences - Budapest

(ricevuto il 6 Aprile 1959)

In the course of the IGY measurements of cosmic ray intensity variations we detected a decrease in the intensity of the penetrating component and the low-energy nucleon component beginning rather sharply on 25th March 1958 at $(17\,46 \pm 6)$ min UT. The intensity variations are plotted in Figs. 1-5. Figs. 1 and 2 show the records of a standard neutron monitor, situated at ground level in Praha (228 m a.s.l.), resp. on the Lomnicky peak (2634 m a.s.l.), while the other Figures show the intensity variations of the μ-mesonic component observed with standard cubical telescopes in Praha (Fig. 3) and on the Lomnicky peak (Fig. 4), resp. with a standard semi-cubical telescope in Budapest (18 m below ground level, 410 m a.s.l., Fig. 5).

A few hours before the onset of the decrease a small geomagnetic storm (sudden increase of H by about $60\,\gamma$) was recorded in Praha and at Tihany [1] (Figs. 6 and 7). It must be mentioned however, that such small geomagnetic disturbances occurred rather frequently before and after the cosmic ray minimum too.

Two days before the onset of the cosmic rays intensity decrease, an extremely bright solar flare (3+) was observed (23-3-58 at 09 50 UT).

One of the most interesting features of the event is the extension of the decrease to the « energetic » μ-mesons

(1) At the Observatory for Geomagnetism which is associated with the Hungarian National « Eötvös Loránd » Institute for Geophysics and which is situated 110 km southwest from Budapest. A part of the experimental data from the observatories Lomnický Štít and Praha is included in the publication: J. Hladký *et. al.*: *Cz. Phys. Journ.* 1959, N. 3, (in press).

responsible for the intensity at a depth of 18 m below ground. The decrease in this region amounts to (6.5 ± 0.6)‰.

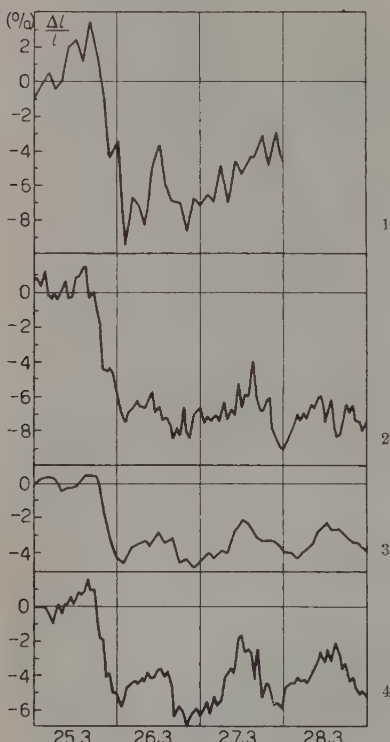

Fig. 1-4.

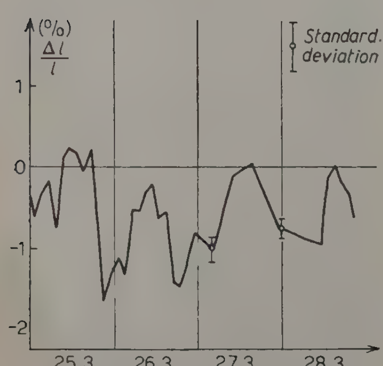

Fig. 5.

Even more interesting is the increase of the amplitude of the daily variation. While on the normal days we observed

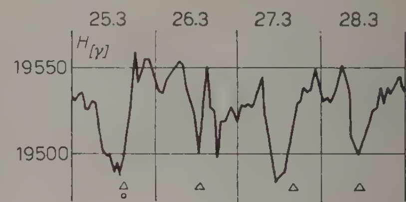

Fig. 6.

a daily period with an amplitude of (0.8 ± 0.1) ‰, the maximum being at $(11\,24 \pm 12)$ UT, on the first day of decrease (25th March 20 00 UT - 26th March 20 00 UT) we obtained a daily amplitude

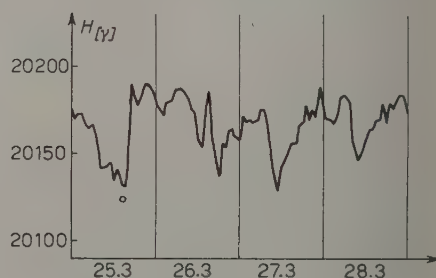

Fig. 7.

of (6.8 ± 1.2) ‰ with a maximum at $(12\,30 \pm 36)$ UT.

These and the analogous results at ground level are listed in Table I. The values for the cubical telescopes are corrected for barometric pressure only and those for the semicubical telescope for both barometric pressure and temperature effect.

Unfortunately, the underground telescope went wrong on 28th March, therefore the end of the decrease could only be observed with surface devices. The normal intensity level was reached exponentially about the 1st April 1958.

TABLE I. – *Amplitude A and time of maximum T of daily variation.*

Detector	A (%)	T (UT)	A (%)	T (UT)
	normal days		March 26, 27, 28	
Cub. Telescope, Praha	0.239 ± 0.035	11 11 ± 33	0.705 ± 0.038	12 19 ± 14
Cub. Telescope, Lom. S.	0.21 ± 0.10	08 10 ± 200	1.18 ± 0.06	11 31 ± 13
Neutron Monit. Praha	0.54 ± 0.15	09 51 ± 100	1.04 ± 0.13	12 14 ± 31
Neutron Monit. Lom. S.	1.27 ± 0.22	06 19 ± 43	0.55 ± 0.14	08 58 ± 55
Semi-cub. Tel. Budapest	0.08 ± 0.01	11 24 ± 12	0.68 ± 0.12 (*)	12 30 ± 36

(*) Obtained from the data of the first day.

IL NUOVO CIMENTO VOL. XII, N. 6 16 Giugno 1959

Preliminary Results Regarding High Energy Interactions of π^- in a He-Bubble Chamber (*).

M. BLOCK (**), B. BRUCKER, C. CHANG, T. KIKUCHI and C. MELTZER
Duke University - Durham, N. C.

F. ANDERSON and A. PEVSNER
Johns Hopkins University - Baltimore, Md.

H. COHN
Oak Ridge National Laboratory - Oak Ridge, Tenn.

E. HARTH and J. LEITNER
Syracuse University - Syracuse, N. Y.

G. BRAUTTI, C. FRANZINETTI and R. TOSI
Istituto di Fisica dell'Università - Trieste
Istituto Nazionale di Fisica Nucleare - Sottosezione di Trieste

(ricevuto il 28 Aprile 1959)

Interactions of high energy π^--mesons with Helium have been studied in the Duke University liquid helium bubble chamber. The sensitive volume of the chamber is a parallelepiped of dimensions of $20\times10\times12$ cm^3 and it is contained in a magnetic field of 14.3 kG.

Exposures have been made to 1.1 (***), 1.8 and 2.4 GeV/c mesons from the Berkeley Bevatron, during early 1958.

The aims of the experiments were the following:

1) *Determination of the relative and absolute parity of* K^+ *and* K^0.

Recently the question of whether or not K^- and K^0's have the same parity has been raised by PAIS (*). The Duke bubble chamber group, then engaged in an experiment to check charge sym-

(*) Presented at the Palermo Conference of the Italian Physical Society, Palermo, 6-11 Nov. 1958.

(**) At present at the Istituto di Fisica della Università, Trieste, on a Guggenheim Fellowship.

(***) This 1.1 GeV/c exposure was made before the magnetic field was installed.

(*) Now appeared in the *Phys. Rev. Letters*, Dec. 1st, 1958.

metry by π^+ and π^--mesons on helium, realized that such studies with a self-conjugate nucleus could give an answer to this question. The investigation of the reactions

$$a) \qquad \pi^- + {}^4\mathrm{He} \to X + \mathrm{K}^0 ,$$

and

$$b) \qquad \pi^- + {}^4\mathrm{He} \to X' + \mathrm{K}^+ ,$$

where X and X' are charge conjugate states, may show a violation of the principle of charge symmetry and would provide evidence for a different parity of the K^0 and K^+.

In particular, examples of the above class of reactions are:

$$(1) \qquad \pi^- + {}^4\mathrm{He} \to {}^4\mathrm{H}_\Lambda + \mathrm{K}^0 ,$$

$$(2) \qquad \pi^+ + {}^4\mathrm{He} \to {}^4\mathrm{He}_\Lambda + \mathrm{K}^+ ,$$

$$(3) \qquad \pi^- + {}^4\mathrm{He} \to \Lambda^0 + {}^3\mathrm{H} + \mathrm{K}^0 ,$$

$$(4) \qquad \pi^+ + {}^4\mathrm{He} \to \Lambda^0 + {}^3\mathrm{He} + \mathrm{K}^+ .$$

It is of course clear that the ratios of occurrence of reactions (1)-(2) and of (3)-(4) respectively are expected to be unity on the basis of charge symmetry, a principle which contains implicitly the statement that K^0 and K^+ are members of the same I-spin doublet and consequently have the same parity. Clearly, any departure from the ratio 1/1 implies a violation of charge symmetry and therefore probably a different parity for K^0 and K^-.

This is true also for the more general case of the reactions a) and b) in which all that is necessary is to compare the cross sections for K^+ and K^0 production from a) and b) respectively. Again any departure of cross section ratios from unity would be indication of a different parity of K^+ and K^0.

The more general reactions a) and b) allow us to improve the statistics, since we measure K^- and K^0 *total* cross section for production. In fact, it is expected that the hyperfragment reactions (1) and (2) would be very rare. Nevertheless, the study of these reactions is important because it would allow a direct determination of the parity assignment of the K^0 and K^-, provided that the spins of the ${}^4\mathrm{He}_\Lambda$ and ${}^4\mathrm{H}_\Lambda$ are zero and the spins of the K's are also zero, and that parity is conserved in strong interactions. It can easily be shown that the observation of the reactions (1) and (2) would prove that the K's are pseudoscalar, whereas the absence of these reactions would indicate that they are scalar.

2) *Study of elastic and inelastic cross sections.*

Preliminary results.

A track length of 5.8 km in the 1.8 GeV/c π^- film has been examined. The total number of observed interactions (including strange particles production, elastic and inelastic scattering) is 1340, which gives a value for the total cross section, — after correction for beam contamination — of the order of 110 mb. Ten V^0-particles have been identified, which gives a preliminary estimate of the cross section of ~ 1 mb. Similarly, the cross section for elastic interaction turns out to be about 5 mb. The angular distribution of the scatters corrected for scanning biases, agrees fairly well with a diffraction scattering curve. From the position of the first diffraction minimum, we estimate a nuclear radius for He of $\sim 2\cdot 10^{-13}$ cm.

At 1.1 GeV/c, the track examined to date is 1.6 km, and the corresponding total cross section is ~ 135 mb.

The companion experiments with exposures to π^+-mesons are now being prepared.

* * *

We would like to acknowledge the hospitality and assistance of Dr. E. LOFGREN and the Berkeley Bevatron staff for making this exposure possible.

1355

J. Jackson – *The Physics of Elementary Particles.* (Princeton University Press, 1958, pagg. 131).

Il libro è diviso in tre parti. Nella prima l'autore tratta l'interazione pione-nucleone, limitandosi alle basse energie (precisamente, nell'intorno della prima risonanza. L'autore sintetizza i principali risultati sperimentali relativi sia allo scattering pione-nucleone che alla fotoproduzione dei pioni da nucleone. Allo scattering pione-nucleone viene applicato il formalismo dello spin isotopico e viene esposta l'analisi in fase. I risultati di questa analisi sono confrontati con le previsioni della « effective range » teoria e delle relazioni di dispersione. Per quel che riguarda la fotoproduzione l'autore discute i vari termini che contribuiscono ad essa (momento magnetico del nucleone, corrente pionica ecc.), distintamente per i pioni neutri e carichi.

La seconda parte è riservata alle « particelle strane ». L'autore inizia con l'esposizione della situazione sperimentale e dello schema di Gell-Mann, Nishijma. L'esposizione è estesa agli iperframmenti ed allo scattering K-nucleone. Sono discusse, anche, le varie forme proposte per l'interazione iperone-nucleone e K-nucleone.

La terza parte riguarda le interazioni deboli. L'autore espone, in dettaglio, quale forma debbano avere le funzioni di distribuzione perchè il decadimento sia invariante per una particolare trasformazione (conservazione della parità, inversione del tempo ecc.). L'autore riassume i principali risultati sul decadimento beta sino ad includere i recenti esperimenti sulla non conservazione della parità e la interpretazione di questi mediante la teoria del neutrino « a due componenti ». Infine sono trattati, più brevemente, il decadimento dei mesoni leggeri e pesanti, e degli iperoni.

Questo libro è stato scritto, come detto nella presentazione inglese e nella prefazione dell'autore, come una introduzione sull'argomento delle particelle elementari. Per ulteriori approfondimenti l'autore rimanda agli articoli originali (la bibliografia è aggiornata al Maggio del 1958).

A mio parere, il testo è una bella sintesi di un campo vasto, quale risulta dalla esposizione del contenuto, e in evoluzione. Il testo però risulta in qualche punto un pò sintetico. Ciò è da credere derivi dalle origini che ha avuto il libro, nato da un breve corso tenuto dall'autore.

M. Grilli

IL NUOVO CIMENTO

INDICI

DEL VOLUME XII - SERIE X

1959

INDICE SISTEMATICO
PER NUMERI SUCCESSIVI DEL PERIODICO

N. 1 - 1° Aprile 1959

N. 2 - 16 Aprile 1959

1559

Lettere alla Redazione:

N. 3 - 1° Maggio 1959

Note Tecniche:

Lettere alla Redazione:

N. 4 - 16 Maggio 1959

N. 5 - 1° Giugno 1959

N. 6 - 16 Giugno 1959

Note Tecniche:

Lettere alla Redazione:

INDICE ALFABETICO DEGLI AUTORI

Le sigle L. e N.T. si riferiscono rispettivamente alle *Lettere alla Redazione* e alle *Note Tecniche.*

INDICE ANALITICO PER MATERIE

Radiazione cosmica.

Radioattività

Elettromagnetismo e Ottica

Astrofisica

Particelle elementari

NUCLEI (FISICA NUCLEARE)

LIQUIDI E SOLIDI - MOLECOLE

Iperframmenti

Idro e Magneto-dinamica

Elettrodinamica e Teoria dei Campi

Apparati, Strumenti e Tecnica Sperimentale

INDICE DELLE RECENSIONI

1571

Fine del Volume XII, Serie X, 1959

Direttore responsabile: G. POLVANI

Tipografia Compositori - Bologna

Questo Fascicolo è stato licenziato dai torchi il 26-VI-1959

1572